PHILOSOPHICAL TRANSACTIONS OF THE ROYAL SOCIETY A MATHEMATICAL, PHYSICAL & ENGINEERING SCIENCES

A Two-Dimensional Model for the Dynamics of Sea Ice

J. M. N. T. Gray and L. W. Morland

Phil. Trans. R. Soc. Lond. A 1994 **347**, 219-290
doi: 10.1098/rsta.1994.0045

A two-dimensional model for the dynamics of sea ice†

By J. M. N. T. Gray and L. W. Morland
School of Mathematics, University of East Anglia, Norwich NR4 7TJ, U.K.

Contents

This paper develops a systematic analysis of a sea ice pack viewed as a thin layer of coherent ice floes and open water regions at the ocean surface. The pack is driven by wind stress and Coriolis force, with responsive water drag on the base of the floes. Integration of the mass and momentum balances through the layer thickness result in a two-dimensional theory for the interface between ocean and atmosphere. The theory is presented for a plane horizontal interface, but the

† This paper was produced from the authors' disk by using the TEX typesetting system.

Phil. Trans. R. Soc. Lond. A (1994) **347**, 219–290
Printed in Great Britain

construction is readily extended to a non-planar interface. An interacting continua framework is adopted to describe the layer mixture of ice and water, which introduces the layer thickness h and ice area fraction A as smoothly varying functions of the plane coordinate and time, on a pack length scale and weather system timescale. It is shown how an evolution equation for A which ignores ridging can lead to the area fraction exceeding unity in maintained converging flow, which is physically invalid. This is a feature and weakness of current models, and is eliminated by artificial cut-off in numerical treatments. Here we formulate a description of the ridging process which redistributes smoothly the excess horizontal ice flux into increasing thickness of a ridging zone of area fraction A_r, and a simple postulate for the vertical ridging flux yields an evolution equation for A which shows how A can approach unity asymptotically, but not exceed unity, in a maintained converging flow. This is a significant feature of the new model, and eliminates a serious physical and numerical flaw in existing models.

The horizontal momentum balance involves the gradients of the extra stress integrated through the layer thickness, extra to the integrated water pressure over the depth of a local floe edge below sea level. These extra stresses are zero in diverging flow and arise as a result of interactions between floes during converging flow. It is shown precisely how a mean stress in a floe is determined by such edge tractions, and in turn provides an interpretation of the local extra stress in the pack. The interpretation introduces the further model function $f(A)$ which defines the fraction of ice–ice contact length over the boundary of a floe, describing an increase of the contact fraction as A increases. Model interaction mechanisms then suggest a qualitative law for the pack stress in terms of relative motions of the floes which define the pack-scale strain rates. A simple viscous law is presented for illustration, but it is shown that even this simple model can reflect a conventional motion of a failure criterion on the stresses in a ridging zone where the convergence greatly exceeds a threshold value. We have therefore defined precisely the two-dimensional ice pack stress arising in the momentum balance, and determined its relation to the contact forces between adjacent floes.

The foregoing analyses hinge on the introduction of dimensionless variables and coordinate scalings which reflect the orders of magnitude of the many physical variables and their gradients in both individual floe and ice pack motions. A variety of small dimensionless parameters arise, which allows the derivation of leading-order equations defining a reduced model which describes the major balances in the motion.

The distinct equations for diverging and converging flow regions indicates the existence of moving boundaries (in the two-dimensional pack domain) in the flow, satisfying appropriate matching conditions to be determined as part of the complete evolution. This feature appears to have been ignored in previous treatments. Here we illustrate the evolution of a moving boundary by constructing an exact solution to a one-dimensional pack motion which describes onshore drift due to increasing, then decreasing, wind stress. During the second phase a region of diverging flow expands from the free edge. The solution demonstrates the influence of various parameters, but, importantly, will provide a test solution for numerical algorithms which must be constructed to determine more complex one and two-dimensional motions.

PHILOSOPHICAL TRANSACTIONS OF THE ROYAL SOCIETY A MATHEMATICAL, PHYSICAL & ENGINEERING SCIENCES

1. Introduction

(*a*) *Sea ice*

Sea ice covers approximately 7% of the oceans throughout the year, covering from 8×10^6 to 15×10^6 km^2 between winter and summer in Arctic waters, and from 3×10^6 to 15×10^6 km^2 between summer and winter in Antarctic waters, with a six month phase difference between Arctic and Antarctic seasons. The presence of extensive sea ice has significant effect on the dynamics and thermodynamics of both atmosphere and ocean, and the motions and thermal responses of all three are strongly coupled. Considerable attention has been given, and continues, to the physical and numerical modelling of processes in the atmosphere and oceans, and the coupling in the absence of ice, but the inclusion of sea ice effects are far less advanced.

As surface cooling occurs and the sea water approaches its freezing point, approximately 271.4 K (−1.8 °C) at a salinity of 35 parts per thousand (p.p.t.), its density increases and there is a convective overturning of the mixed layer above the pycnocline. Ice does not form on the surface until the entire mixed layer approaches the freezing point. As the ice forms some of the salt is trapped in brine pockets within the crystal lattice, but the rest is rejected to increase the salinity of the near surface water. Such adjustments of the temperature and salinity distributions strongly influence the ocean dynamics. The initial skim of frazil ice continues to thicken due to thermodynamic growth into a smooth sheet in calm water, or may be fractured into ice pancakes by wave action, which interact and raft over each other to freeze again into a single, less smooth, ice floe. Floes can reach 3 m in thickness by thermodynamic growth in the central Arctic (Maykut & Untersteiner 1971), and become thicker off the northern coast of Greenland by mechanical deformation (ridging). Floe diameters range from tens of metres in the marginal ice zone (MIZ), to several kilometres in the interior. An ice pack is a mosaic of many floes separated by leads of open water and frazil ice, which may extend for 1000 km. The system is driven by the wind and ocean currents, reaching velocities of 10^{-1} m s^{-1} (8.64 km per day).

The relative motions between floes due to the non-homogeneous wind forcing and the different inertias causes opening and closing of the leads, and interactions between the floes. Newly open water in expanding leads can freeze rapidly and the latent heat is responsible for substantial heat exchange with the ocean. In addition, the much greater albedo of ice compared to that of water results in much greater reflection of solar radiation, creating a colder atmosphere and further freezing. The strong katabatic winds blowing off the Antarctic coast drive the ice offshore, creating coastal polynyas, large enclosed leads (Gordon & Comiso 1988), in which new ice is generated in vast quantities. The ice is easily blown into warmer regions in which freezing would not necessarily occur, resulting in a more northerly ice margin in Antarctica and a greater volume of ice than would otherwise be expected. The Antarctic ice pack then is largely composed of first year ice approximately 1 m thick (Wadhams 1987). In the enclosed Arctic basin there is considerable convergence of the floes, resulting in ridges with ice pushed up to form a sail on the surface, and down to form a keel on the base, which can extend to 15 m or more below the water surface. With 50% of the Arctic ice volume in ridges (Wadhams 1981; Bourke & Garret 1987), the mean thickness is approximately 5 m, and comprises mainly multi-year ice.

PHILOSOPHICAL TRANSACTIONS OF THE ROYAL SOCIETY A MATHEMATICAL, PHYSICAL & ENGINEERING SCIENCES

While the thermal and salinity effects of ice in the ocean are essentially due to the thermodynamics of freezing and melting, the distribution of ice over the ocean surface at any time is governed by the coupled atmosphere, ice and ocean dynamics. The most simple description will comprise a prescribed pressure and tangential wind stress distribution over the ice/ocean surface, and prescribed sensible heat and radiation fluxes, all varying in time, essentially uncoupling the atmosphere motion. At the base of an ice floe there is the water pressure and a tangential drag prescribed in terms of relative tangential velocity, a freezing point condition, and a heat flux. Individual ice floes will move essentially as rigid bodies, but the interaction of converging flows give rise to large-scale in-plane stress gradients which influence the non-uniform large-scale ice dynamics. A model must therefore, in some well-defined sense, reflect the interaction mechanisms of converging ice floes, including the ridging process, and the thermal processes of freezing and melting at the surface and base of floes, and in leads, to determine the evolution of the ice thickness and concentration.

(*b*) *Previous modelling*

The first descriptions of an individual ice floe drift were based on different balances between wind stress, water drag and Coriolis force (Nansen 1902; Rossby & Montgomery 1935; Schulekin 1938), while the presence, but not the motion, of surrounding floes was parametrized with an additional frictional force by Sverdrup (1928). Nikiforov (1957) introduced the representation of the ice pack by a collection of rigid floating bodies defined on the large-scale by the area fraction of total area covered (concentration), which changes due to the divergence of the floe drift and to the advective process, but ignored the thermodynamic influence. Ruzin (1959) and Reed & Campbell (1960) treated the ice as a thin film of viscous liquid, introducing the concept of a large-scale ice rheology to describe the floe interaction mechanisms. The thermodynamic processes governing thickness variation were described in a one-dimensional model by Maykut & Untersteiner (1971), Maykut (1976) and Semtner (1976), ignoring the dynamics. An ice floe collision model for sparse ice distribution in an MIZ has been developed by Shen *et al.* (1986, 1987), based on fluid–solid constitutive relations (Shen & Ackermann 1982, 1984), but is not applicable to the extensive ice cover.

A major thrust towards a large-scale description of the dynamics of an ice pack was made by the Arctic Ice Dynamics Joint Experiment (AIDJEX) team at the University of Washington between 1970 and 1978, which is reported in 40 AIDJEX Bulletins and a final AIDJEX Symposium Proceedings (Pritchard 1980*a*). This substantial pioneering research programme drew together empirical observation, theoretical modelling and numerical investigations, to provide the basis of sea ice applications over the last decade. At the outset AIDJEX recognized that a tractable large-scale model must view the ice pack as a highly fractured two-dimensional continuum acting as an interface between the ocean and atmosphere, with the in-plane stress-deformation relations on the large-scale the consequence of interactions between individual floes, though it was realized that individual floes with 10 km diameter were not small elements on the scale of a 100 km pack extent (Rothrock 1970; Solomon 1970). A two-dimensional rheology for the ice pack as an anisotropic viscous fluid (Campbell & Rasmussen 1970*a*), was noted by Glen (1970) to violate frame-indifference, so modified (Campbell & Rasmussen 1970*b*) to a nonlinearly viscous (isotropic) fluid with large viscosity in conver-

gence and low viscosity in divergence. Subsequent viscous models (Timokhov 1971; Yegerov 1971) adopted constant viscosity. Pai & Li (1971) recognized that the ice pack should be viewed as a two-constituent mixture, ice and water, and later (Pai & Li 1975) derived an ice concentration relation from mass balance conservation, but an incorrect momentum equation for the ice. This approach was not pursued. Nye (1973) interpreted the directly postulated two-dimensional stress tensor in terms of the depth integrated stresses, but a derivation and justification of the two-dimensional conservation laws and constitutive relations from the fundamental three-dimensional equations has not been presented until now. Nye & Thomas (1974) demonstrated by satellite photographs that the ice pack deformation on the large-scale was essentially due to the relative motion between rigid floes, supporting this continuum mixture model approach.

On scales of 10 km ice packs contain ice of many thicknesses, and the notion of a thickness distribution was introduced (Thorndike & Maykut 1973; Thorndike *et al.* 1975), with the bulk ice properties determined by area fraction weightings of properties associated with each thickness. For practical application only a few discrete intervals of thickness were used. However, these property relations were never clear, nor were the effects of ridging on the thickness distribution. A ridging model based on Coon's (1972) mechanism of breaking in bending was developed by Parmerter & Coon (1972, 1973), calculating a horizontal stress required to perform the work expended to produce the potential energy in the ridge, depending on the ridge thickness. They deduced that this rate-independent ridging mechanism leads to a limiting value for the sail and keel thicknesses, after which continued fracturing leads to a hummock field. The strong visual similarity between pack ice deformations from satellite photographs and the behaviour of granular materials (soils), reinforced by the work dissipation in ridge formations, led to the major AIDJEX proposal of a plasticity model for the two-dimensional ice pack rheology (Coon *et al.* 1974). Elementary one-dimensional numerical simulations were constructed by Pritchard & Colony (1974) and Pritchard & Schwaegler (1975), and two-dimensional algorithms were constructed by Colony & Pritchard (1975) and applied to simulate Arctic and Beaufort sea ice conditions within available computer capacity (Colony 1975; Pritchard *et al.* 1976; Pritchard 1980*b*). This outline highlights the central thread of the AIDJEX developments.

Following the disbanding of AIDJEX, the thrust in sea ice dynamics research moved to Hibler at the Cold Regions Research and Engineering Laboratories in Hanover, New Hampshire. Attention was focused on a precise two-layer model of thick and thin ice with the area fraction of thick ice defining the ice concentration (Hibler 1979, 1980*a–d*, 1984, 1985*a*, *b*, 1986; Hibler *et al.* 1983; Leppäranta & Hibler 1985). A viscous model was applied by Hibler & Tucker (1979), but the main theme has been the construction of a viscoplastic model (Hibler 1979), with Hibler's (1980*b*) numerical algorithm receiving widespread use (Hibler & Ackley 1983; Walsh *et al.* 1985; Preller 1985; Preller & Posey 1989*a*, *b*; Lemke *et al.* 1990; Stössel *et al.* 1990; Preller *et al.* 1990). Owens & Lemke (1990) further introduced a snow layer and allowed the viscoplastic stresses to operate only when the ice thickness exceeded a specific value. Hibler's generalization of the AIDJEX plasticity model has moved away from direct association with underlying floe interaction mechanisms. It is, furthermore, numerically complex, and requires extensive computation for an uncoupled ice dynamics problem, so that investigation of coupled ocean-ice dynamics (Hibler & Bryan 1987) becomes very

PHILOSOPHICAL TRANSACTIONS OF THE ROYAL SOCIETY A MATHEMATICAL, PHYSICAL & ENGINEERING SCIENCES

large-scale computation. There has also been no proper distinction between converging and diverging flows. The yield criterion is only constrained to lie outside the stress region of tensile principal stresses without reference to the flow field, which allows a viscoplastic stress contribution to apply in a region of diverging flow. Strictly, the ice pack stress derives from floe interactions that arise during converging flow. This artificial stress in diverging flow results in an unstable system of governing equations, which was demonstrated by Gray (1992) for a simple one-dimensional flow configuration. Furthermore, for numerical expediency the model equations have been applied over prescribed fixed domains to avoid the more difficult moving boundary problem. In reality the ice pack domain is varying and appropriate boundary conditions are required on the moving edge. Additionally, interior regions of open water may open, also bounded by a moving margin.

Plasticity difficulties have been avoided by the use of cavitating fluid models (Nikiforov *et al.* 1967; Parkinson & Washington 1979; Flato & Hibler 1989, 1990, 1992). These are essentially free drift models, but at each time step the ice velocity in converging zones is corrected, in an *ad hoc* fashion, to restrict the build up of ice thickness and concentration. The algorithms do not calculate actual solutions of the differential equations over the ice pack domain, but are, of course, numerically much simpler than plasticity models, and so more tractable to ocean coupling. There remains the question of how well, if at all, they reflect the floe interactions in any real ice pack.

(*c*) *Present theory*

Addressing the concern in numerical oceanographic modelling for a tractable model to incorporate the effects of a sea ice interface with the atmosphere, it was immediately apparent that a more rigorous theory of an ice–water layer is required to properly interpret the two-dimensional model and recognize both the rational approximations and the more tenuous assumptions necessary for such a reduction. This is accomplished by integrating the full three-dimensional mass and momentum equations through the layer thickness and exploiting the small thickness to span ratio, together with the assumption of a smooth variation in thickness (on the large scale) with very small gradient. A proper choice of dimensionless, normalized variables based on geometry and the dominant physical forcing variables, and a coordinate/velocity scaling using the small parameter defined by the aspect ratio, determines a reduced two-dimensional model governed by the leading-order equations. This is the analogue of successful reduced model derivations for the flow of nonlinearly viscous grounded ice sheets by Fowler (1979), Morland & Johnson (1980, 1982), Hutter (1982), Morland (1984), and for floating ice shelves by Morland & Shoemaker (1982) and Morland (1987).

The reduction is first carried out for a single coherent ice floe – the fundamental element of an ice pack – driven by a surface wind traction with responsive ocean drag at the base, and subject to surface and base freezing/melting with related heat flux and temperature conditions. Here the integrated edge stresses are given by the integrated water pressure on open sections, and by interaction forces on sections in contact with other floes. The ice pack is now viewed as a layer of smoothly varying thickness $h(x_\alpha, t)$ comprising the coherent ice floes and air/water/thin-ice in the open leads, where t denotes time and x_α $(\alpha = 1, 2)$ are coordinates in the surface. For simplicity the theory is presented for a plane surface, but generalization to a non-planar surface to include the effects of curvature

PHILOSOPHICAL TRANSACTIONS OF THE ROYAL SOCIETY A MATHEMATICAL, PHYSICAL & ENGINEERING SCIENCES

and geographical location will follow the same procedures. The smooth extension of the floe ice base across the leads represents the upper boundary of the ocean, and while the in-plane motion of the layer water in the leads is described by the in-plane pack motions, there is also a basal flux into, or out of, the ocean domain, which is determined by the full mass conservation equation. The ice floe concentration is defined by an area fraction $A(x_\alpha, t)$ so that $1 - A$ is the area fraction of open water. The necessary assumption that $A(x_\alpha, t)$ is a smoothly varying function is physically apt only on length scales much greater than floe diameters, and is therefore invalid where the coherent floes are very large, but it is hoped that mean effects over large scales will still be reasonable. To overcome this weakness it would be necessary to identify and track ice floes, which is considered beyond the scope of a tractable model. Subsequently, the area fraction A is explicitly separated into area fractions A_r of ice available for ridging and A_c of coherent ice, with associated thickness distributions h_r and h_c respectively. The ice pack motion is defined by a single in-plane smoothly varying velocity field $\boldsymbol{v}(x_\alpha, t)$, supposing that the in-plane open water velocity field is essentially determined by the adjacent ice floes. The smooth variation in $\boldsymbol{v}$ describes the large-scale relative motions of the individual ice floes, which is again suspect when floes are large. A mixture (interacting continua) theory for the three constituents, ridging ice, coherent ice and open water, with common in-plane velocity $\boldsymbol{v}$ is developed, and again reduced to a two-dimensional theory by integration through the layer and exploiting the small aspect ratio and small in-plane gradients. The evolution of different thicknesses and area fractions are coupled, determined by the integrated individual constituent mass balances incorporating the surface and base energy fluxes into latent heats of freezing and melting, which are more explicit, and complete, than previous formulations of evolution equations. This development is drawn from earlier mixture theory formulations Morland (1972, 1978, 1992) with specific applications to melting and freezing in snowpacks (Kelly *et al.* 1990).

The resulting two-dimensional theory for the ice pack involves $\boldsymbol{v}$, h, h_r, h_c, A, A_r ($A_c = A - A_r$), together with a two-dimensional extra stress tensor $\boldsymbol{N}^e$. This is the stress extra to the local water pressure, integrated through the layer. It is generated by compressive and frictional contacts between converging ice floes. As an alternative to direct postulates for the in-plane rheology, it is shown how in a mean sense, the ice stress can be related to the large-scale deformation in terms of contact mechanisms between converging floes. A two-dimensional mean stress theorem determines the mean of each stress component over a floe domain of arbitrary shape (an element of the mixture theory) in terms of the distribution of tractions around its edge. In turn, postulated laws for the ice–ice contact forces in terms of the relative (rigid) motions and displacements interpreted in terms of strain rates or strains associated with the velocity field $\boldsymbol{v}(x_\alpha, t)$, result in a constitutive law for the mean local ice stress in terms of the velocity field $\boldsymbol{v}(x_\alpha, t)$, the assumed floe geometry and dimensions, and the thickness distribution. The total extra stress $\boldsymbol{N}^e$ is now related to the mean integrated ice stress by incorporating the area weighting A and a contact length factor $f(A)$ which distinguishes ice–ice and ice–water contact length around the floe. A first theory assumes that the contact fraction is simply a nonlinear function of the ice concentration A, zero when $A = 0$ and approaching unity as $A \to 1$. Comparisons and distinctions are drawn with previous theories.

PHILOSOPHICAL TRANSACTIONS OF THE ROYAL SOCIETY A MATHEMATICAL, PHYSICAL & ENGINEERING SCIENCES

There are two physical requirements for a valid evolution equation for the ice concentration A. Firstly, it is necessarily positive everywhere since the mixture equations demand the presence of some ice in each mixture element. It is shown that in a constant velocity divergence, A approaches zero asymptotically, and does not become negative, except with large maintained melting. Secondly, in a converging flow, A must not exceed unity. The conventional evolution equation leads to A increasing indefinitely in a flow with constant velocity convergence (negative divergence), so in general allows A to exceed unity. This required Hibler (1979) to artificially correct the ice concentration in the numerical scheme by resetting $A \equiv 1$ whenever A exceeded unity, and adjusting the thickness h to conserve the ice column volume Ah. Here a ridging mechanism is introduced in which A is partitioned into area fraction A_c of coherent ice, and an area fraction A_r of ice available for ridging and redistribution over the coherent ice when the floes converge. The total ice concentration A evolution and thickness h evolution now involve A_r, a ridging ice thickness h_r and the vertical ridging velocity, but in a combination which defines the ratio α of the vertical volume flux to the horizontal flux. In a diverging flow $\alpha \equiv 0$, and in a converging flow we assume a simple trial model in which α is a monotonically increasing function of A, zero at $A = 0$ and possibly for A less than some critical value, and approaching unity as A approaches unity, to reflect the conceived ridging process. It then follows that in continually converging flow A approaches unity asymptotically, and does not exceed unity, and mass (volume) is preserved smoothly by redistribution of thickness.

In summary, the present analysis provides a systematic reduction of the three-dimensional equations for a mixture of ice and water in a smoothly varying layer at the ocean surface, to a two-dimensional theory. It draws out the approximations and assumptions, and provides precise definitions of the physical variables used. The necessary concept of ice–ice contact length fraction is introduced, and self consistent ice area fraction and thickness evolution equations are derived to describe a smooth ridging process in converging flow. The in-plane stress in converging flow is related to the large-scale strain or strain rate through ice–ice contact mechanisms, as an alternative to directly postulated rheology, which provides a framework to explore the effects of different contact mechanisms. The model can be coupled to the ocean dynamics through a prescribed water drag relation at the ice base together with the thermal conditions and resulting phase changes.

A summary of the two-dimensional model equations is presented in § 4. The new features are noted, and a comparison is made with the model used in current numerical applications which shows also the differences in the basic physical balances. In § 5 a complete analytic solution is constructed for a one-dimensional flow problem, ignoring the lateral Coriolis effect. It describes a pack driven by wind stress against a rigid coast with all regions in convergence, then reduction and reversal of the wind stress so that a diverging region expands monotonically from the free rear edge to the coast. No thermal effects are included. The construction is an inverse method, starting from a continuously changing deformation field which reflects the above features, and determining the area fraction and thickness evolution in both phases of the motion, in both converging and diverging regions in the second phase. The necessary wind stress and drag resultant can then be determined for any adopted constitutive law for the pack stress. Illustra-

PHILOSOPHICAL TRANSACTIONS OF THE ROYAL SOCIETY A MATHEMATICAL, PHYSICAL & ENGINEERING SCIENCES

tions are presented for a linearly viscous law, for both linear and quadratic basal drag relations. Such an analytic solution provides a valuable test case for a direct numerical treatment which also has to determine the moving interface between converging and diverging regions, with different equation structures on the two sides. This is the first analytic construction for a nonlinear model incorporating the converging and diverging dynamics, and a ridging process.

2. Single ice floe

(*a*) *Floe geometry and coordinate system*

An ice floe is represented as a disk of solid coherent ice floating at the surface of the ocean, with smoothly varying thickness, in space and in time t, and with a small thickness to diameter ratio. On the scale of the diameter, its edge will be considered everywhere vertical so that the horizontal cross-section is uniform, defined by $S(t)$ with a bounding contour $C(t)$ which is supposed smooth except possibly at a finite number of vertices. Roughly 90% of the ice volume, hence thickness, is submerged below the water surface.

Let Ox_i $(i = 1, 2, 3)$ be a rectangular cartesian coordinate system fixed with respect to the rotating Earth and hence defining a non-inertial frame. The origin O is at a fixed geographical location and on the ocean surface, and Ox_3 is the vertically upward direction normal to the geopotential mean sea surface, with Ox_1x_2 the local horizontal tangent plane, where Ox_1 points to the east and Ox_2 points to the north. For simplicity the theory for the entire ice pack will be presented as if the mean sea surface over its domain lies in the same tangent plane, neglecting the Earth's surface curvature and the effects of varying centrifugal force with location on the surface. Greek subscripts α, β $(= 1, 2)$ will denote the in-plane coordinates x_1, x_2 only. The unit coordinate base vectors are denoted by $\boldsymbol{i}$, $\boldsymbol{j}$, $\boldsymbol{k}$.

The dynamic water surface is defined by

$$x_3 = z_{\mathrm{w}}(x_\alpha, t), \tag{2 a 1}$$

and the floe base and surface are defined by

$$x_3 = z_{\mathrm{b}}(x_\alpha, t), \quad x_3 = z_{\mathrm{s}}(x_\alpha, t), \tag{2 a 2}$$

respectively, so that the ice thickness $h(x_\alpha, t)$ and the ice draught (depth below sea level) $h_{\mathrm{w}}(x_\alpha, t)$ are given respectively by

$$h = z_{\mathrm{s}} - z_{\mathrm{b}}, \quad h_{\mathrm{w}} = z_{\mathrm{w}} - z_{\mathrm{b}}. \tag{2 a 3}$$

Figure 1 illustrates a horizontal plan view and figure 2 illustrates a vertical section $x_2 = \text{const.}$ (typical of any vertical section) of an ice floe bounded by a contour $C(t)$. The unit outward normal to the edge of $C(t)$ is denoted by $\boldsymbol{n}^{\mathrm{c}}$, to the surface by $\boldsymbol{n}^{\mathrm{s}}$, and to the base by $\boldsymbol{n}^{\mathrm{b}}$. The normal $\boldsymbol{n}^{\mathrm{c}}$ is horizontal and $\boldsymbol{s}^{\mathrm{c}}$ is the horizontal tangent vector such that $\boldsymbol{n}^{\mathrm{c}}$, $\boldsymbol{s}^{\mathrm{c}}$, $\boldsymbol{k}$ form a right-handed triad; thus

$$\boldsymbol{n}^{\mathrm{c}} = (n_1^{\mathrm{c}}, n_2^{\mathrm{c}}, 0), \quad \boldsymbol{s}^{\mathrm{c}} = (-n_2^{\mathrm{c}}, n_1^{\mathrm{c}}, 0). \tag{2 a 4}$$

The base and surface normals are given by

$$\boldsymbol{n}^{\mathrm{b}} = \frac{1}{\Delta_{\mathrm{b}}}\left(\frac{\partial z_{\mathrm{b}}}{\partial x_1}, \frac{\partial z_{\mathrm{b}}}{\partial x_2}, -1\right), \quad \boldsymbol{n}^{\mathrm{s}} = \frac{1}{\Delta_{\mathrm{s}}}\left(-\frac{\partial z_{\mathrm{s}}}{\partial x_1}, -\frac{\partial z_{\mathrm{s}}}{\partial x_2}, 1\right), \tag{2 a 5}$$

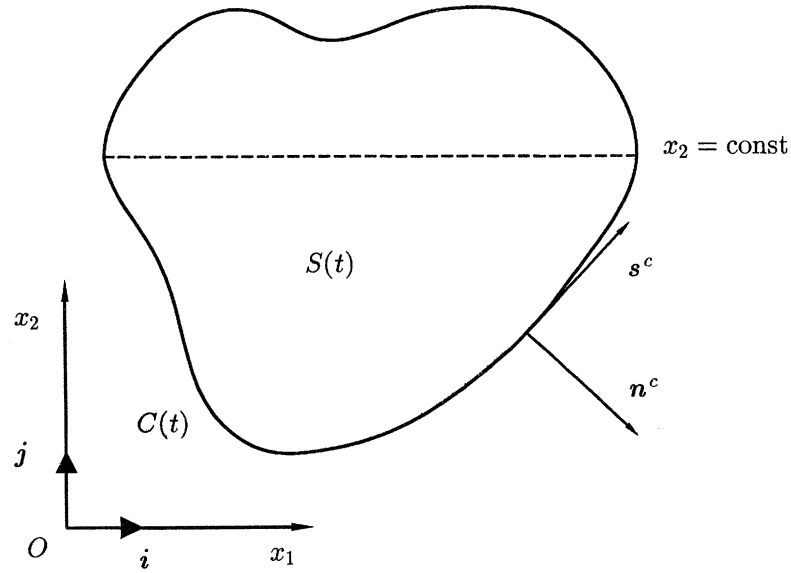

Figure 1. Horizontal plan view of a sea ice floe.

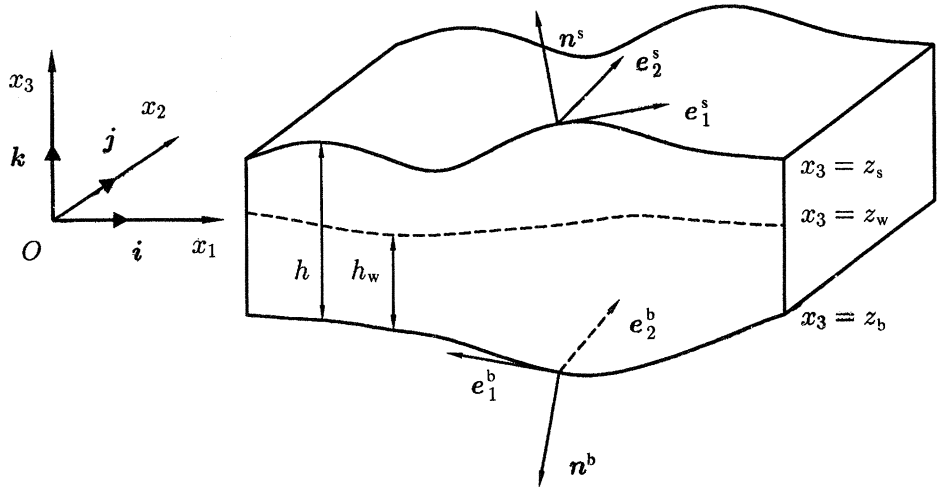

Figure 2. Vertical section through a sea ice floe.

where

$$\Delta_b = \left\{1 + \left(\frac{\partial z_b}{\partial x_1}\right)^2 + \left(\frac{\partial z_b}{\partial x_2}\right)\right\}^{1/2}, \quad \Delta_s = \left\{1 + \left(\frac{\partial z_s}{\partial x_1}\right)^2 + \left(\frac{\partial z_s}{\partial x_2}\right)\right\}^{1/2}. \quad (2\,a\,6)$$

Associated tangent vectors forming right-handed orthonormal triads $\boldsymbol{e}_1^b$, $\boldsymbol{e}_2^b$, $\boldsymbol{n}^b$, and $\boldsymbol{e}_1^s$, $\boldsymbol{e}_2^s$, $\boldsymbol{n}^s$, for base and surface respectively, with $\boldsymbol{e}_1^b$ and $\boldsymbol{e}_1^s$ lying in $x_2 =$ const. and $\boldsymbol{e}_2^b$, $\boldsymbol{e}_2^s$ having positive components in the x_2 direction, are given for both the surface and base by

$$\left.\begin{aligned} \boldsymbol{e}_1 &= (n_1^2 + n_3^2)^{-1/2}(n_3, 0, -n_1), \\ \boldsymbol{e}_2 &= (n_1^2 + n_3^2)^{-1/2}(-n_1 n_2, n_1^2 + n_3^2, -n_3 n_2). \end{aligned}\right\} \quad (2\,a\,7)$$

(*b*) *Physical balances and boundary conditions*

The coherent ice is treated as an incompressible material of constant uniform density $\rho = 918\ \mathrm{kg\,m^{-3}}$. Let $\boldsymbol{v}(x_i, t)$ denote the particle velocity field, which will later be viewed as the sum of a rigid body translation and rotation about a vertical axis and a distortional velocity field. The particle acceleration relative to the Earth is given by

$$a_i = \dot{v}_i = \frac{\mathrm{D}v_i}{\mathrm{D}t} = \frac{\partial v_i}{\partial t} + v_j \frac{\partial v_i}{\partial x_j}, \tag{2 b 1}$$

where the superposed dot denotes a material time derivative. The summation convention is used throughout, over 1, 2 and 3 for a repeated roman suffix and over 1 and 2 for a repeated greek suffix. We suppose that the Earth is rotating with constant angular velocity $\boldsymbol{\Omega}$ about its North–South axis with respect to an inertial frame, so that the particle acceleration in the inertial frame is

$$a_i^{\mathrm{N}} = a_i + a_i^{\mathrm{c}}, \tag{2 b 2}$$

where $\boldsymbol{a}^{\mathrm{c}}$ is the Coriolis acceleration given by

$$\boldsymbol{a}^{\mathrm{c}} = 2\boldsymbol{\Omega} \wedge \boldsymbol{v}. \tag{2 b 3}$$

In terms of the rotating coordinate axes the angular velocity is given by

$$\boldsymbol{\Omega} = \Omega(\sin\phi \boldsymbol{k} + \cos\phi \boldsymbol{j}) \tag{2 b 4}$$

at latitude ϕ, with magnitude

$$\Omega = 0.729 \times 10^{-4}\ \mathrm{rad\ s^{-1}}. \tag{2 b 5}$$

The vertical and gravity definitions also depend on $\boldsymbol{\Omega}$, and hence on ϕ, and on the position $\boldsymbol{x}$ relative to the chosen origin, through

$$-g\boldsymbol{k} = \boldsymbol{g}^* - \boldsymbol{\Omega} \wedge (\boldsymbol{\Omega} \wedge \boldsymbol{x}), \tag{2 b 6}$$

where $\boldsymbol{g}^*$ is the gravity due to the Earth's mass. While the vertical component of $\boldsymbol{\Omega} \wedge (\boldsymbol{\Omega} \wedge \boldsymbol{x})$ is negligible compared to g, its horizontal component is of order $10^{-3}\ \mathrm{m\,s^{-2}}$ at distances of 10^5 m, and so is comparable with the term $\boldsymbol{\Omega} \wedge \boldsymbol{v}$ when $|\boldsymbol{v}| \sim 10^{-1}\ \mathrm{m\ s^{-1}}$, the typical maximum velocity. This possible influence of location is customarily incorporated in the definition of $\boldsymbol{g}$, which is commonly still assumed to be constant. We also suppose $\boldsymbol{g}$ is constant and do not take proper account of the non-planar surface. Since the ice pack motion is essentially horizontal and confined to the plane $x_3 = 0$, the Coriolis acceleration components are

$$a_1^{\mathrm{c}} = -2\Omega \sin\phi\, v_2, \quad a_2^{\mathrm{c}} = 2\Omega \sin\phi\, v_1, \quad a_3^{\mathrm{c}} = -2\Omega \cos\phi\, v_1. \tag{2 b 7}$$

Since a_3^{c} is negligible in comparison to g, the Coriolis effect is essentially

$$-a_\alpha^{\mathrm{c}} = 2\Omega \sin\phi \varepsilon_{\alpha\beta 3} v_\beta = f_{\mathrm{c}} \varepsilon_{\alpha\beta 3} v_\beta, \quad a_3^{\mathrm{c}} = 0, \tag{2 b 8}$$

where ε_{ijk} are components of the alternating tensor. The Coriolis parameter

$$f_{\mathrm{c}} = 2\Omega \sin\phi \tag{2 b 9}$$

ranges from zero at the equator to $\pm\ 1.46\times\ 10^{-4}$ rad s^{-1} at the poles.

The Cauchy stress tensor $\boldsymbol{\sigma}^{\mathrm{I}}(x_i, t)$ determines the traction $\boldsymbol{t}^{\mathrm{I}}$ per unit area on

a section with unit outward normal $\boldsymbol{n}$ by

$$\boldsymbol{t}^{\mathrm{I}} = \boldsymbol{\sigma}^{\mathrm{I}}\boldsymbol{n}, \quad t_i^{\mathrm{I}} = \sigma_{ij}^{\mathrm{I}} n_j, \tag{2 b 10}$$

and the tangential traction is denoted by $\boldsymbol{t}_{\mathrm{s}}^{\mathrm{I}}$, the normal traction by $t_{\mathrm{n}}^{\mathrm{I}}$. The temperature field in the ice is denoted by $\Theta^{\mathrm{I}}(x_i, t)$, and the ice is supposed to have constant thermal conductivity $K^{\mathrm{I}} = 2.2\ \mathrm{N\ K^{-1}\ s^{-1}}$ and constant specific heat $C^{\mathrm{I}} = 2 \times 10^3\ \mathrm{J\ kg^{-1}\ K^{-1}}$.

Mass conservation is simply the incompressibility condition

$$\rho = \text{const.}, \quad \operatorname{div} \boldsymbol{v} = \frac{\partial v_k}{\partial x_k} = 0. \tag{2 b 11}$$

The linear momentum balance implies that

$$\frac{\partial \sigma_{\alpha j}^{\mathrm{I}}}{\partial x_j} - \rho a_\alpha^{\mathrm{c}} = \rho \dot{v}_\alpha \quad (\alpha = 1, 2), \tag{2 b 12}$$

$$\frac{\partial \sigma_{3j}^{\mathrm{I}}}{\partial x_j} - \rho g = 0, \tag{2 b 13}$$

where g is the constant gravity acceleration, and vertical particle acceleration is negligible compared to $g = 9.81\ \mathrm{m\ s^{-2}}$. For an incompressible material and negligible stress working at the low shear stress and strain rate occurring here, energy conservation is given by the thermal balance,

$$\rho C^{\mathrm{I}} \dot{\Theta}^{\mathrm{I}} - K^{\mathrm{I}} \operatorname{div} \operatorname{grad} \Theta^{\mathrm{I}} - r^{\mathrm{I}} = 0, \tag{2 b 14}$$

where r^{I} is the energy deposit per unit volume per unit time due to radiation.

The upper ice surface is subject to atmospheric pressure and tangential tractions $\boldsymbol{\tau}^{\mathrm{s}}$ induced by wind action – the wind stress. Variation of atmospheric pressure over a single floe is not significant, so atmospheric pressure at the surface is assumed constant and defines the zero stress level. With surface melting or freezing , the surface is non-material and there are discontinuities of particle velocity and of traction. However, these discontinuities are extremely small (Hutter 1983), and the surface traction is therefore

$$x_3 = z_{\mathrm{s}}: \quad \boldsymbol{t}_{\mathrm{s}}^{\mathrm{s}} = \boldsymbol{\tau}^{\mathrm{s}}, \quad t_{\mathrm{n}}^{\mathrm{s}} = \boldsymbol{t}^{\mathrm{s}} \cdot \boldsymbol{n} = 0, \tag{2 b 15}$$

which is the major driving force for the ice floe motion. On the base the normal traction is essentially the water pressure p^{W} and the tangential traction is a drag τ^{b} related to the relative motion between the ice and water, continuous with the tangential viscous stresses in the water. We make the common approximation that the bulk viscosity of water is negligible, so that the normal viscous stress is negligible and the pressure is essentially hydrostatic. Thus the basal traction is

$$x_3 = z_{\mathrm{b}}: \quad \boldsymbol{t}_{\mathrm{s}}^{\mathrm{b}} = \boldsymbol{\tau}^{\mathrm{b}}, \quad t_{\mathrm{n}}^{\mathrm{b}} = \boldsymbol{t}^{\mathrm{b}} \cdot \boldsymbol{n} = -p^{\mathrm{W}}, \tag{2 b 16}$$

where

$$x_3 < z_{\mathrm{w}}: \quad p^{\mathrm{W}} = \rho_{\mathrm{w}} g (z_{\mathrm{w}} - x_3), \quad p^{\mathrm{W}}|_{z_{\mathrm{b}}} = \rho_{\mathrm{w}} g h_{\mathrm{w}}, \tag{2 b 17}$$

and the constant water density near the ocean surface is $\rho_{\mathrm{w}} = 10^3\ \mathrm{kg\ m^{-3}}$. These impose conditions on the surface and base values of the ice stress tensor. On the surface, using (2 b 10), and (2 a 7) to determine the components of $\boldsymbol{\tau}^{\mathrm{s}}$,

$$x_3 = z_{\mathrm{s}}: \quad \boldsymbol{n}^{\mathrm{s}} = (n_1^{\mathrm{s}}, n_2^{\mathrm{s}}, n_3^{\mathrm{s}}), \quad \sigma_{ij}^{\mathrm{I}} n_j^{\mathrm{s}} = \tau_i^{\mathrm{s}}, \tag{2 b 18}$$

and similarly on the base

$$x_3 = z_\mathrm{b}: \quad \boldsymbol{n}^\mathrm{b} = (n_1^\mathrm{b}, n_2^\mathrm{b}, n_3^\mathrm{b}), \quad \sigma_{ij}^\mathrm{I} n_j^\mathrm{b} = \tau_i^\mathrm{b} - \rho_\mathrm{w} g h_\mathrm{w} n_i^\mathrm{b}, \tag{2 b 19}$$

where the components of $\boldsymbol{n}^\mathrm{s}$ and $\boldsymbol{n}^\mathrm{b}$ are given by (2 *a* 5).

On the vertical edge contour C there will be sections in contact with water – all of C for an isolated floe – and sections in contact with other floes. Interactions between floes are a major feature of ice pack dynamics, and are treated in a later section. On the sections of contour in contact with water only, C_w say, the edge traction $\boldsymbol{t}^C$ is simply the hydrostatic water pressure acting over the submerged part

$$x_3 < z_\mathrm{w}: \quad \boldsymbol{t}^C = -\rho_\mathrm{w} g (z_\mathrm{w} - x_3) \boldsymbol{n}^\mathrm{c}, \tag{2 b 20}$$

where $\boldsymbol{n}^\mathrm{c}$ is horizontal. The total force per unit length of contour in water contact is therefore

$$\boldsymbol{T}^C = \int_{z_\mathrm{b}}^{z_\mathrm{w}} \boldsymbol{t}^C \,\mathrm{d}x_3 = -\tfrac{1}{2} \rho_\mathrm{w} g {h_\mathrm{w}}^2 \boldsymbol{n}^\mathrm{c} = -P^\mathrm{W} \boldsymbol{n}^\mathrm{c}. \tag{2 b 21}$$

The total horizontal force per unit width on any vertical plane in the ice floe, with horizontal normal $\boldsymbol{n}^h$, is given by

$$T_\alpha^\mathrm{I} = \int_{z_\mathrm{b}}^{z_\mathrm{s}} t_\alpha^\mathrm{I} \,\mathrm{d}x_3 = \int_{z_\mathrm{b}}^{z_\mathrm{s}} \sigma_{\alpha\beta}^\mathrm{I} n_\beta^h \,\mathrm{d}x_3 = N_{\alpha\beta}^\mathrm{I} n_\beta^h, \tag{2 b 22}$$

where

$$N_{\alpha\beta}^\mathrm{I} = \int_{z_\mathrm{b}}^{z_\mathrm{s}} \sigma_{\alpha\beta}^\mathrm{I} \,\mathrm{d}x_3 = N_{\beta\alpha}^\mathrm{I} \tag{2 b 23}$$

is the depth integrated stress. Thus on an edge section in contact with water,

$$C_\mathrm{w}: \quad N_{\alpha\beta}^\mathrm{I} n_\beta^\mathrm{c} = -P^\mathrm{W} n_\alpha^\mathrm{c}. \tag{2 b 24}$$

These are the results required in § 2 *c* where the equations are integrated through the thickness.

The upper ice surface is modified by snow accretion or melt. Let q be the equivalent volume flow of ice entering the floe per unit area per unit time – the accumulation rate, negative when ablation occurs – and let u_n be the normal speed of a surface point along the outward normal $\boldsymbol{n}^\mathrm{s}$, then

$$u_\mathrm{n} - \boldsymbol{v} \cdot \boldsymbol{n}^\mathrm{s} = q. \tag{2 b 25}$$

Now the surface is defined by

$$x_3 - z_\mathrm{s}(x_1, x_2, t) \equiv 0, \tag{2 b 26}$$

and hence

$$-\frac{\partial z_\mathrm{s}}{\partial t} + u_\mathrm{n} \boldsymbol{n}^\mathrm{s} \cdot \left(-\frac{\partial z_\mathrm{s}}{\partial x_1}, -\frac{\partial z_\mathrm{s}}{\partial x_2}, 1 \right) = 0, \tag{2 b 27}$$

where $\boldsymbol{n}^\mathrm{s}$ is given by (2 *a* 5). Eliminating u_n between (2 *b* 25) and (2 *b* 27) gives the surface accumulation condition

$$x_3 = z_\mathrm{s}: \quad \frac{\partial z_\mathrm{s}}{\partial t} + v_1 \frac{\partial z_\mathrm{s}}{\partial x_1} + v_2 \frac{\partial z_\mathrm{s}}{\partial x_2} - v_3 = \Delta_\mathrm{s} q. \tag{2 b 28}$$

Similarly, if b is the volume flux of ice ablating from the floe base per unit area

PHILOSOPHICAL TRANSACTIONS OF THE ROYAL SOCIETY A MATHEMATICAL, PHYSICAL & ENGINEERING SCIENCES

per unit time – the melt rate, negative when freezing occurs – then the basal melt condition is

$$x_3 = z_\mathrm{b}: \quad \frac{\partial z_\mathrm{b}}{\partial t} + v_1 \frac{\partial z_\mathrm{b}}{\partial x_1} + v_2 \frac{\partial z_\mathrm{b}}{\partial x_2} - v_3 = \Delta_\mathrm{b} b. \tag{2 b 29}$$

We consider a maximum for q or b to be 10^{-6} m s^{-1} (approximately 10 m per year).

In general, surface and basal melting or freezing are governed by the thermal interactions with the atmosphere and ocean. The surface and base are non-material singular surfaces, with outward mass fluxes $-\rho q$, ρb respectively, then, since particle velocity jumps $[\boldsymbol{v}]$ across these surfaces are small, the respective traction jumps $[\boldsymbol{t}] = -\rho q[\boldsymbol{v}]$ and $\rho \mathrm{b}[\boldsymbol{v}]$ are negligible in comparison with water pressures or wind stresses. Continuity of traction has already been imposed. Further, the kinetic energy and stress working jumps are negligible compared to the latent heat $L = 3.3 \times 10^5$ J kg^{-1}, so energy conservation requires

$$x_3 = z_\mathrm{s}: \quad \left[K \frac{\partial \Theta}{\partial n}\right] = -\rho q L, \qquad x_3 = z_\mathrm{b}: \quad \left[K \frac{\partial \Theta}{\partial n}\right] = \rho b L, \tag{2 b 30}$$

where [ ] denotes jump in the positive $\boldsymbol{n}$ direction, i.e. outward from the floe. These formally relate q and b to temperature gradient jumps between air and ice at the surface and between water and ice at the base in a fully coupled system. This result ignores the presence of any snow layer at the surface and of accretion of existing frazil ice from below the base.

It is sensible to assume that the melting and freezing at the base occurs at a melting–freezing temperature Θ_M associated with the local salinity and pressure of the water, which is a thermal boundary condition for the energy balance (2 b 14). An empirical relation for Θ_M has been presented by Millero (1978), but a useful simple approximation is constant $\Theta_M = 271$ K associated with a fixed salinity of 34 p.p.t. and a fixed constant pressure 10^5 N m^{-2}. Then either the normal temperature gradient $\partial\Theta/\partial n$ in the water must be prescribed to determine b by (2 b 30) which is required in the basal condition (2 b 29), or the mass exchange ρb must be prescribed directly, if the equations governing the ice response are to be uncoupled from those of the ocean. Surface ablation would require a melt temperature condition, but accretion can take place on a cold ice surface, governed by the prescription of positive q together with a cold surface temperature or heat flux in the air, or some combination. The most simple idealization is to suppose that $q = 0$, which ignores accretion or ablation at the surface in comparison with basal melting and freezing, and prescribe a surface temperature $\Theta^\mathrm{s}(x_\alpha, t)$. We therefore consider surface and base conditions:

$$x_3 = z_\mathrm{s}: \quad \Theta^\mathrm{I} = \Theta^\mathrm{s}(x_\alpha, t), \qquad x_3 = z_\mathrm{b}: \quad \Theta^\mathrm{I} = \Theta_M. \tag{2 b 31}$$

(c) *Depth integration*

Anticipating the construction of a reduced two-dimensional description in terms of the mean or total quantities with respect to ice thickness, it is instructive to consider the integration of the full balance equations of the previous section, to highlight the importance of the approximations which are necessary to achieve such a two-dimensional theory.

Define the horizontal ice flux per unit width of vertical section by

$$Q_\alpha(x_\alpha, t) = \int_{z_b}^{z_s} v_\alpha(x_j, t)\,\mathrm{d}x_3, \tag{2 c 1}$$

then integration of the mass conservation (2 *b* 11) through the floe thickness, subject to the kinematic boundary conditions (2 *b* 28) and (2 *b* 29) and thickness definition (2 *a* 3) shows that

$$\frac{\partial h}{\partial t} + \frac{\partial Q_1}{\partial x_1} + \frac{\partial Q_2}{\partial x_2} = \Delta_s q - \Delta_b b. \tag{2 c 2}$$

Integrating the horizontal momentum balances (2 *b* 12) through the thickness, using (2 *b* 8), (2 *b* 18) and (2 *b* 19) with the relations (2 *a* 5) and (2 *a* 6), gives

$$\frac{\partial N^I_{\alpha\beta}}{\partial x_\beta} + \left[\Delta_s \tau^s_\alpha + \rho v_\alpha \frac{\partial z_s}{\partial t}\right]_{z_s} + \left[\Delta_b \tau^b_\alpha - \Delta_b p^W n_\alpha - \rho v_\alpha \frac{\partial z_b}{\partial t}\right]_{z_b} + \rho f_c \varepsilon_{\alpha\beta 3} Q_\beta = \rho \frac{\partial Q_\alpha}{\partial t} + \rho \int_{z_b}^{z_s} v_j \frac{\partial v_\alpha}{\partial x_j}\,\mathrm{d}x_3. \tag{2 c 3}$$

There is no useful integral of the energy balance (2 *b* 14). Now Δ_s, Δ_b depend on gradients of z_s and z_b independently, so in general (2 *c* 2) does not simply relate the thickness h and fluxes Q_1, Q_2. Similarly, τ^b_α, τ^s_α, n_α on surface and base depend on gradients of z_s and z_b, $(v_\alpha \partial z_s/\partial t)_s - (v_\alpha \partial z_b/\partial t)_b = v_\alpha \partial h/\partial t$ only if $v_\alpha|_{z_s} = v_\alpha|_{z_b}$, and there is no explicit integral of the final term in (2 *c* 3) unless v_α is independent of x_3. Thus, (2 *c* 3) does not in general determine the integrated stress gradients $\partial N^I_{\alpha\beta}/\partial x_\beta$ in terms of the other integrated quantities. Furthermore, any nonlinear or temperature-dependent relation for the ice stress $\boldsymbol{\sigma}^I$ will not integrate to relations for $\boldsymbol{N}^I$. It is evident that explicit integration of the mass and momentum equations in terms of the integrated quantities will require small surface and base gradients which can be neglected compared to unity, and negligible variation of the horizontal velocity components v_α with depth.

It is useful to express the ice stress as the hydrostatic water pressure (zero above sea level) and an extra stress, thus

$$\boldsymbol{\sigma}^I = -p^W \mathbf{1} + \boldsymbol{\sigma}^E, \quad \boldsymbol{N}^I = -P^W \mathbf{1} + \boldsymbol{N}^E. \tag{2 c 4}$$

By (2 *a* 3), (2 *a* 5) and (2 *b* 21),

$$\Delta_b n_\alpha|_{z_b} = \frac{\partial z_w}{\partial x_\alpha} - \frac{\partial h_w}{\partial x_\alpha}, \quad \frac{\partial P^W}{\partial x_\alpha} = \rho_w g h_w \frac{\partial h_w}{\partial x_\alpha}, \tag{2 c 5}$$

and so (2 *c* 3) becomes

$$\frac{\partial N^E_{\alpha\beta}}{\partial x_\beta} + \Delta_s \tau^s_\alpha + \Delta_b \tau^b_\alpha - \rho_w g h_w \frac{\partial z_w}{\partial x_\alpha} = \rho h \bar{a}^N_\alpha, \tag{2 c 6}$$

where the mean horizontal acceleration $\bar{\boldsymbol{a}}^N$ in the rotating frame is defined by

$$\bar{a}^N_\alpha = \frac{1}{h}\left\{\frac{\partial Q_\alpha}{\partial t} - f_c \varepsilon_{\alpha\beta 3} Q_\beta - v_\alpha|_{z_s} \frac{\partial z_s}{\partial t} + v_\alpha|_{z_b} \frac{\partial z_b}{\partial t} + \int_{z_b}^{z_s} v_j \frac{\partial v_\alpha}{\partial x_j}\,\mathrm{d}x_3\right\}. \tag{2 c 7}$$

On the edge C,

$$C: \quad N^{\mathrm{E}}_{\alpha\beta} n^{\mathrm{c}}_{\beta} = T^{C}_{\alpha} + P^{\mathrm{W}} n^{\mathrm{c}}_{\alpha} = T^{\mathrm{E}}_{\alpha}, \tag{2 c 8}$$

where T^{E}_{α} is zero on the section C_{w} in contact with water. The vertical momentum balance will be integrated explicitly in § 2 *d*.

(*d*) *Rigid floe model*

The motion of the ice pack and adjacent ocean is driven by the wind stress, and the temporal and spatial scales of the variation are those of the weather system. Typical timescales of variation are several days, say $t^* = 10^6$ s, and horizontal length scales are a thousand kilometres, say $l^* = 10^6$ m. Ice pack extents are similar. Mean ice thicknesses range from 1 to 5 m, and it is useful to introduce a vertical length scale $h^* = 5$ m which is the length scale on which the ice stress (pressure and shear) makes its maximum changes. The basic element of the ice pack is the ice floe which has a diameter in the range 10^3–10^4 m, so there is a further horizontal length scale $l_{\mathrm{f}} = 10^3$ m. The pack or weather system and floe aspect ratios define two small parameters

$$\epsilon^* = h^*/l^* = 5 \times 10^{-6} \ll \epsilon_{\mathrm{f}} = h^*/l_{\mathrm{f}} = 5 \times 10^{-3} \ll 1. \tag{2 d 1}$$

Now ice floes are observed to have maximum (horizontal) translational velocities of order $v^* = 10^{-1}$ m s^{-1} and maximum angular velocities (about the vertical) of order $\omega^* = 10^{-5}$ rad s^{-1}, and insignificant vertical velocity by comparison. These physical magnitudes and parameters, and subsequent magnitudes introduced in the balances, are collected together in table 1 for convenience. It is convenient therefore to represent the ice particle velocity as the sum of a rigid translation and a rotation in the horizontal plane and a distortional velocity field; thus

$$v_{\alpha} = v^{\mathrm{p}}_{\alpha} - \varepsilon_{\alpha\beta 3}\omega(x_{\beta} - r^{\mathrm{p}}_{\beta}) + v^{\mathrm{D}}_{\alpha}, \quad v_3 = v^{\mathrm{D}}_3, \tag{2 d 2}$$

where $\boldsymbol{v}^{\mathrm{p}}(t)$ is the horizontal velocity of a given particle P at position $\boldsymbol{r}^{\mathrm{p}}(t)$, $\omega(t)\,\boldsymbol{k}$ is the angular velocity, and $\boldsymbol{v}^{\mathrm{D}}(\boldsymbol{x}, t)$ is the distortional velocity field.

A typical wind stress magnitude is $\tau^* = 10^{-1}$ N m^{-2} and we suppose that the ocean interaction is a responsive drag, not exceeding τ^* in magnitude and possibly much smaller. The shear stress in the horizontal plane can therefore vary by up to τ^* through the thickness of the floe. The vertical stress will vary from zero at the surface to the basal hydrostatic water pressure, $\rho_{\mathrm{w}} g h_{\mathrm{w}} \approx 5 \times 10^4$ N m^{-2}.

Edge stresses due to interactions with adjacent converging floes will exceed the water pressure, but it is supposed that any significant distortional effect is alleviated by post-fracture ridging. The strain rates (velocity gradients) across the coherent floe are those induced by tangential wind and drag stresses, and edge tractions. The magnitudes of strain rates and strains depend on the constitutive properties of the coherent ice.

It is customary to adopt a temperature-dependent nonlinearly viscous incompressible fluid model for the long-time response of ice, i.e. the floe of ice sheets and shelves over hundreds and thousands of years. The maximum strain rates occur near melting, with the ice becoming much more viscous as temperature decreases, and moderately less viscous as the deviatoric stress increases. Data correlation uses the minimum strain rate at constant stress supposing this is achieved in laboratory tests up to six months, and correlation of Glen's (1955) uni-axial data at the melt point by Smith & Morland (1981) implies a viscosity in the range

Table 1. *Physical parameters*

parameter	magnitude
gravity acceleration, g	9.81 m s^{-2}
Coriolis parameter, $f_c = 2\Omega \sin\phi$	$0 - 1.58 \times 10^{-4}$ rad s^{-1}
ice thermal conductivity, K^I	2.2 N K^{-1} s^{-1}
ice specific heat, C^I	2×10^3 J kg^{-1} K^{-1}
ice latent heat, L	3.3×10^5 J kg^{-1}
ice density, ρ	918 kg m^{-3}
water (saline) density, ρ_w	10^3 kg m^{-3}
melting point, Θ_M	271.4 K
linear drag coefficient, c_1	0.55×10^{-3} m s^{-1}
quadratic drag coefficient, c_2	0.55×10^{-2}
timescale, t^*	10^6 s
ice thickness, h^*	5 m
ice pack and weather system span, l^*	10^6 m
ice floe span, l_f	10^3 m
pack aspect ratio, $\epsilon^* = h^*/l^*$	5×10^{-6}
floe aspect ratio, $\epsilon_f = h^*/l_f$	5×10^{-3}
horizontal velocity, v^*	10^{-1} m s^{-1}
angular velocity about vertical, ω^*	10^{-5} rad s^{-1}
wind stress, water drag, τ^*	10^{-1} N m^{-2}
stress ratio, $\kappa = \tau^*/\rho g h^*$	2×10^{-6}

5–0.7×10^{12} N m^{-2} s for shear stress 0–10^5 N m^{-2}. This would imply a horizontal velocity change over a thickness of 5 m, due to wind stress 10^{-1} N m^{-2}, of order 10^{-13} m s^{-1}. The shorter time response is viscoelastic, reviewed by Mellor (1980) and by Hutter (1983), with initial creep decelerating at constant stress. Even if the strain rate above is enhanced by a factor 10^6 the velocity change with depth is at most 10^{-7} m s^{-1}, which is still negligible compared to the rigid body velocity of 10^{-1} m s^{-1}. Vertical particle velocity will be less than surface accumulation and basal melting and freezing rates, which mainly induce thickness changes, and so we suppose vertical velocities and strain rates are of order 10^{-8} m s^{-1} and 10^{-8} s^{-1} respectively at most. The mass conservation equation (2 *b* 11) then implies that the horizontal strain rates are of the same magnitude, so that horizontal velocity changes across the floe span should not exceed 10^{-4} m s^{-1}, also negligible compared to a rigid body velocity 10^{-1} m s^{-1}. On these assumptions we therefore make the approximation,

$$v_\alpha = v_\alpha^{\mathrm{p}}(t) - \varepsilon_{\alpha\beta 3}\omega(t)(x_\beta - r_\beta^{\mathrm{p}}), \quad v_3 = 0, \tag{2 d 3}$$

which neglects creep within the coherent ice in a single floe compared to the rigid body velocity, and which is a horizontal velocity not varying through the thickness of the floe. Now, the depth integrations (2 *c* 1), (2 *c* 2) and (2 *c* 6) become

$$Q_\alpha = h v_\alpha, \tag{2 d 4}$$

$$\frac{\mathrm{D}h}{\mathrm{D}t} = \frac{\partial h}{\partial t} + \frac{\partial}{\partial x_\alpha}(h v_\alpha) = \Delta_s q - \Delta_b b, \tag{2 d 5}$$

PHILOSOPHICAL TRANSACTIONS OF THE ROYAL SOCIETY A MATHEMATICAL, PHYSICAL & ENGINEERING SCIENCES

since $\partial v_\alpha/\partial x_\alpha = 0$ by (2 *d* 3),

$$\frac{\mathrm{D}v_\alpha}{\mathrm{D}t} = \dot{v}^{\mathrm{p}}_\alpha - \omega^2(x_\alpha - r^{\mathrm{p}}_\alpha) - \varepsilon_{\alpha\beta 3}\dot{\omega}(x_\beta - r^{\mathrm{p}}_\beta), \tag{2 d 6}$$

$$\frac{\partial N^{\mathrm{E}}_{\alpha\beta}}{\partial x_\beta} + \Delta_{\mathrm{s}}\tau^{\mathrm{s}}_\alpha + \Delta_{\mathrm{b}}\tau^{\mathrm{b}}_\alpha - \rho_{\mathrm{w}} g h_{\mathrm{w}}\frac{\partial z_{\mathrm{w}}}{\partial x_\alpha} + \rho f_{\mathrm{c}} h \varepsilon_{\alpha\beta 3} v_\beta = \rho h \frac{\mathrm{D}v_\alpha}{\mathrm{D}t}, \tag{2 d 7}$$

which involve z_{s}, z_{b} separately through Δ_{s} and Δ_{b} and τ^{s}_α, τ^{b}_α.

The essential reduction rests on the assumption that horizontal gradients of all variables are small compared to vertical gradients, supposing that changes across a floe span l_{f} are smooth and no greater than changes through the thickness h^*, but changes across the pack or weather system scale l^* will compare with changes through the thickness. This is formalized by a coordinate scaling,

$$x_\alpha = lX_\alpha = \epsilon^{-1}h^* X_\alpha, \quad x_3 = h^* X_3, \quad \epsilon^* \leqslant \epsilon \leqslant \epsilon_{\mathrm{f}} \ll 1, \tag{2 d 8}$$

together with the statement that derivatives in X_α and X_3 have the same status, where l and ϵ are determined by the balances. Define

$$z_{\mathrm{w}} = h^*\tilde{z}_{\mathrm{w}}, \quad z_{\mathrm{b}} = h^*\tilde{z}_{\mathrm{b}}, \quad z_{\mathrm{s}} = h^*\tilde{z}_{\mathrm{s}}, \quad h = h^*\tilde{h}, \quad h_{\mathrm{w}} = h^*\tilde{h}_{\mathrm{w}}, \tag{2 d 9}$$

so that $\tilde{z}_{\mathrm{b}}$, $\tilde{z}_{\mathrm{s}}$, $\tilde{z}_{\mathrm{w}}$, $\tilde{h}$, $\tilde{h}_{\mathrm{w}}$ are all order unity variables. Now

$$\frac{\partial z_{\mathrm{s}}}{\partial x_\alpha} = \epsilon\frac{\partial \tilde{z}_{\mathrm{s}}}{\partial X_\alpha}, \quad \frac{\partial z_{\mathrm{b}}}{\partial x_\alpha} = \epsilon\frac{\partial \tilde{z}_{\mathrm{b}}}{\partial X_\alpha}, \tag{2 d 10}$$

and hence to leading order, neglecting ϵ compared to unity, by (2 *a* 5)–(2 *a* 7),

$$\left.\begin{aligned} \Delta_{\mathrm{s}} = \Delta_{\mathrm{b}} = 1, \quad \boldsymbol{n}^{\mathrm{b}} = (0,0,-1), \quad \boldsymbol{n}^{\mathrm{s}} = (0,0,1), \\ \boldsymbol{e}^{\mathrm{b}}_1 = (-1,0,0) = -\boldsymbol{i}, \quad \boldsymbol{e}^{\mathrm{b}}_2 = (0,1,0) = \boldsymbol{j}, \\ \boldsymbol{e}^{\mathrm{s}}_1 = (1,0,0) = \boldsymbol{i}, \quad \boldsymbol{e}^{\mathrm{s}}_2 = (0,1,0) = \boldsymbol{j}, \end{aligned}\right\} \tag{2 d 11}$$

where $\boldsymbol{i}$, $\boldsymbol{j}$, $\boldsymbol{k}$ are the coordinate base vectors. The base and surface are therefore horizontal to leading order. All subsequent reductions are to leading order in ϵ. The surface condition (2 *b* 15) becomes

$$X_3 = \tilde{z}_{\mathrm{s}}: \quad \sigma^{\mathrm{I}}_{\alpha 3} = \tau^{\mathrm{s}}_\alpha, \quad \sigma^{\mathrm{I}}_{33} = 0, \tag{2 d 12}$$

and the basal condition (2 *b* 16) with (2 *b* 17) becomes

$$X_3 = \tilde{z}_{\mathrm{b}}: \quad \sigma^{\mathrm{I}}_{\alpha 3} = -\tau^{\mathrm{b}}_\alpha, \quad \sigma^{\mathrm{I}}_{33} = -\rho_{\mathrm{w}} g h^*(\tilde{z}_{\mathrm{w}} - \tilde{z}_{\mathrm{b}}), \tag{2 d 13}$$

where $\boldsymbol{\tau}^{\mathrm{s}}$ and $\boldsymbol{\tau}^{\mathrm{b}}$ are now horizontal vectors. The vertical equilibrium (2 *b* 13) with the surface and base conditions (2 *d* 12) and (2 *d* 13) give immediately that

$$\sigma^{\mathrm{I}}_{33} = -\rho g h^*(\tilde{z}_{\mathrm{s}} - X_3), \quad \rho_{\mathrm{w}}\tilde{h}_{\mathrm{w}} = \rho\tilde{h} = m/h^*, \tag{2 d 14}$$

where m is the mass of the ice column per unit horizontal cross-sectional area, and the horizontal momentum equations (2 *d* 7) become

$$\frac{\epsilon}{h^*}\frac{\partial N^{\mathrm{E}}_{\alpha\beta}}{\partial X_\beta} + \tau^{\mathrm{s}}_\alpha + \tau^{\mathrm{b}}_\alpha - mg\epsilon\frac{\partial \tilde{z}_{\mathrm{w}}}{\partial X_\alpha} + \varepsilon_{\alpha\beta 3} f_{\mathrm{c}} m v_\beta = m\frac{\mathrm{D}v_\alpha}{\mathrm{D}t}. \tag{2 d 15}$$

If the ratio ϵ corresponds to the weather system length scale so that $\partial\tilde{z}_{\mathrm{w}}/\partial X_\alpha \lesssim 1$,

then this dynamic pressure term may be comparable with the wind stress since $mg/\tau^* \sim 5 \times 10^5$.

The vertical and in-plane stresses will have at least the magnitude of the basal water pressure or weight of column of ice due to basal and edge conditions, so define

$$\boldsymbol{\sigma}^{\mathrm{I}} = \rho g h^* \tilde{\boldsymbol{\sigma}}^{\mathrm{I}}, \quad \boldsymbol{N}^{\mathrm{I}} = \rho g (h^*)^2 \tilde{\boldsymbol{N}}^{\mathrm{I}}, \tag{2 d 16}$$

then $\tilde{\boldsymbol{\sigma}}^{\mathrm{I}}$ and $\tilde{\boldsymbol{N}}^{\mathrm{I}}$ have some components of order unity (or greater). Note that there may be larger in-plane stresses if floe interaction forces are much greater. The surface and basal tangential tractions are of order $\tau^* = 10^{-1}$ N m^{-2}, so define

$$\tau_\alpha^{\mathrm{b}} = \tau^* \tilde{\tau}_\alpha^{\mathrm{b}}, \quad \tau_\alpha^{\mathrm{s}} = \tau^* \tilde{\tau}_\alpha^{\mathrm{s}}, \tag{2 d 17}$$

where $\tilde{\tau}_\alpha^{\mathrm{b}}$, $\tilde{\tau}_\alpha^{\mathrm{s}}$ are of order unity (or less for the basal traction), and the stress ratio

$$\kappa = \tau^*/\rho g h^* \approx 2 \times 10^{-6} \ll 1. \tag{2 d 18}$$

The rigid body velocity has magnitude v^* which will impose a restriction on the net edge force determined by integration of the rigid body momentum equation for the floe over the timescale $t^* = 10^6$ s of a maintained wind stress. Define

$$v_\alpha = v^* \tilde{v}_\alpha, \quad t = t^* \tilde{t}, \tag{2 d 19}$$

so that $\tilde{v}_\alpha$, $\tilde{t}$ are order unity variables. The thickness evolution equation (2 *d* 5) becomes

$$\frac{D\tilde{h}}{D\tilde{t}} = \frac{\partial \tilde{h}}{\partial \tilde{t}} + \epsilon \frac{v^* t^*}{h^*} \tilde{v}_\beta \frac{\partial \tilde{h}}{\partial X_\beta} = \frac{t^*}{h^*}(q - b) = \tilde{q}, \tag{2 d 20}$$

where $\tilde{q} \lesssim 1$ and the momentum equations (2 *d* 15) become

$$\frac{\partial \tilde{N}_{\alpha\beta}^{\mathrm{E}}}{\partial X_\beta} + \epsilon^{-1} \kappa \tilde{\tau}_\alpha - \tilde{m} \frac{\partial \tilde{z}_{\mathrm{w}}}{\partial X_\alpha} + \epsilon^{-1} \left(\frac{f_{\mathrm{c}} v^*}{g} \right) \tilde{m} \varepsilon_{\alpha\beta 3} \tilde{v}_\beta = \epsilon^{-1} \left(\frac{v^*}{g\, t^*} \right) \tilde{m} \frac{D\tilde{v}_\alpha}{D\tilde{t}}, \tag{2 d 21}$$

where

$$\tilde{\tau}_\alpha = \tilde{\tau}_\alpha^{\mathrm{s}} + \tilde{\tau}_\alpha^{\mathrm{b}}, \quad \tilde{m} = m/\rho h^* = O(1). \tag{2 d 22}$$

Magnitudes of the respective terms in the momentum balance (2 *d* 21), and of the implied velocity and angular velocity, must be estimated to determine restrictions on the total force and moment of force implied by observed motions. In addition, they are necessary for a crucial reduction of the mean floe stress constructed in § 2 *e*, which is the basis of the ice pack stress interpretation in § 3 *e*.

Now, from (2 *d* 3),

$$\tilde{v}_\alpha = \tilde{v}_\alpha^{\mathrm{p}}(\tilde{t}) - \varepsilon_{\alpha\beta 3} \tilde{\omega}(\tilde{t})(X_\beta - R_\beta^{\mathrm{p}}(\tilde{t})), \tag{2 d 23}$$

where

$$\tilde{\omega}(\tilde{t}) = \epsilon^{-1}(h^*/v^*)\omega(t), \quad \boldsymbol{r}^{\mathrm{p}} = \epsilon^{-1} h^* \boldsymbol{R}^{\mathrm{p}}, \tag{2 d 24}$$

and differentiating,

$$\frac{D\tilde{v}_\alpha}{D\tilde{t}} = \dot{\tilde{v}}_\alpha^{\mathrm{p}} - \varepsilon_{\alpha\beta 3} \dot{\tilde{\omega}}(X_\beta - R_\beta^{\mathrm{p}}) - \epsilon \left(\frac{v^* t^*}{h^*} \right) \tilde{\omega}^2 (X_\alpha - R_\alpha^{\mathrm{p}}), \tag{2 d 25}$$

where the superposed $\cdot$ now denotes differentiation with respect to the argument $\tilde{t}$. Note that the velocity due to rotation is bounded by v^*, which requires $\omega l_{\mathrm{f}} \lesssim v^*$

or

$$\omega \lesssim \epsilon_{\rm f} v^*/h^*, \quad \tilde{\omega}\epsilon/\epsilon_{\rm f} \lesssim 1, \tag{2 d 26}$$

which is satisfied by observed angular velocities

$$\omega \lesssim \omega^* = 10^{-5} \text{rad s}^{-1}. \tag{2 d 27}$$

If the gradients of extra stress and dynamic surface $z_{\rm w}$ are zero (or negligible), which is possible, then the wind stress and water drag must be balanced by the acceleration and, or, Coriolis force. Since $f_{\rm c} t^* \approx 10^2$ near the poles recalling the magnitudes of $f_{\rm c}$ and t^* given in table 1, a developed motion, with $|\boldsymbol{v}|$ approaching v^*, must then balance the wind stress and water drag with the Coriolis term; thus

$$v^* = g\kappa/f_{\rm c} \approx 10^{-1} \text{ m s}^{-1}, \tag{2 d 28}$$

which is the observed, and assumed, maximum magnitude in a pack motion.

The rigid body velocity and angular velocity are determined by the integrals of the linear and angular momentum equations over the floe. Let $\boldsymbol{r}^{\rm p}(t)$ be the instantaneous centre of mass of the floe with horizontal location $R^{\rm p}_\alpha(\tilde{t})$ in $(X_\alpha, \tilde{t})$. This will not remain at a fixed particle P, due to profile changes caused by base, surface and edge melting and freezing, and ridging. Let $\tilde{S}(\tilde{t})$, $\tilde{C}(\tilde{t})$ be the floe domain and boundary in $(X_\alpha, \tilde{t})$, so $\tilde{S}$ has a linear dimension $\epsilon/\epsilon_{\rm f}$ on the X_α scale in view of the scalings (2 d 1) and (2 d 8). Then

$$\tilde{M} R^{\rm p}_\alpha = \int_{\tilde{S}} \tilde{m} X_\alpha \, {\rm d}\tilde{S}, \quad \tilde{M} = \int_{\tilde{S}} \tilde{m} \, {\rm d}\tilde{S} = O(\epsilon^2/\epsilon_{\rm f}^2), \tag{2 d 29}$$

where the floe mass M is given by

$$M = \rho h^{*3} \epsilon^{-2} \tilde{M}. \tag{2 d 30}$$

On the edge $\tilde{C}$,

$$\tilde{C}: \quad \tilde{N}^{\rm E}_{\alpha\beta} n^{\rm c}_\beta = \tilde{T}^{\rm E}_\alpha = T^{\rm E}_\alpha/(\rho g h^{*2}). \tag{2 d 31}$$

Integrating (2 d 21) over $\tilde{S}$ gives

$$\int_{\tilde{C}} \tilde{T}^{\rm E}_\alpha \, {\rm d}\tilde{s} + \int_{\tilde{S}} \left(\epsilon^{-1} \kappa \tilde{\tau}_\alpha - \tilde{m} \frac{\partial \tilde{z}_{\rm w}}{\partial X_\alpha} \right) {\rm d}\tilde{S} = \tilde{M} \frac{\epsilon^{-1} v^*}{g t^*} \left\{ \dot{\tilde{v}}^{\rm p}_\alpha - f_{\rm c} t^* \varepsilon_{\alpha\beta 3} \tilde{v}^{\rm p}_\beta \right\}, \tag{2 d 32}$$

since the integrals involving $\boldsymbol{X} - \boldsymbol{R}^{\rm p}$ vanish by (2 d 29). With the acceleration upper bound (2 d 29) and the magnitude (2 d 29) for $\tilde{M}$, and the identity (2 d 28), the right-hand side of (2 d 32) has magnitude $(\epsilon/\epsilon_{\rm f})^2(\kappa/\epsilon)$ at greatest, which is also the magnitude of the first term of the surface integral. Further, the length scale of variation of $\tilde{z}_{\rm w}$ in X_α is $l^*/l = \epsilon l^*/h^* = \epsilon/\epsilon^*$. Thus the $\tilde{z}_{\rm w}$ gradient contribution has magnitude $(\epsilon/\epsilon_{\rm f})^2(\epsilon^*/\epsilon)$, which does not exceed the magnitude $(\epsilon/\epsilon_{\rm f})^2(\kappa/\epsilon)$ provided that $\epsilon^* \leqslant \kappa$, and this is satisfied by the physical parameters listed in table 1. Thus

$$\left| \tilde{\boldsymbol{F}}^{\rm E} \right| = \left| \int_{\tilde{C}} \tilde{\boldsymbol{T}}^{\rm E} \, {\rm d}\tilde{s} \right| \lesssim \frac{\epsilon^2}{\epsilon_{\rm f}^2} \epsilon^{-1} \kappa, \tag{2 d 33}$$

which is simply the physical statement

$$|\boldsymbol{F}^{\rm E}| = \left| \int_C \boldsymbol{T}^{\rm E} \, {\rm d}s \right| \lesssim l_{\rm f}^2 \tau^*. \tag{2 d 34}$$

Given that the estimate (2 *d* 28) is the observed velocity magnitude we will assume that (2 *d* 34) holds, which is a restriction on the forces generated by the floe interactions, in turn driven by wind stress and Coriolis force. Note that the small parameter ϵ chosen to induce the small horizontal gradients is not defined by the rigid body balances, but we now impose a convenient, and consistent, estimate

$$\epsilon \approx \kappa \approx \epsilon^*. \tag{2 d 35}$$

Taking moments of (2 *d* 21) about a vertical axis through P and integrating over the floe domain $\tilde{S}$ gives the angular momentum equation,

$$\varepsilon_{3\gamma\alpha}\left\{\int_{\tilde{C}}(X_\gamma - R^{\mathrm{p}}_\gamma)\tilde{T}^{\mathrm{E}}_\alpha \,\mathrm{d}\tilde{s} + \int_{\tilde{S}}(X_\gamma - R^{\mathrm{p}}_\gamma)\left[\epsilon^{-1}\kappa\tilde{\tau}_\alpha - \tilde{m}\frac{\partial \tilde{z}_{\mathrm{w}}}{\partial X_\alpha}\right]\mathrm{d}\tilde{S}\right\}$$
$$= \epsilon^{-1}\,(v^*/gt^*)\,\tilde{I}\dot{\tilde{\omega}}, \tag{2 d 36}$$

where

$$\tilde{I} = \int_{\tilde{S}} \tilde{m}(X_\alpha - R^{\mathrm{p}}_\alpha)^2 \,\mathrm{d}\tilde{S} = O(\epsilon^4/\epsilon_{\mathrm{f}}^4), \tag{2 d 37}$$

since $|X_\alpha - R^{\mathrm{p}}_\alpha|$ is of order $\epsilon/\epsilon_{\mathrm{f}}$ over $\tilde{S}$, and

$$I = \rho h^{*5}\epsilon^{-4}\tilde{I} \tag{2 d 38}$$

is the moment of inertia of the floe about this axis. If the stresses are maintained for a time t^*, $\tilde{t} = 1$, $\dot{\tilde{\omega}} \approx \tilde{\omega} \lesssim (\epsilon_{\mathrm{f}}/\epsilon)$ by (2 *d* 26), and (2 *d* 36) is a restriction on the moments of contact and surface forces. Over the floe span we suppose that $\tilde{\tau}_\alpha$ and $\partial\tilde{z}_{\mathrm{w}}/\partial X_\alpha$ are nearly uniform, since their variation is over the scale $l^* = 10^6$ m, and if uniform their moment integral is identically zero. With the above angular acceleration bound and estimate (2 *d* 37) for $\tilde{I}$, and the results (2 *d* 28), (2 *d* 29), (2 *d* 35) with table 1 parameter values, the moment requirements are

$$\left.\begin{aligned} \varepsilon_{3\gamma\alpha}\left(\frac{\epsilon_{\mathrm{f}}}{\epsilon}\right)^2 \int_{\tilde{C}}(X_\gamma - R^{\mathrm{p}}_\gamma)\tilde{T}^{\mathrm{E}}_\alpha \,\mathrm{d}\tilde{s} &\lesssim 10^{-5}, \\ \varepsilon_{3\gamma\alpha}\left(\frac{\epsilon_{\mathrm{f}}}{\epsilon}\right)^3 \int_{\tilde{S}}(X_\gamma - R^{\mathrm{p}}_\gamma)\left[\epsilon^{-1}\kappa\tilde{\tau}_\alpha - \tilde{m}\frac{\partial \tilde{z}_{\mathrm{w}}}{\partial X_\alpha}\right]\mathrm{d}\tilde{S} &\lesssim 10^{-2}. \end{aligned}\right\} \tag{2 d 39}$$

The factors $(\epsilon_{\mathrm{f}}/\epsilon)^2$ and $(\epsilon_{\mathrm{f}}/\epsilon)^3$ before the integrals make these terms moments in the dimensionless floe coordinates, and highlight the strong restrictions which are required to limit angular velocities to the observed magnitude ω^*. They are assumed to hold therefore. Solutions of the pack equations for given driving forces and interactions $\boldsymbol{T}^{\mathrm{E}}$ must confirm, or not, the observed magnitudes.

(*e*) *Mean floe stress*

The extra stress $\tilde{\boldsymbol{N}}^{\mathrm{E}}$ is indeterminate, not determined by the point balance (2 *d* 21) subject to edge tractions $\tilde{T}^{\mathrm{E}}$, due to the rigid body approximation. Any stress field

$$\tilde{N}^*_{11} = \frac{\partial^2 U}{\partial X_2^2}, \quad \tilde{N}^*_{12} = -\frac{\partial^2 U}{\partial X_1 \partial X_2}, \quad \tilde{N}^*_{22} = \frac{\partial^2 U}{\partial X_1^2}, \tag{2 e 1}$$

in terms of a twice differentiable stress function $U(X_1, X_2)$ subject only to homogeneous boundary conditions,

$$\tilde{N}^*_{\alpha\beta} n^{\mathrm{c}}_{\beta} = 0, \tag{2 e 2}$$

is self-equilibrating, and can be added to a solution of (2 d 21). However, we will treat a floe as a basic element of the ice-pack, supposedly small on the pack scale so that variations across the floe are not significant. It is therefore the *mean stress* over a floe which represents the local (point) stress in the ice pack. Define the mean extra stress $\bar{\tilde{\boldsymbol{N}}}^{\mathrm{E}}$ by

$$\tilde{S}\bar{\tilde{N}}^{\mathrm{E}}_{\alpha\beta} = \int_{\tilde{S}} \tilde{N}^{\mathrm{E}}_{\alpha\beta}\, \mathrm{d}\tilde{S}, \tag{2 e 3}$$

where $\tilde{S}$ also denotes the area of the domain $\tilde{S}$. If $\tilde{\boldsymbol{N}}^{\mathrm{E}}$ satisfies the equilibrium equation

$$\frac{\partial \tilde{N}^{\mathrm{E}}_{\alpha\beta}}{\partial X_\beta} + \tilde{B}_\alpha = 0, \tag{2 e 4}$$

with body force $\tilde{\boldsymbol{B}}$, by applying the two-dimensional divergence theorem we find the mean stress is given by

$$\tilde{S}\bar{\tilde{N}}^{\mathrm{E}}_{\alpha\gamma} = \int_{\tilde{C}} (X_\gamma - R^{\mathrm{p}}_\gamma)\tilde{T}^{\mathrm{E}}_\alpha \,\mathrm{d}\tilde{s} + \int_{\tilde{S}} (X_\gamma - R^{\mathrm{p}}_\gamma)\tilde{B}_\alpha \,\mathrm{d}\tilde{S}, \tag{2 e 5}$$

which is the analogue of Signorini's mean stress theorem. The mean stress therefore depends on the edge tractions which will be related to the floe interactions, and on the body force $\tilde{\boldsymbol{B}}$.

We can express (2 d 21) in the form (2 e 4) by appropriate definition of $\tilde{\boldsymbol{B}}$. However, a more convenient form of $\tilde{\boldsymbol{B}}$ is obtained by eliminating the centre of mass (P) term $\dot{\tilde{v}}^{\mathrm{p}}_\alpha - f_{\mathrm{c}} t^* \varepsilon_{\alpha\beta 3} \tilde{v}^{\mathrm{p}}_\beta$ through (2 d 32) when the expressions (2 d 23) and (2 d 25) are used in (2 d 21). Then

$$\begin{aligned}\tilde{B}_\alpha = &-\frac{\tilde{m}}{\tilde{M}} \int_{\tilde{C}} \tilde{T}^{\mathrm{E}}_\alpha \,\mathrm{d}\tilde{s} + \epsilon^{-1}\kappa \left[\tilde{\tau}_\alpha - \frac{\tilde{m}}{\tilde{M}} \int_{\tilde{S}} \tilde{\tau}_\alpha \,\mathrm{d}\tilde{S}\right] - \left[\tilde{m}\frac{\partial \tilde{z}_{\mathrm{w}}}{\partial X_\alpha} - \frac{\tilde{m}}{\tilde{M}} \int_{\tilde{S}} \tilde{m} \frac{\partial \tilde{z}_{\mathrm{w}}}{\partial X_\alpha} \,\mathrm{d}\tilde{S}\right] \\ &+ \frac{v^* \tilde{m}}{\epsilon g t^*} \left\{ \varepsilon_{\alpha\beta 3} \dot{\tilde{\omega}} (X_\beta - R^{\mathrm{p}}_\beta) + \tilde{\omega} t^* \left(\frac{\epsilon v^*}{h^*} \tilde{\omega} + f_{\mathrm{c}} \right) (X_\alpha - R^{\mathrm{p}}_\alpha) \right\}. \end{aligned} \tag{2 e 6}$$

Recall that our scaling is

$$\kappa \simeq \epsilon^* = \epsilon \ll \epsilon_{\mathrm{f}}, \quad \delta = \epsilon/\epsilon_{\mathrm{f}} = 10^{-3} \ll 1, \tag{2 e 7}$$

so that

$$|\boldsymbol{X} - \boldsymbol{R}^{\mathrm{p}}| = O(\delta), \quad \tilde{S} = O(\delta^2), \quad \tilde{M} = O(\delta^2). \tag{2 e 8}$$

The contour integral in (2 e 5) therefore makes a contribution of order $|\tilde{\boldsymbol{T}}^{\mathrm{E}}|$ to $\bar{\tilde{\boldsymbol{N}}}^{\mathrm{E}}$, which we suppose is order unity or greater so that the integrated extra edge tractions and the stress are comparable to the integrated water pressure, and the floe interactions make a significant contribution to the ice pack dynamics. The surface integral makes a contribution of order $|\tilde{\boldsymbol{B}}|\delta$ to $\bar{\tilde{\boldsymbol{N}}}^{\mathrm{E}}$, so terms in $\tilde{B}_\alpha$ of order unity or less do not contribute significantly. By (2 d 33), the term $\tilde{m}\tilde{M}^{-1}\tilde{\boldsymbol{F}}^{\mathrm{E}}$ is order unity, and so insignificant. Similarly the terms in $\tilde{\tau}_\alpha$ and $\partial \tilde{z}_{\mathrm{w}}/\partial X_\alpha$ are order

unity, and insignificant. Given that ω reaches a magnitude ω^* when stresses are maintained for a time t^* ($\tilde{t} = 1$), then

$$\dot{\tilde{\omega}} = \tilde{\omega} = \epsilon^{-1} h^* \omega^* / v^* \tag{2 e 9}$$

represent maximum magnitudes. The three angular velocity terms in (2 *e* 6) therefore have magnitudes,

$$\frac{l_f \omega^*}{\epsilon g t^*}(1, \omega^* t^*, f_c t^*), \tag{2 e 10}$$

of which the Coriolis term is greatest but with magnitude less than unity, again insignificant. Thus the mean stress is given by

$$\bar{\tilde{N}}^{\mathrm{E}}_{\alpha\gamma} = \frac{1}{\tilde{S}} \int_{\tilde{C}} (X_\gamma - R^{\mathrm{p}}_\gamma) \tilde{T}^{\mathrm{E}}_\alpha \, \mathrm{d}\tilde{s}, \tag{2 e 11}$$

or in physical components by

$$\bar{N}^{\mathrm{E}}_{\alpha\gamma} = \frac{1}{S} \int_C (x_\gamma - r^{\mathrm{p}}_\gamma) T^{\mathrm{E}}_\alpha \, \mathrm{d}s. \tag{2 e 12}$$

The symmetry of $\bar{\boldsymbol{N}}^{\mathrm{E}}$ is equivalent to the edge traction $\boldsymbol{T}^{\mathrm{E}}$ being self-equilibrating with zero net force and moment. This is a key result in the later interpretation of the ice pack stress field and its relation to the large-scale deformation or deformation rate which describes the relative (rigid) motions of the floe elements. The various physical magnitudes and dimensionless parameters introduced in the balance and scaling arguments are collected in table 1 for convenience.

3. Multi-floe ice pack

(*a*) *The ice–water layer*

An ice pack is a mosaic of individual floes which occupy a large fraction of the area of the pack domain, separated by open water leads and contact interfaces with adjacent floes. The pattern changes as the pack is driven non-uniformly by the wind-stress and Coriolis force, involving regions with diverging floes and with converging floes, and a ridging process can occur in converging regions. We view the pack as a thin layer containing coherent ice floes and 'trapped water' within the layer. There is, though, a vertical flux of water into or out of this layer, from or into the ocean, as adjacent floes diverge and converge, but it is useful to define a layer of thickness $h(x_\alpha, t)$ as a continuous extension of adjacent floes. The layer therefore has base $x_3 = z_{\mathrm{b}}(x_\alpha, t)$ and surface $x_3 = z_{\mathrm{s}}(x_\alpha, t)$, and $z_{\mathrm{b}}(x_\alpha, t)$ also defines the base of the 'trapped water'. The water surface is $x_3 = z_{\mathrm{w}}(x_\alpha, t)$, and there is overlying trapped air, of negligible mass, filling the remaining space available. Figure 3 illustrates the layer concept and figure 4 illustrates a local floe surface pattern with ice–water and ice–ice contacts.

The area fraction of ice in a horizontal plane, that is the area of ice surface per unit pack surface area is denoted by $A(x_\alpha, t)$, and f represents the mean proportion of ice–ice contact length on floe boundaries. In practice the proportion f must depend on floe shapes and detailed motion, all lost in the present large-scale view of the pack motion, and the assumption $f = f(A)$ is an attempt to reflect a dependence on concentration in a simple manner. Thus, $f(A)$ is a model function, that is, a constitutive postulate, to be prescribed subject to

PHILOSOPHICAL TRANSACTIONS OF THE ROYAL SOCIETY A MATHEMATICAL, PHYSICAL & ENGINEERING SCIENCES

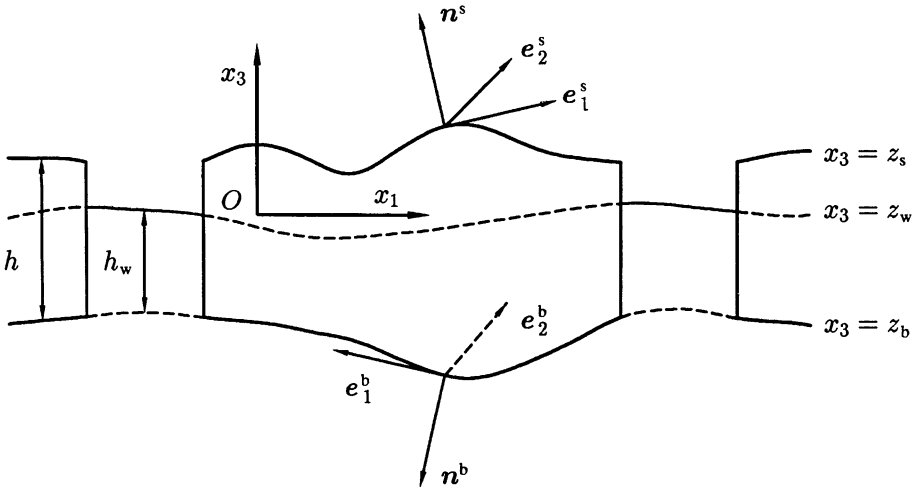

Figure 3. Vertical section through a segment of the ice pack layer.

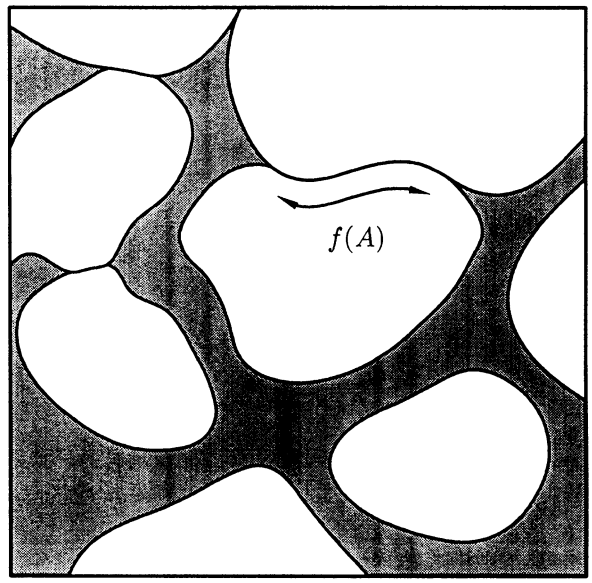

Figure 4. Horizontal plan view of a segment of the ice ice pack layer.

$f(0) = 0$ and $f(1) = 1$. It will influence the ice floe stress. We suppose that $f(A)$ is monotonically increasing to reflect an increasing contact length with increase of ice concentration and generally expect $f(A)$ to be nonlinear.

An essential assumption is that all physical variables change smoothly over the pack and weather system length scale l^*, so that they reflect mean values over the floe scale and all irregularities on the floe scale are ignored. The appropriate coordinate scaling is

$$x_\alpha = l^* X_\alpha = \epsilon^{-1} h^* X_\alpha, \quad x_3 = h^* X_3, \quad \epsilon = \epsilon^* \ll 1, \tag{3 a 1}$$

where X_α and X_3 derivatives have the same status, and the leading-order relations in ϵ for the ice base and surface normals and tangents, and the traction conditions,

are again (2 *d* 11)–(2 *d* 13), and the vertical stress results (2 *d* 14) follow. This justifies the view of the pack as a horizontal layer of slowly varying (ice) thickness and the integration through the depth to construct a two-dimensional theory for the integrated stresses and horizontal velocity field. Further, since only mean values on the floe scale are considered, the pack is described as a two-dimensional (horizontal) mixture (interacting continua) of ice and water columns forming the layer, with overlapping horizontal velocity fields $\boldsymbol{v}^{\mathrm{i}}(x_\alpha, t)$, $\boldsymbol{v}^{\mathrm{w}}(x_\alpha, t)$, and partial densities $\rho^{\mathrm{i}}(x_\alpha, t)$, $\rho^{\mathrm{w}}(x_\alpha, t)$ defined everywhere. Partial density is the mass of constituent per unit mixture volume. This supposes that the floe and open water spaces are very small compared to the pack span, so that a mixture element contains sufficient of each for mean values to be sensible, and identification of the actual constituents at each point is not necessary. With actual floe spans of 10^3–10^4 m this is not a good approximation, but is consistent with, and necessary for, a theory which ignores individual floe detail. The slowly varying horizontal ice velocity field $\boldsymbol{v}^{\mathrm{i}}(x_\alpha, t)$ describes the relative motions of the rigid floes in a mean sense, and is independent of x_3, and there is no vertical ice velocity. Later, the ice fraction A is partitioned to describe the ridging process.

In a layer of pack with unit horizontal cross-sectional area the mass of ice is $\rho A h$ and the layer volume is h, so the mass per unit layer volume, partial density of ice, is

$$\rho^{\mathrm{i}} = A\rho. \tag{3 a 2}$$

The mass of water is $\rho_{\mathrm{w}}(1-A)h_{\mathrm{w}}, = (1-A)\rho h$ by (2 *d* 14), so the partial density of water is

$$\rho^{\mathrm{w}} = (1-A)\rho, \tag{3 a 3}$$

and the total density $\rho^{\mathrm{i}} + \rho^{\mathrm{w}} = \rho$, which is the intrinsic ice density. Note that the air within the layer volume h per unit horizontal cross-section has been assigned zero mass. The mass of the ice and water columns per unit horizontal cross-section are therefore

$$m^{\mathrm{i}} = \rho^{\mathrm{i}} h = Am, \quad m^{\mathrm{w}} = \rho^{\mathrm{w}} h = (1-A)m, \tag{3 a 4}$$

and $m^{\mathrm{i}} + m^{\mathrm{w}} = m$, which follows because the ice and water depths are related by the equal column mass result (2 *d* 14). The traction t_i on a unit pack horizontal cross-section is the sum of the partial tractions (forces per unit pack horizontal cross-section) t_i^{i}, t_i^{w} carried by the ice and water respectively; thus

$$\boldsymbol{n} = (0, 0, \pm 1): \quad t_i = t_i^{\mathrm{i}} + t_i^{\mathrm{w}}. \tag{3 a 5}$$

The force on the ice is actually over an area A, and that on the water over an area $1 - A$, so

$$\boldsymbol{n} = (0, 0, \pm 1): \quad t_i^{\mathrm{i}} = At_i^{\mathrm{I}}, \quad t_i^{\mathrm{w}} = (1-A)t_i^{\mathrm{W}}, \tag{3 a 6}$$

where $\boldsymbol{t}_i^{\mathrm{I}}$, $\boldsymbol{t}_i^{\mathrm{W}}$ are the intrinsic ice and water tractions – forces per unit ice and water cross-sections respectively. The relations (3 *a* 5), (3 *a* 6) will apply to the base and surface conditions. A capital superscript will always denote an intrinsic variable, one associated with an element of the constituent, in contrast to lower case for a partial variable associated with an element of the mixture. While the constituent velocity fields $\boldsymbol{v}^{\mathrm{i}}$, $\boldsymbol{v}^{\mathrm{w}}$ are associated with the mixture in the sense that $\rho^{\mathrm{i}}\boldsymbol{v}^{\mathrm{i}}$ and $\rho^{\mathrm{w}}\boldsymbol{v}^{\mathrm{w}}$ determine the mass fluxes, a consistent theory requires that $\boldsymbol{v}^{\mathrm{i}}$, $\boldsymbol{v}^{\mathrm{w}}$ define mean intrinsic velocities of the ice and water, so here there is no

PHILOSOPHICAL TRANSACTIONS OF THE ROYAL SOCIETY A MATHEMATICAL, PHYSICAL & ENGINEERING SCIENCES

distinction. A detailed formulation of three-dimensional mixture theory with such interpretations and conclusions is presented by Morland (1992), and the present two-dimensional theory follows closely.

In contrast to an unstructured three-dimensional mixture we recognize that vertical sections do not intersect an array of ice and water layers, and tractions are generally across ice–ice or water–water interfaces except at vertical floe edges. We introduce a partition $f(A)$, $1-f(A)$ of unit contour length into ice–ice and ice–water contact, that is, an area partition hf, $h(1-f)$ of a vertical section area h, which will be used in the interpretation of the mean stress result (2 *e* 12). For the purposes of applying the constituent momentum balances of mixture theory we formally define the partial tractions $\boldsymbol{t}^{\mathrm{i}}$, $\boldsymbol{t}^{\mathrm{w}}$ on any mixture plane as the forces per unit mixture area carried by the ice and water respectively, then the momentum balance, with the usual smoothness assumptions, defines partial stresses $\boldsymbol{\sigma}^{\mathrm{i}}$, $\boldsymbol{\sigma}^{\mathrm{w}}$ by the relations

$$t_i^{\mathrm{i}} = \sigma_{ij}^{\mathrm{i}} n_j, \quad t_i^{\mathrm{w}} = \sigma_{ij}^{\mathrm{w}} n_j, \tag{3 a 7}$$

for any unit vector $\boldsymbol{n}$. The total traction and stress is then given by

$$t_i = t_i^{\mathrm{i}} + t_i^{\mathrm{w}}, \quad \sigma_{ij} = \sigma_{ij}^{\mathrm{i}} + \sigma_{ij}^{\mathrm{w}}. \tag{3 a 8}$$

It has been noted that the vertical water velocity v_3^{w} is distinct from that of the zero ice velocity v_3^{i} since the layer water moves in and out of the underlying ocean as the adjacent floes converge and diverge. However, the horizontal water motion in the leads must be strongly governed by the motion of adjacent floes, which would be reflected by a mean local velocity assumption

$$v_\alpha^{\mathrm{w}} = v_\alpha^{\mathrm{i}} = v_\alpha; \tag{3 a 9}$$

that is, a common horizontal ice and water velocity field. This serves to eliminate unknown interactions and simplify the equations of motion. This may be too strong a restriction, but is adopted in the present theory. Any alternative will require the prescription of an interaction drag between layer water and ice. We formally suppose that the distinct $v_3^{\mathrm{i}}(=0)$, v_3^{w} are defined everywhere.

(*b*) *The mass and thermal balances*

Reference to water will imply the water instantaneously within the layer. The general mixture relations are taken from Morland (1992).

With neglect of any vertical velocity of the ice, mass conservation for the ice is expressed by

$$\frac{\partial \rho^{\mathrm{i}}}{\partial t} + \frac{\partial}{\partial x_\alpha}(\rho^{\mathrm{i}} v_\alpha) = k, \tag{3 b 1}$$

where k is the mass transfer per unit pack volume per unit time into the ice due to phase change at floe edges, assumed uniform through the depth of layer water to be consistent with ρ^{i}, v_α uniform in x_3. In § 3 *c* we reintroduce a vertical ice velocity in a ridging ice zone. Equation (3 *b* 1) gives the evolution equation for A:

$$\frac{\partial A}{\partial t} + \frac{\partial}{\partial x_\alpha}(A v_\alpha) = \frac{\mathrm{D}A}{\mathrm{D}t} + A\frac{\partial v_\alpha}{\partial x_\alpha} = \frac{k}{\rho}. \tag{3 b 2}$$

Now, analogous to (2 *b* 28), (2 *b* 29), the surface and base kinematic conditions for

the ice are

$$\frac{\partial z_s}{\partial t} + v_\alpha \frac{\partial z_s}{\partial x_\alpha} = q^I, \quad \frac{\partial z_b}{\partial t} + v_\alpha \frac{\partial z_b}{\partial x_\alpha} = b^I, \tag{3 b 3}$$

recalling the leading-order results $\Delta_s = \Delta_b = 1$, where q^I, b^I are volume fluxes per unit horizontal area of ice floe. Thus, differencing these two relations,

$$\frac{Dh}{Dt} = \frac{\partial h}{\partial t} + v_\alpha \frac{\partial h}{\partial x_\alpha} = q^I - b^I, \tag{3 b 4}$$

which describes the evolution of ice thickness. The theory holds only while h remains positive. Combining (3 *b* 2) and (3 *b* 4) gives a further relation

$$\frac{Dh^i}{Dt} + h^i \frac{\partial v_\alpha}{\partial x_\alpha} = \frac{\partial h^i}{\partial t} + \frac{\partial}{\partial x_\alpha}(h^i v_\alpha) = \frac{h^i k}{\rho A} + (q^i - b^i), \tag{3 b 5}$$

where

$$h^i = Ah, \quad q^i = Aq^I, \quad b^i = Ab^I, \tag{3 b 6}$$

define a partial ice thickness – the thickness of a continuous ice layer which has the same ice volume as the ice pack, and partial fluxes q^i, b^i per unit pack horizontal cross-section. Note that it is the intrinsic ice fluxes q^I, b^I which will enter the ice surface and base thermal processes, and coupling with atmosphere and ocean.

Ignoring internal freezing in the leads, mass conservation for the layer water is expressed by

$$\frac{\partial \rho^w}{\partial t} + \frac{\partial}{\partial x_\alpha}(\rho^w v_\alpha) + \frac{\partial}{\partial x_3}(\rho^w v_3^w) = -k, \tag{3 b 7}$$

where $-k$ is the mass transfer from the ice to water, and integrating through the thickness h_w using (3 *a* 3) gives

$$h_w \left\{ -\frac{DA}{Dt} + (1-A)\frac{\partial v_\alpha}{\partial x_\alpha} \right\} + [(1-A)v_3^w]_{z_b}^{z_w} = -\frac{h_w k}{\rho}. \tag{3 b 8}$$

Now the basal condition for the layer water is

$$\frac{\partial z_b}{\partial t} + v_\alpha \frac{\partial z_b}{\partial x_\alpha} - v_3^w|_{z_b} = b^W, \tag{3 b 9}$$

where b^W is the downward water flux needed to maintain the layer base at $x_3 = z_b$ continuous with the adjacent floe base. The surface condition is

$$\frac{\partial z_w}{\partial t} + v_\alpha \frac{\partial z_w}{\partial x_\alpha} - v_3^w|_{z_w} = q^W - E^W, \tag{3 b 10}$$

where q^W is the accumulation rate of water volume per unit water surface area, and E^W is the evaporation rate. Note that q^W, E^W could arise separately in the water–atmosphere coupling. Differencing shows that

$$[v_3^w]_{z_b}^{z_w} = \frac{\partial h_w}{\partial t} + v_\alpha \frac{\partial h_w}{\partial x_\alpha} - (q^W - b^W) + E^W, \tag{3 b 11}$$

and eliminating h_w by (2 *d* 14) and Dh/Dt by (3 *b* 4) gives

$$[v_3^w]_{z_b}^{z_w} = \frac{\rho}{\rho_w}(q^I - b^I) - (q^W - b^W) + E^W. \tag{3 b 12}$$

Note that $\rho_w q^W = \rho q^I$ if there is surface accumulation converting to ice and water fluxes respectively over floes and open water, but floe surface melt ($q^I < 0$) is not proportionally related to q^W. Eliminating v_3^w between (3 *b* 8) and (3 *b* 12), and DA/Dt by (3 *b* 2) determines the trapped water flux into the ocean,

$$b^W = q^W - E^W - \frac{\rho}{\rho_w}(q^I - b^I) - \frac{h_w}{1-A}\frac{\partial v_\alpha}{\partial x_\alpha}. \tag{3 b 13}$$

The first four terms are contributions needed to maintain the layer configuration due to fluxes on the ice surface and base and water surface, and the final term adds a positive downward flux when $\partial v_\alpha/\partial x_\alpha < 0$ (converging floes) and an upward flux when $\partial v_\alpha/\partial x_\alpha > 0$ (diverging floes).

The prime rôle of b^W is as a coupling interface condition with the ocean, which, per unit area of the layer base $x_3 = z_b$, receives a water volume flux

$$\frac{\rho}{\rho_w}Ab^I + (1-A)b^W = -h_w\frac{\partial v_\alpha}{\partial x_\alpha} + \frac{\rho}{\rho_w}b^I + (1-A)\left\{q^W - E^W - \frac{\rho q^I}{\rho_w}\right\}. \tag{3 b 14}$$

Salt exchange, though, is associated specifically with b^I.

The thermal balance for the ice, neglecting all mechanical working, becomes

$$\rho AC^I\dot{\Theta}^I - K^I \mathrm{div}\, A\,\mathrm{grad}\,\Theta^I = Ar^I + \psi, \tag{3 b 15}$$

where ψ is the energy absorption by the ice per unit layer volume due to phase change, freezing or melting, at layer water interfaces. With a postulate of symmetric partitioning of energy production between the phases (Morland 1992),

$$\psi = \tfrac{1}{2}kL, \tag{3 b 16}$$

where $L = 3.3 \times 10^5$ J kg^{-1} is the latent heat. Note that there is an identical energy absorption by the layer water, and the total 2ψ is the energy release by phase change. In view of the scaling (3 *a* 1), to leading order the temperature equation is

$$\rho AC^I\left(\frac{\partial\Theta^I}{\partial t} + v_\alpha\frac{\partial\Theta^I}{\partial x_\alpha}\right) - AK^I\frac{\partial^2\Theta^I}{\partial x_3^2} = \tfrac{1}{2}kL + Ar^I, \tag{3 b 17}$$

where diffusion is only significant in the vertical direction. Maximum temperature change occurs between surface and base, and for a 25 K change over $h^* = 5$ m, an estimate of the diffusion term is 2 J m^{-3} s^{-1}, probably larger with a higher gradient in a warm basal layer. Local heating and horizontal advection must be of the same magnitude, but we need estimates of k and r^I to assess the influence of the source terms. Now k is determined by the layer water energy balance, as follows. We assume the layer water is maintained at a uniform temperature Θ_M by adjacent ice floes, so there is no local heating advection or diffusion, and no flux from the conceptual base in the absence of a temperature gradient. Thus there is a balance between the surface energy flux Q^W into the water per unit water area and the radiation energy R^W absorbed into a water column of unit cross-sectional area per unit time, with the latent heat used by the phase change. That is

$$(1-A)(Q^W + R^W) = -\tfrac{1}{2}kLh_w \tag{3 b 18}$$

determines the mass transfer k in terms of Q^{W}, R^{W} and A and h_{w}, which completes the thermal balances. Note that (3 *b* 2), (3 *b* 4), (3 *b* 17) and (3 *b* 18), with (2 *d* 14) to express h_{w} in terms of h, are four scalar equations for A, h, k, Θ^{I}, if the two velocity components v_α are known, and coupling with two horizontal momentum equations will complete the system.

If we suppose that the area fraction requires (at least) time t^* to change by order unity, then since $|\partial v_\alpha/\partial x_\alpha| < 1/t^*$ with the proposed magnitudes, (3 *b* 2) requires

$$|k| \lesssim \rho/t^* \approx 10^{-3}\ \mathrm{kg\ m^{-3}\ s^{-1}}, \tag{3 b 19}$$

so (3 *b* 18) implies

$$|kL|,\ |R^{\mathrm{W}}/h_{\mathrm{w}}|,\ |Q^{\mathrm{W}}/h_{\mathrm{w}}| \lesssim 3 \times 10^2\ \mathrm{J\ m^{-3}\ s^{-1}}. \tag{3 b 20}$$

Now $R^{\mathrm{W}} \approx h_{\mathrm{w}} r^{\mathrm{W}}$ where r^{w} is the deposit per unit depth analogous to r^{I}. For a given incoming radiation at the surface of the pack there is a greater reflection from the ice than from the water, so that the net absorptions satisfy $|r^{\mathrm{I}}| \lesssim |r^{\mathrm{W}}|$. However, their magnitudes are comparable and hence both source terms in (3 *b* 17) can be significant. Further, k, determined by (3 *b* 18), must be retained in the area fraction equation (3 *b* 2) unless the prescribed q^{W}, r^{W} define much smaller values than the upper bound (3 *b* 19).

At this stage it is necessary to analyse the dynamic implications of the area fraction evolution (3 *b* 2) in view of previous invalid numerical solutions predicting $A > 1$, and we will examine the behaviour both as $A \to 1$ and $A \to 0$. Define

$$\frac{\partial v_\alpha}{\partial x_\alpha} = \eta, \quad \frac{k}{\rho} = (1 - A)u, \tag{3 b 21}$$

where $\eta \gtrless 0$ represents floes diverging and converging respectively, and by (3 *b* 21), $u \gtrless 0$ represents freezing and melting respectively due to phase change with layer water, incorporating the A dependence of k given by (3 *b* 18). Now (3 *b* 2) becomes

$$\frac{\mathrm{D}A}{\mathrm{D}t} + A(\eta + u) = u. \tag{3 b 22}$$

During a small change of A we can suppose η and u are constants, and we assert that η and u can be prescribed arbitrarily since they represent the effects of the large-scale floe dynamics and the external thermal inputs. Let $A = A_0$ at $t = 0$, then the solution to (3 *b* 22) for small changes of A from A_0 at a fixed element is

$$\left.\begin{aligned} A &= \frac{u}{\eta + u} + \left(A_0 - \frac{u}{\eta + u}\right) \exp\left(-(\eta + u)t\right) \\ \frac{\mathrm{D}A}{\mathrm{D}t} &= \left[(1 - A_0)u - A_0\eta\right] \exp\left(-(\eta + u)t\right) \end{aligned}\right\} \quad (\eta + u \neq 0), \tag{3 b 23}$$

or

$$A = A_0 + ut, \quad \frac{\mathrm{D}A}{\mathrm{D}t} = u, \quad (\eta + u = 0). \tag{3 b 24}$$

First consider A near zero with $0 < A_0 \ll 1$. We see that

$$\frac{\mathrm{D}A}{\mathrm{D}t} \geqslant 0 \quad \text{if} \quad \begin{cases} A_0\eta \leqslant (1 - A_0)u, & \eta \neq -u, \\ \eta = -u \leqslant 0, \end{cases} \tag{3 b 25}$$

when A does not decrease from A_0. Alternatively,

$$\frac{\mathrm{D}A}{\mathrm{D}t} < 0 \quad \text{if} \quad \begin{cases} A_0\eta > (1-A_0)u, & \eta \neq -u, \\ \eta = -u > 0, \end{cases} \tag{3 b 26}$$

when A decreases from A_0. The concentration A will then reach zero at a finite time t_0, and subsequently become negative, if

$$\left.\begin{aligned} \eta \neq -u: \qquad & t_0 = \frac{1}{\eta+u} \ln\left[\frac{A_0\eta - (1-A_0)u}{-u}\right], \\ \eta = -u > 0: \qquad & t_0 = \frac{A_0}{(-u)}, \end{aligned}\right\} \tag{3 b 27}$$

are real and positive. This follows immediately in the case $\eta = -u > 0$. For $\eta \neq -u$, in view of (3 b 26), it again requires $u < 0$, and since

$$\frac{A_0\eta - (1-A_0)u}{-u} = 1 + \left(\frac{A_0}{-u}\right)(\eta+u) \gtrless 1 \quad \text{as} \quad \eta + u \gtrless 0, \tag{3 b 28}$$

t_0 is positive for either sign of $\eta+u$. The remaining possibility $(3\,b\,26)_1$ with $u \geqslant 0$ (no melting and necessarily divergence $\eta > 0$) has no finite solution t_0, and

$$A \to \frac{u}{\eta+u} < A_0 \quad \text{as} \quad t \to \infty, \tag{3 b 29}$$

by (3 b 23) and $(3\,b\,26)_1$. Thus, continued edge melting $u < 0$ with divergence $\eta > 0$, or convergence $\eta < 0$ satisfying $(3\,b\,26)_1$, removes the local ice cover and the pack equations no longer apply, but must be adjoined to open water equations across a developing internal boundary. This is not a commonly expected situation.

Next consider $0 < 1 - A_0 \ll 1$, then $D(1-A)/\mathrm{D}t \geqslant 0$ if $A_0\eta \geqslant (1-A_0)u$ or $u = -\eta \leqslant 0$, and A does not exceed unity. However,

$$(1-A_0)u > A_0\eta \quad \text{or} \quad u = -\eta > 0 \quad \Rightarrow \quad \frac{\mathrm{D}}{\mathrm{D}t}(1-A) < 0, \tag{3 b 30}$$

and A becomes unity, then exceeds unity, at a finite time if

$$\frac{(1-A_0)u - A_0\eta}{\eta} < 0 \quad \text{or} \quad u = -\eta > 0. \tag{3 b 31}$$

Conditions (3 b 30) and (3 b 31) hold if

$$\eta < 0 \quad \text{and} \quad (1-A_0)u > A_0\eta \quad \text{or} \quad u = -\eta > 0; \tag{3 b 32}$$

i.e. for convergence and melting or convergence and freezing satisfying (3 b 32). Since here A_0 is close to unity, (3 b 32) is satisfied for large $(-u)$, so converging flow will almost always cause A to exceed unity if A is governed by (3 b 2). Such flow is a common situation.

In all current numerical treatments this invalid situation is avoided by artificial devices. Nikiforov *et al.* (1967) simply removed the onshore component of velocity when the concentration reached unity and Parkinson & Washington (1979) iteratively corrected the velocity so that the concentration remained below unity. These schemes do not conserve linear momentum and are a contrived coupling

which would not emerge naturally from the physical balances. Similarly, a correction scheme in a numerical solution (Hibler 1979) which, when A exceeds unity, resets new values h^{H}, A^{H} of thickness and area fraction by

$$h^{\mathrm{H}} = Ah, \quad A^{\mathrm{H}} = 1, \tag{3 b 33}$$

to preserve ice volume (mass) does not follow from the governing differential equations. However, this approach recognizes the need to redistribute ice volume through thickness change as A approaches unity in converging flow, to reflect the effects of ridging. We will now formulate a simple ridging process which leads to evolution equations which have the required asymptotic behaviour $A \to 1$ in a maintained converging flow, and which replace (3 *b* 1)–(3 *b* 5).

(*c*) *Ridging model*

A maintained converging flow at an already high ice concentration (A→ 1) region induces increasing contact forces between adjacent floes which are relieved by fracture, crushing and vertical displacement to form sails above, and keels below, the coherent ice. This ridging process is an impressive physical phenomenon, and pressure ridges are a significant proportion of the ice mass in the Arctic (Weeks 1976). The process is irreversible, with the ridged profiles remaining when the floes diverge. Figure 5 illustrates a sequence describing the convergence of two adjacent floes accompanied by ridging and the subsequent divergence in which the ice thickness does not change.

Detailed description of a ridging process depends on the stress field and on the adopted failure criteria and subsequent deformation for which there is no established theory. The detailed process is, in fact, too complex to incorporate in a large-scale model, but model calculations of local failure and deformation such as Hopkins & Hibler (1991) may lead to better forms for large-scale relations. Here we formulate directly a process in which ridging ice during convergence is redistributed smoothly over the layer surface and base to replace area fraction increase by thickness increase. We suppose that during convergence the area fraction A can be partitioned into fractions A_{c} of coherent ice not in failure, which moves horizontally, and a fraction A_{r} at failure which has an additional vertical velocity component v_3^{r} which transports ice into sails and keels, but has the same horizontal velocity as the coherent ice and layer water. Thus

$$A = A_{\mathrm{c}} + A_{\mathrm{r}}. \tag{3 c 1}$$

Let h_{c} and h_{r} be the thicknesses of the coherent and ridging ice respectively, but on the timescale t^* of the pack evolution it is supposed that the ridged ice is instantaneously redistributed to form a layer of thickness h which is smoothly varying on the pack scale l^*. Mass conservation determines the mean thickness h by

$$Ah = A_{\mathrm{c}}h_{\mathrm{c}} + A_{\mathrm{r}}h_{\mathrm{r}}. \tag{3 c 2}$$

The ice pack dynamics is therefore described in terms of a binary mixture of ice and layer water, with A, h defining the ice area fraction and thickness, but the embedded ridging process is described in terms of three constituents: layer water, coherent ice and ridging ice.

The partial densities ρ^{c}, ρ^{r} of coherent and ridging ice viewed as columns of

PHILOSOPHICAL TRANSACTIONS OF THE ROYAL SOCIETY A MATHEMATICAL, PHYSICAL & ENGINEERING SCIENCES

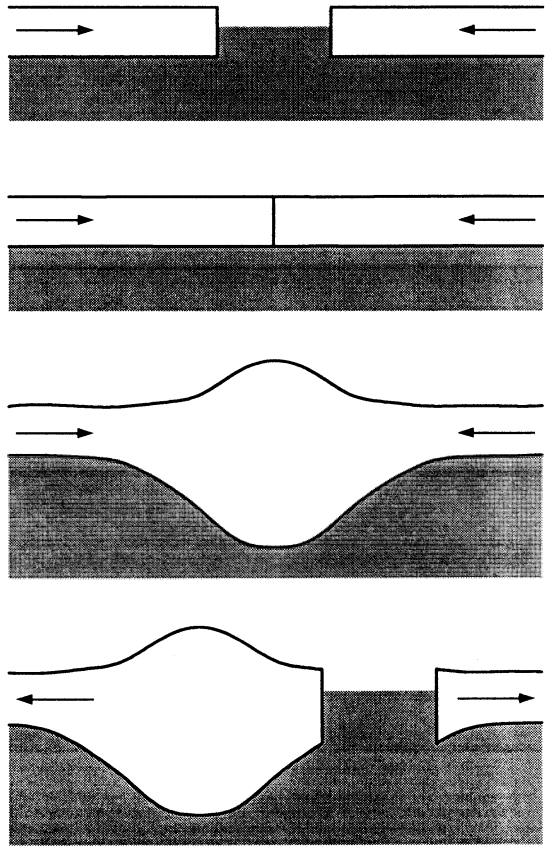

Figure 5. Convergence and divergence of adjacent floes illustrating the ridging process.

thickness h are given by

$$\rho^{\mathrm{c}} = \frac{A_{\mathrm{c}} h_{\mathrm{c}}}{h}\rho, \quad \rho^{\mathrm{r}} = \frac{A_{\mathrm{r}} h_{\mathrm{r}}}{h}\rho, \quad \rho^{\mathrm{c}} + \rho^{\mathrm{r}} = A\rho = \rho^{\mathrm{i}}, \tag{3.3}$$

where ρ^{i} is the partial density of ice in the layer. Let k^{r} be the mass transfer per unit time per unit layer volume from coherent to ridging ice, and partition the phase change transfer k arising at the floe edges by the coherent and ridging area fractions, then the respective mass conservation equations are

$$\frac{D\rho^{\mathrm{c}}}{\mathrm{D}t} + \rho^{\mathrm{c}}\eta = -k^{\mathrm{r}} + \frac{A_{\mathrm{c}}}{A}k, \tag{3.4}$$

$$\frac{D\rho^{\mathrm{r}}}{\mathrm{D}t} + \rho^{\mathrm{r}}\eta + \frac{\partial}{\partial x_3}(\rho^{\mathrm{r}} v_3^{\mathrm{r}}) = k^{\mathrm{r}} + \frac{A_{\mathrm{r}}}{A}k. \tag{3.5}$$

Here we retain the total derivative notation

$$\frac{\mathrm{D}}{\mathrm{D}t} = \frac{\partial}{\partial t} + v_\alpha \frac{\partial}{\partial x_\alpha} \tag{3.6}$$

involving only the horizontal advection. The unknown k^{r} is eliminated by sum-

ming to obtain the ice mass balance

$$\frac{D\rho^{\mathrm{i}}}{\mathrm{D}t} + \rho^{\mathrm{i}}\eta + \frac{\partial}{\partial x_3}(\rho^{\mathrm{r}} v_3^{\mathrm{r}}) = k. \tag{3 c 7}$$

Note that the ridging mechanism incorporates a vertical velocity v_3^{r} in the ridging zone which contributes to the mass divergence in (3 *c* 7), whereas purely coherent ice described in (3 *b* 1) has no vertical velocity. Integrating (3 *c* 7) through the layer thickness h gives

$$\frac{\mathrm{D}A}{\mathrm{D}t} + A\eta + \frac{A_{\mathrm{r}} h_{\mathrm{r}}}{h^2}\,[v_3^{\mathrm{r}}]_h = \frac{k}{\rho}, \tag{3 c 8}$$

where $[v_3^{\mathrm{r}}]_h$ is the velocity difference between surface and base. Now the vertical flux per unit layer cross-section out of the layer, recalling the contribution of a vertical velocity v_3 to the surface and base kinematic conditions (2 *b* 28) and (2 *b* 29) not present in (3 *b* 3), is

$$\rho^{\mathrm{r}}\,[v_3^{\mathrm{r}}]_h - \rho^{\mathrm{r}}\frac{\mathrm{D}h}{\mathrm{D}t} - \rho^{\mathrm{c}}\frac{\mathrm{D}h}{\mathrm{D}t} = -\rho A(q^{\mathrm{I}} - b^{\mathrm{I}}), \tag{3 c 9}$$

and hence

$$\frac{\mathrm{D}h}{\mathrm{D}t} = q^{\mathrm{I}} - b^{\mathrm{I}} + \frac{A_{\mathrm{r}} h_{\mathrm{r}}}{Ah}\,[v_3^{\mathrm{r}}]_h\,. \tag{3 c 10}$$

Combining (3 *c* 8) and (3 *c* 10) shows that

$$\frac{\mathrm{D}}{\mathrm{D}t}(Ah) + Ah\eta = A(q^{\mathrm{I}} - b^{\mathrm{I}}) + \frac{kh}{\rho}, \tag{3 c 11}$$

which confirms that the total volume evolution (3 *b* 5) is not influenced by the partitioning into coherent and ridging ice. The two equations (3 *c* 8) and (3 *c* 10) replace (3 *b* 2) and (3 *b* 4) for the evolution of A and h, but involve the ridging area fraction A_{r} and thickness h_{r}, and the vertical ridging velocity difference $[v_3^{\mathrm{r}}]_h$ across the layer, which must be determined by a model of the ridging process . In diverging flow, $\eta > 0$, the model will impose $[v_3^{\mathrm{r}}]_h = 0$ and the original equations (3 *b* 2) and (3 *b* 4) apply.

Now $\rho^{\mathrm{r}}[v_3^{\mathrm{r}}]_h$ is the vertical flux of mass per unit cross-section from the layer of fixed thickness h instantaneously overlapping the ice layer, and $-\rho^{\mathrm{i}}\eta h$ is the horizontal mass flux into this region. Their ratio, using (3 *c* 3),

$$-\frac{\rho^{\mathrm{r}}[v_3^{\mathrm{r}}]_h}{\rho^{\mathrm{i}}\eta h} = -\frac{A_{\mathrm{r}} h_{\mathrm{r}}}{A\eta h^2}[v_3^{\mathrm{r}}]_h = \alpha, \tag{3 c 12}$$

is zero in diverging flow and can be assumed to have the following properties during converging flow:

$$\eta < 0: \quad 0 \leqslant \alpha \leqslant 1, \quad \alpha \to 1 \quad \text{as} \quad A \to 1. \tag{3 c 13}$$

The most elementary model of ridging is to assume

$$\left.\begin{array}{ll} \eta \geqslant 0: & \alpha = 0, \\ \eta < 0: & \alpha = \alpha(A), \quad \alpha(0) = 0, \quad \alpha'(A) \geqslant 0, \quad \alpha \to 1 \quad \text{as} \quad A \to 1, \end{array}\right\} \tag{3 c 14}$$

which we adopt for the further analysis and illustrations. Then (3 *c* 8) and (3 *c* 10)

for converging flow and (3 *b* 2) and (3 *b* 4) for diverging flow are described by the common evolution equations

$$\frac{\mathrm{D}A}{\mathrm{D}t} + A\eta\,[1 - \alpha(A)H(-\eta)] = \frac{k}{\rho}, \tag{3 c 15}$$

$$\frac{\mathrm{D}h}{\mathrm{D}t} = q^{\mathrm{I}} - b^{\mathrm{I}} - \eta h\alpha(A)H(-\eta), \tag{3 c 16}$$

where $H(\theta)$ is the Heaviside unit function, which can be solved in turn for A and h. Before determining the behaviour of A for maintained convergence near $A = 1$, we can construct a model for the evolutions of the distinct ridging and coherent regions and show how they reduce to (3 *c* 15) and (3 *c* 16) for A and h, with auxiliary equations for A_{r}, A_{c}, h_{r}, h_{c}.

The partial densities of coherent and ridging ice with distinct column thicknesses h_{c} and h_{r} are given by

$$\tilde{\rho}^{\mathrm{c}} = A_{\mathrm{c}}\rho, \quad \tilde{\rho}^{\mathrm{r}} = A_{\mathrm{r}}\rho, \quad \tilde{\rho}^{\mathrm{c}} + \tilde{\rho}^{\mathrm{r}} = A\rho = \rho^{\mathrm{i}}. \tag{3 c 17}$$

Let $\tilde{k}^{\mathrm{r}}$ be the mass transfer per unit time per unit mixture volume from coherent to ridging ice, which takes place only over the common thickness h_{c} so that

$$\tilde{k}^{\mathrm{r}} h_{\mathrm{c}} = k^{\mathrm{r}} h. \tag{3 c 18}$$

The respective mass conservation equations are

$$\frac{\mathrm{D}\tilde{\rho}^{\mathrm{c}}}{\mathrm{D}t} + \tilde{\rho}^{\mathrm{c}}\eta = -\tilde{k}^{\mathrm{r}} + \frac{A_{\mathrm{c}}}{A}k, \tag{3 c 19}$$

$$\frac{\mathrm{D}\tilde{\rho}^{\mathrm{r}}}{\mathrm{D}t} + \tilde{\rho}^{\mathrm{r}}\eta + \frac{\partial}{\partial x_3}(\tilde{\rho}^{\mathrm{r}} v_3^{\mathrm{r}}) = \tilde{k}^{\mathrm{r}} + \frac{A_{\mathrm{r}}}{A}k, \tag{3 c 20}$$

with the understanding that $\tilde{k}^{\mathrm{r}} = 0$ over the excess ridging thickness

$$h_d = h_{\mathrm{r}} - h_{\mathrm{c}}. \tag{3 c 21}$$

Integrating (3 *c* 19) and (3 *c* 20) over the common thickness h_{c} gives

$$\frac{\mathrm{D}A_{\mathrm{c}}}{\mathrm{D}t} + A_{\mathrm{c}}\eta = -\frac{\tilde{k}^{\mathrm{r}}}{\rho} + \frac{A_{\mathrm{c}}}{A}\frac{k}{\rho}, \tag{3 c 22}$$

$$\frac{\mathrm{D}A_{\mathrm{r}}}{\mathrm{D}t} + A_{\mathrm{r}}\eta + \frac{A_{\mathrm{r}}}{h_{\mathrm{c}}}[v_3^{\mathrm{r}}]_{\mathrm{c}} = \frac{\tilde{k}^{\mathrm{r}}}{\rho} + \frac{A_{\mathrm{r}}}{A}\frac{k}{\rho}, \tag{3 c 23}$$

where $[v_3^{\mathrm{r}}]_{\mathrm{c}}$ is the vertical velocity difference over the thickness h_{c}. Integrating (3 *c* 20) over the excess thickness h_d with no transfer of coherent into ridging ice gives

$$\frac{\mathrm{D}A_{\mathrm{r}}}{\mathrm{D}t} + A_{\mathrm{r}}\eta + \frac{A_{\mathrm{r}}}{h_d}[v_3^{\mathrm{r}}]_d = \frac{A_{\mathrm{r}}}{A}\frac{k}{\rho}, \tag{3 c 24}$$

and comparison with (3 *c* 23) shows that

$$[v_3^{\mathrm{r}}]_d = \frac{h_d}{h_{\mathrm{c}}}[v_3^{\mathrm{r}}]_{\mathrm{c}} - \frac{h_{\mathrm{d}}\tilde{k}^{\mathrm{r}}}{\rho A_{\mathrm{r}}}, \tag{3 c 25}$$

PHILOSOPHICAL TRANSACTIONS OF THE ROYAL SOCIETY A MATHEMATICAL, PHYSICAL & ENGINEERING SCIENCES

so that, using (3 *c* 18), (3 *c* 21), the velocity difference over the ridging column is

$$[v_3^{\mathrm{r}}]_{\mathrm{r}} = [v_3^{\mathrm{r}}]_{\mathrm{c}} + [v_3^{\mathrm{r}}]_d = \frac{h_{\mathrm{r}}}{h_{\mathrm{c}}}[v_3^{\mathrm{r}}]_{\mathrm{c}} - \frac{h_d h}{\rho A_{\mathrm{r}}}\frac{k^{\mathrm{r}}}{h_{\mathrm{c}}}. \tag{3 c 26}$$

Summing (3 *c* 22) and (3 *c* 23) gives

$$\frac{\mathrm{D}A}{\mathrm{D}t} + A\eta + \frac{A_{\mathrm{r}}}{h_{\mathrm{c}}}[v_3^{\mathrm{r}}]_{\mathrm{c}} = \frac{k}{\rho}. \tag{3 c 27}$$

The surface and base kinematic conditions for the coherent and ridging ice give respectively

$$\frac{\mathrm{D}h_{\mathrm{c}}}{\mathrm{D}t} = q^{\mathrm{I}} - b^{\mathrm{I}}, \quad \frac{\mathrm{D}h_{\mathrm{r}}}{\mathrm{D}t} = q^{\mathrm{I}} - b^{\mathrm{I}} + [v_3^{\mathrm{r}}]_{\mathrm{r}}. \tag{3 c 28}$$

Correlation with a single layer of thickness h, defined by (3 *c* 2) to preserve total mass, is obtained by requiring that the mean vertical mass flux of ridging ice per unit cross section per unit thickness in the transfer region of thickness h_{c} is identified with that in the single layer of thickness h which is supposed to be formed instantaneously, thus

$$\frac{\tilde{\rho}^{\mathrm{r}}}{h_{\mathrm{c}}}[v_3^{\mathrm{r}}]_{\mathrm{c}} = \frac{\rho^{\mathrm{r}}}{h}[v_3^{\mathrm{r}}]_h. \tag{3 c 29}$$

Hence

$$[v_3^{\mathrm{r}}]_{\mathrm{c}} = \frac{h_{\mathrm{r}} h_{\mathrm{c}}}{h^2}[v_3^{\mathrm{r}}]_h, \tag{3 c 30}$$

so that the evolution equation (3 *c* 27) for A is again (3 *c* 8), and the evolution of h_{r} $(3\,c\,28)_2$ becomes

$$\frac{\mathrm{D}h_{\mathrm{r}}}{\mathrm{D}t} = q^{\mathrm{I}} - b^{\mathrm{I}} + \frac{h_{\mathrm{r}}^2}{h^2}[v_3^{\mathrm{r}}]_h - \frac{h_d h}{\rho A_{\mathrm{r}}}\frac{k^{\mathrm{r}}}{h_{\mathrm{c}}}. \tag{3 c 31}$$

Now the horizontal mass flux per unit cross-section of ridging ice is interpreted as the sum of the flux over the common thickness h_{c} and the mass transfer over the thickness h_{c}, that is

$$-\tilde{\rho}^{\mathrm{r}}\eta h_{\mathrm{r}} = -\tilde{\rho}^{\mathrm{r}}\eta h_{\mathrm{c}} + \tilde{k}^{\mathrm{r}} h_{\mathrm{c}}, \tag{3 c 32}$$

which implies that the mass transfer is given by

$$h_{\mathrm{c}}\tilde{k}^{\mathrm{r}} = -\rho A_{\mathrm{r}} h_d \eta. \tag{3 c 33}$$

Hence (3 *c* 31), using (3 *c* 18), becomes

$$\frac{\mathrm{D}h_{\mathrm{r}}}{\mathrm{D}t} = q^{\mathrm{I}} - b^{\mathrm{I}} + \frac{h_{\mathrm{r}}^2}{h^2}[v_3^{\mathrm{r}}]_h + \frac{h_d^2}{h_{\mathrm{c}}}\eta, \tag{3 c 34}$$

and (3 *c* 23) becomes, using (3 *c* 30) and (3 *c* 18),

$$\frac{\mathrm{D}A_{\mathrm{r}}}{\mathrm{D}t} + \frac{h_{\mathrm{r}}}{h_{\mathrm{c}}}A_{\mathrm{r}}\eta = \frac{A_{\mathrm{r}}}{A}\frac{k}{\rho} - \frac{A_{\mathrm{r}} h_{\mathrm{r}}}{h^2}[v_3^{\mathrm{r}}]_h. \tag{3 c 35}$$

Finally, combining (3 *c* 1), (3 *c* 2), (3 *c* 8), $(3\,c\,28)_1$, (3 *c* 34), (3 *c* 35) shows that

$$\frac{\mathrm{D}}{\mathrm{D}t}(A_{\mathrm{c}}h_{\mathrm{c}} + A_{\mathrm{r}}h_{\mathrm{r}}) = A(q^{\mathrm{I}} - b^{\mathrm{I}}) + \frac{kh}{\rho} - Ah\eta, \tag{3 c 36}$$

PHILOSOPHICAL TRANSACTIONS OF THE ROYAL SOCIETY A MATHEMATICAL, PHYSICAL & ENGINEERING SCIENCES

which confirms the total volume evolution (3 *c* 11), and hence with (3 *c* 8) recovers (3 *c* 10) for the evolution of h. The evolution equations are therefore (3 *c* 8) and (3 *c* 10) for A and h with auxiliary equations (3 *c* 35) and (3 *c* 28), (3 *c* 34) for A_r, h_c, h_r, and (3 *c* 1) for A_c. The model assumption (3 *c* 14) allows successive solution of (3 *c* 15), (3 *c* 16) for A and h, and (3 *c* 28) for h_c, but (3 *c* 34) and (3 *c* 35) are coupled equations for h_r and A_r. Note that their initial conditions at a time t_c at which convergence begins are

$$h_c(t_c) = h_r(t_c) = h(t_c), \quad A_r(t_c) = 0, \tag{3 c 37}$$

reflecting the commencement of ridging from the coherent layer at the end of diverging flow. Note that without the simplifying model assumption (3 *c* 14) the system of differential equations for A, h, A_r, h_r are coupled.

We can now return to the simplified uncoupled equation (3 *c* 15) for the evolution of A, and examine the influence of the ridging function $\alpha(A)$ in converging flow for A near zero and A near unity. For diverging flow, $\eta \geqslant 0$, (3 *c* 15) is just (3 *b* 2) and the previous conclusions apply. Near $A = 0$ we assume

$$\alpha(A) \sim \alpha_0 A \quad \text{as} \quad A \to 0, \quad \alpha_0 \geqslant 0, \tag{3 c 38}$$

so (3 *c* 15) is approximated by (3 *b* 2) and the earlier conclusions apply. Near $A = 1$ we assume

$$\alpha(A) \sim 1 - \alpha_1(1 - A) \quad \text{as} \quad A \to 1, \quad \alpha_1 \geqslant 0, \tag{3 c 39}$$

so with (3 *b* 2), (3 *c* 15) is approximated for $\eta < 0$ by

$$\eta < 0: \quad \frac{\mathrm{D}}{\mathrm{D}t}(1 - A) + (u - \alpha_1\eta)(1 - A) = 0, \tag{3 c 40}$$

where $u \gtrless 0$ represents freezing and melting respectively, subject to an initial condition

$$t = 0: \quad A = A_0 < 1, \quad A_0 \sim 1. \tag{3 c 41}$$

The solution is

$$\left.\begin{aligned} u \neq \alpha_1\eta: &\quad 1 - A = (1 - A_0)\exp\left[-(u - \alpha_1\eta)t\right], \\ u = \alpha_1\eta: &\quad 1 - A = 1 - A_0, \end{aligned}\right\} \tag{3 c 42}$$

so that $1 - A$ remains positive, and A approaches unity asymptotically if $-\alpha_1\eta > -u$, and A decreases from A_0 if $-\alpha_1\eta < -u$ which requires $u < 0$ (melting). That is, in maintained convergence, with either edge melting or freezing, the evolution equation (3 *c* 15) does not permit A to reach unity in finite time, removing the validity failure associated with the non-ridging equation (3 *b* 2).

(*d*) *Momentum balances*

We need consider only the binary mixture of the ice layer of thickness h and contained water, described in § 3 *a* and § 3 *b*. The horizontal momentum balances for ice and water are

$$\frac{\partial \sigma^{\mathrm{i}}_{\alpha\beta}}{\partial x_\beta} + \frac{\partial \sigma^{\mathrm{i}}_{\alpha 3}}{\partial x_3} + \varepsilon_{\alpha\beta 3} f_c \rho^{\mathrm{i}} v_\beta + \rho\beta^{\mathrm{i}}_\alpha + \rho\hat{\beta}^{\mathrm{i}}_\alpha = \rho^{\mathrm{i}} \frac{\mathrm{D}v_\alpha}{\mathrm{D}t}, \tag{3 d 1}$$

$$\frac{\partial \sigma^{\mathrm{w}}_{\alpha\beta}}{\partial x_\beta} + \frac{\partial \sigma^{\mathrm{w}}_{\alpha 3}}{\partial x_3} + \varepsilon_{\alpha\beta 3} f_c \rho^{\mathrm{w}} v_\beta - \rho\beta^{\mathrm{i}}_\alpha + \rho\hat{\beta}^{\mathrm{w}}_\alpha = \rho^{\mathrm{w}} \frac{\mathrm{D}v_\alpha}{\mathrm{D}t}, \tag{3 d 2}$$

PHILOSOPHICAL TRANSACTIONS OF THE ROYAL SOCIETY A MATHEMATICAL, PHYSICAL & ENGINEERING SCIENCES

where $\rho\beta^{\mathrm{i}}_{\alpha}$ are the interaction drag components per unit mixture volume on the ice due to the water (the body drag), and $\rho\hat{\beta}^{\mathrm{i}}_{\alpha}$, $\rho\hat{\beta}^{\mathrm{w}}_{\alpha}$ are the corresponding thrusts due to momentum production with phase change. The latter are negligible (Morland 1992), and the body drag components $\rho\beta^{\mathrm{i}}_{\alpha}$ are determined by the common velocity v_α assumption, being the interaction necessary to maintain the common velocity in both momentum balances. The individual ice and water balances (3 *d* 1) and (3 *d* 2) are used in § 4 *b*. Adding (3 *d* 1) and (3 *d* 2) gives a total stress equation

$$\frac{\partial \sigma_{\alpha\beta}}{\partial x_\beta} + \frac{\partial \sigma_{\alpha 3}}{\partial x_3} + \varepsilon_{\alpha\beta 3} f_{\mathrm{c}} \rho v_\beta = \rho \frac{\mathrm{D}v_\alpha}{\mathrm{D}t} \tag{3 d 3}$$

for v_α, recalling $\rho^{\mathrm{i}} + \rho^{\mathrm{w}} = \rho$, then (3 *d* 1) or (3 *d* 2) determines the necessary $\rho\beta^{\mathrm{i}}_{\alpha}$ once constitutive relations for the stresses are given. Integrating (3 *d* 3) through the layer thickness and applying the previous scaling arguments shows that

$$\frac{\partial N_{\alpha\beta}}{\partial x_\beta} + t_\alpha|_{z_{\mathrm{s}}} + t_\alpha|_{z_{\mathrm{b}}} + \varepsilon_{\alpha\beta 3} f_{\mathrm{c}} m v_\beta = m \frac{\mathrm{D}v_\alpha}{\mathrm{D}t}, \tag{3 d 4}$$

where $m = \rho h$ and the integrated horizontal stress for the pack is

$$N_{\alpha\beta} = \int_{z_{\mathrm{b}}}^{z_{\mathrm{s}}} \sigma_{\alpha\beta}\, \mathrm{d}x_3 = \int_{z_{\mathrm{b}}}^{z_{\mathrm{s}}} (\sigma^{\mathrm{i}}_{\alpha\beta} + \sigma^{\mathrm{w}}_{\alpha\beta})\, \mathrm{d}x_3. \tag{3 d 5}$$

The vertical equilibrium equations are

$$\frac{\partial \sigma^{\mathrm{i}}_{33}}{\partial x_3} + \frac{\partial \sigma^{\mathrm{i}}_{3\beta}}{\partial x_\beta} - \rho^{\mathrm{i}} g = 0, \quad \frac{\partial \sigma^{\mathrm{w}}_{33}}{\partial x_3} + \frac{\partial \sigma^{\mathrm{w}}_{3\beta}}{\partial x_\beta} - \rho^{\mathrm{w}} g = 0, \tag{3 d 6}$$

subject to surface and base conditions

$$\left.\begin{aligned} x_3 = z_{\mathrm{s}}: &\quad \sigma^{\mathrm{i}}_{33} = 0, \\ x_3 = z_{\mathrm{w}}: &\quad \sigma^{\mathrm{w}}_{33} = 0, \\ x_3 = z_{\mathrm{b}}: &\quad \sigma^{\mathrm{i}}_{33} = -A\rho_{\mathrm{w}} g h_{\mathrm{w}}, \\ &\quad \sigma^{\mathrm{w}}_{33} = -(1-A)\rho_{\mathrm{w}} g h_{\mathrm{w}}, \end{aligned}\right\} \tag{3 d 7}$$

using the partial traction relation (3 *a* 6) and leading-order results $\Delta_{\mathrm{s}} = \Delta_{\mathrm{b}} = 1$. Since $\partial/\partial x_\alpha$ is higher order in ϵ than $\partial/\partial x_3$ by the scaling, the leading-order solutions are

$$\sigma^{\mathrm{i}}_{33} = -\rho^{\mathrm{i}} g (z_{\mathrm{s}} - x_3), \quad \sigma^{\mathrm{w}}_{33} = -\rho^{\mathrm{w}} g (z_{\mathrm{w}} - x_3), \tag{3 d 8}$$

which, with (3 *a* 2), (3 *a* 3) and the intrinsic traction definitions (3 *a* 6), and basal traction condition (3 *d* 7), shows that

$$\left.\begin{aligned} \sigma^{\mathrm{i}}_{33} = A\sigma^{\mathrm{I}}_{33} = -A\rho g (z_{\mathrm{s}} - x_3), \quad \rho h = \rho_{\mathrm{w}} h_{\mathrm{w}}, \\ \sigma^{\mathrm{w}}_{33} = (1-A)\sigma^{\mathrm{W}}_{33} = -(1-A)\rho_{\mathrm{w}} g (z_{\mathrm{w}} - x_3), \end{aligned}\right\} \tag{3 d 9}$$

where σ^{I}_{33}, σ^{W}_{33} are intrinsic stress components and σ^{W}_{33} is continuous across z_{b}. In the two-dimensional depth integrated momentum equations (3 *d* 4), the shear stress $\sigma_{3\alpha}$ on horizontal planes enters only through the surface and base tangential tractions. In the water, the in-plane viscous shear stresses are negligible compared

to the pressure p^{w}, so that

$$\sigma^{\mathrm{w}}_{\alpha\beta} = -p^{\mathrm{w}}\delta_{\alpha\beta}, \quad p^{\mathrm{w}} = -\tfrac{1}{3}(\sigma^{\mathrm{w}}_{\alpha\alpha} + \sigma^{\mathrm{w}}_{33}) = -\sigma^{\mathrm{w}}_{33}. \tag{3 d 10}$$

Now on the surface the tangential wind stress acts on both ice and water, but interface roughness differences may impose different tractions, thus

$$t_\alpha|_{z_{\mathrm{s}}} = A\tau^{\mathrm{sI}}_\alpha + (1-A)\tau^{\mathrm{sW}}_\alpha, \tag{3 d 11}$$

where the superscripts I and W denote intrinsic ice and water tractions. On the base there is normal water pressure everywhere, an intrinsic tangential drag $\tau^{\mathrm{bI}}_\alpha$ acting on the ice base, and an intrinsic tangential traction $\tau^{\mathrm{bW}}_\alpha$ in the water interface. Here we suppose that the shear traction on horizontal planes in the water will not change significantly between surface and base since the viscous stresses and depth h_{w} are small. Thus

$$t_\alpha|_{z_{\mathrm{b}}} = A\left\{\tau^{\mathrm{bI}}_\alpha - p^{\mathrm{W}}n_\alpha\right\}_{z_{\mathrm{b}}} + (1-A)\left\{-\tau^{\mathrm{sW}}_\alpha - p^{\mathrm{W}}n_\alpha\right\}_{z_{\mathrm{b}}}, \tag{3 d 12}$$

and hence

$$t_\alpha|_{z_{\mathrm{s}}} + t_\alpha|_{z_{\mathrm{b}}} = A(\tau^{\mathrm{sI}}_\alpha + \tau^{\mathrm{bI}}_\alpha) - (p^{\mathrm{W}}n_\alpha)_{z_{\mathrm{b}}}, \tag{3 d 13}$$

where

$$(p^{\mathrm{W}}n_\alpha)_{z_{\mathrm{b}}} = \rho g h \frac{\partial z_{\mathrm{b}}}{\partial x_\alpha} \tag{3 d 14}$$

using (2 a 5) with $\Delta_{\mathrm{b}} = 1$, and (3 d 9) and (3 d 10). The integrated stress balance (3 d 4) becomes

$$\frac{\partial N_{\alpha\beta}}{\partial x_\beta} + A(\tau^{\mathrm{sI}}_\alpha + \tau^{\mathrm{bI}}_\alpha) - mg\frac{\partial z_{\mathrm{b}}}{\partial x_\alpha} + \varepsilon_{\alpha\beta 3} f_{\mathrm{c}} m v_\beta = m\frac{\mathrm{D}v_\alpha}{\mathrm{D}t}. \tag{3 d 15}$$

Defining extra total stress and extra integrated total stress $\boldsymbol{\sigma}^{\mathrm{e}}$, $\boldsymbol{N}^{\mathrm{e}}$, extra to the intrinsic water pressure, and integrated intrinsic water pressure, by

$$\left.\begin{aligned} \sigma_{\alpha\beta} &= \sigma^{\mathrm{e}}_{\alpha\beta} - p^{\mathrm{W}}\delta_{\alpha\beta}, & p^{\mathrm{W}} &= \rho_{\mathrm{w}} g h_{\mathrm{w}}, \\ N_{\alpha\beta} &= N^{\mathrm{e}}_{\alpha\beta} - P^{\mathrm{W}}\delta_{\alpha\beta}, & P^{\mathrm{W}} &= \tfrac{1}{2}\rho_{\mathrm{w}} g h^2_{\mathrm{w}}, \end{aligned}\right\} \tag{3 d 16}$$

analogous to (2 c 4), gives the extra stress balance

$$\frac{\partial N^{\mathrm{e}}_{\alpha\beta}}{\partial x_\beta} + A(\tau^{\mathrm{sI}}_\alpha + \tau^{\mathrm{bI}}_\alpha) - mg\frac{\partial z_{\mathrm{w}}}{\partial x_\alpha} + \varepsilon_{\alpha\beta 3} f_{\mathrm{c}} m v_\beta = m\frac{\mathrm{D}v_\alpha}{\mathrm{D}t}. \tag{3 d 17}$$

The model is completed by prescribing constitutive relations for the integrated extra pack stress $\boldsymbol{N}^{\mathrm{e}}$ in terms of the large-scale pack deformation associated with the velocity field $\boldsymbol{v}(x_\alpha, t)$.

(e) *Constitutive models*

The extra total pack stress $\boldsymbol{N}^{\mathrm{e}}$, and its gradients in the balance (3 d 17), arise from the stress field induced in the coherent ice floes by contact forces from adjacent floes during convergence. During divergence with no local contacts, the stress field is simply the water pressure and $\boldsymbol{N}^{\mathrm{e}} \equiv \boldsymbol{0}$. Now with the partial stress-intrinsic stress scalings $\boldsymbol{\sigma}^{\mathrm{i}} = A\boldsymbol{\sigma}^{\mathrm{I}}$, $p^{\mathrm{w}} = (1-A)p^{\mathrm{W}}$ consistent with the traction scalings (3 a 6), the integrated total stress given by (3 d 5) has the decomposition

$$\boldsymbol{N} = A\boldsymbol{N}^{\mathrm{I}} - (1-A)P^{\mathrm{W}}\boldsymbol{1}. \tag{3 e 1}$$

Then by $(3\,d\,16)$ the extra integrated stress is

$$\boldsymbol{N}^{\mathrm{e}} = A(\boldsymbol{N}^{\mathrm{I}} + P^{\mathrm{W}}\mathbf{1}) = A\boldsymbol{N}^{\mathrm{E}} \tag{3\,e\,2}$$

when the intrinsic stresses $\boldsymbol{N}^{\mathrm{I}}$, $\boldsymbol{N}^{\mathrm{E}}$ are interpreted as the single coherent floe stresses given by $(2\,c\,4)$. We further suppose that on the mixture length scale $\boldsymbol{N}^{\mathrm{E}}$ can be interpreted as the mean integrated extra stress in the (local) floe determined by the edge tractions induced by interactions with adjacent converging floes, extra to the water pressure. This mean stress is given by $(2\,e\,11)$ or $(2\,e\,12)$ in terms of the extra integrated tractions $\boldsymbol{T}^{\mathrm{E}}$ around the floe boundary. We noted earlier that ice–ice and ice–water contact over a floe boundary will be partitioned in some mean fractions f and $1-f$. An elementary model $f = f(A)$ was proposed to reflect simple dependence on ice concentration A, with f increasing smoothly from zero at $A = 0$ to unity at $A = 1$. On the fraction $1-f$ of the floe boundary, $\boldsymbol{T}^{\mathrm{E}} = \mathbf{0}$. We therefore propose that the mean stress integral $(2\,e\,12)$ should be applied with $\boldsymbol{T}^{\mathrm{E}}$ denoting edge tractions due to complete contact around the boundary with adjacent floes, and the reduction due to the non-contact sections modelled by the inclusion of the weighting fraction $f(A)$. Thus we make the identification

$$N^{\mathrm{e}}_{\alpha\beta} = Af\bar{N}^{\mathrm{E}}_{\alpha\beta} = \frac{Af}{S}\int_C (x_\beta - r^{\mathrm{p}}_\beta)T^{\mathrm{E}}_\alpha \,\mathrm{d}s. \tag{3\,e\,3}$$

The integral $(3\,e\,3)$ implies a dependence of $\boldsymbol{N}^{\mathrm{e}}$ on the assumed geometry and the assumed mechanisms which determine $\boldsymbol{T}^{\mathrm{E}}$. If a reference pack configuration is chosen with non-uniform floe geometries and orientations, then a non-homogeneous constitutive law would result. Further, if the adopted force mechanisms depend on displacements (deformations) from the reference configuration, even if initially isotropic, subsequent configurations would exhibit anisotropy. At this stage such models are too ambitious, and we will focus on uniform geometry and dependence only on deformation rates, a viscous model, to illustrate the application of $(3\,e\,3)$. The choice of geometry and mechanisms allows a variety of responses.

The contact interactions will depend on the relative normal and tangential velocities of the adjacent rigid floes at the interface. Recall that a failure mechanism transfers the excess horizontal flux into vertical flux in the ridging process. It is observed (Olmsted 1991) that tightly packed floes rotate as groups rather than as individuals, and we make the approximation that all floes adjacent to the central floe rotate as a rigid group. We therefore choose coordinates $x^\dagger_\alpha$ fixed in the central floe, with origin at the centre of mass of the group, so the velocity gradient $\boldsymbol{L}^\dagger$ at $\mathcal{P}$ with respect to $x^\dagger_\alpha$ is a pure strain rate $\boldsymbol{D}^\dagger$ with zero spin $\boldsymbol{W}^\dagger$; that is

$$L^\dagger_{\alpha\beta} = \frac{\partial v^\dagger_\alpha}{\partial x^\dagger_\beta} = \tfrac{1}{2}\left(\frac{\partial v^\dagger_\alpha}{\partial x^\dagger_\beta} + \frac{\partial v^\dagger_\beta}{\partial x^\dagger_\alpha}\right) = D^\dagger_{\alpha\beta}, \tag{3\,e\,4}$$

$$W^\dagger_{\alpha\beta} = \tfrac{1}{2}\left(\frac{\partial v^\dagger_\alpha}{\partial x^\dagger_\beta} - \frac{\partial v^\dagger_\beta}{\partial x^\dagger_\alpha}\right) = 0. \tag{3\,e\,5}$$

The pack velocity field $\boldsymbol{v}(x^\dagger_\alpha, t)$ is interpreted to define the velocities of centres of mass of local floes. Consider a central floe labelled by its centre of mass $\mathcal{P}$, and

PHILOSOPHICAL TRANSACTIONS OF THE ROYAL SOCIETY A MATHEMATICAL, PHYSICAL & ENGINEERING SCIENCES

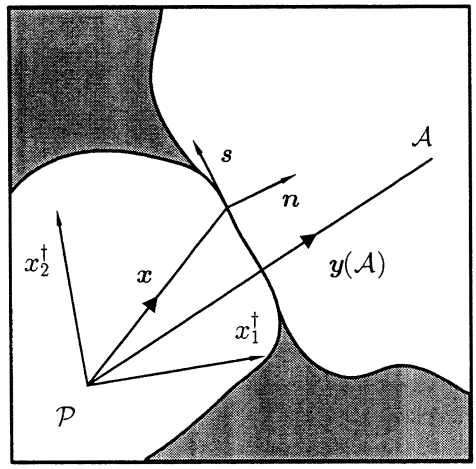

Figure 6. Geometry of adjacent floes.

an adjacent floe labelled by its centre of mass $\mathcal{A}$, illustrated in figure 6, where $\mathcal{A}$ has position vector $\boldsymbol{y}(\mathcal{A})$ relative to $\mathcal{P}$.

In $x_\alpha^\dagger$ both floes have zero spin, so the relative velocity of $\mathcal{A}$ to $\mathcal{P}$ is given by the linear Taylor series approximation

$$v_\alpha^\dagger(\mathcal{A}) - v_\alpha^\dagger(\mathcal{P}) = D_{\alpha\beta}^\dagger y_\beta^\dagger(\mathcal{A}), \tag{3 e 6}$$

since changes on the floe scale are very small compared to the pack scale. Thus, relative to $\mathcal{P}$, all points of floe $\mathcal{A}$ have a velocity

$$\check{v}_\alpha^\dagger(\mathcal{A}) = D_{\alpha\beta}^\dagger y_\beta^\dagger(\mathcal{A}), \tag{3 e 7}$$

and in particular interface points with position $\boldsymbol{x}^\dagger$ relative to $\mathcal{P}$. The normal and tangential relative velocities at $\boldsymbol{x}^\dagger$ are then

$$\check{v}_{\mathrm{n}}(\mathcal{A}, \boldsymbol{x}^\dagger) = D_{\alpha\beta}^\dagger y_\beta^\dagger(\mathcal{A}) n_\alpha^\dagger, \quad \check{v}_{\mathrm{s}}(\mathcal{A}, \boldsymbol{x}^\dagger) = D_{\alpha\beta}^\dagger y_\beta^\dagger(\mathcal{A}) s_\alpha^\dagger, \tag{3 e 8}$$

where $\boldsymbol{n}$, $\boldsymbol{s}$ are the unit normal and tangent vectors at $\boldsymbol{x}^\dagger$ shown in figure 6. Negative $\check{v}_{\mathrm{n}}(\mathcal{A}, \boldsymbol{x}^\dagger)$ is required to induce a non-zero extra stress $\boldsymbol{T}^{\mathrm{E}}$ at $\boldsymbol{x}^\dagger$. Interaction models will relate $\boldsymbol{T}^{\mathrm{E}}(\mathcal{A}, \boldsymbol{x}^\dagger)$ to the relative velocity $\check{\boldsymbol{v}}(\mathcal{A}, \boldsymbol{x}^\dagger)$ on each floe contact interface.

Application of the integral relation (3 e 3) needs an assumed local floe configuration. Consider the regular array of identical square floes as shown in figure 7, each with side l_{f}. We suppose that the ridging does not significantly adjust the domain of the floe. The relative normal and tangential velocities are uniform over each side, and by (3 e 8)

$$\left.\begin{aligned} &\check{v}_{\mathrm{n}}(\mathcal{A}) = \check{v}_{\mathrm{n}}(\mathcal{C}) = l_{\mathrm{f}} D_{11}^\dagger, \quad \check{v}_{\mathrm{n}}(\mathcal{B}) = \check{v}_{\mathrm{n}}(\mathcal{D}) = l_{\mathrm{f}} D_{22}^\dagger, \\ &\check{v}_{\mathrm{s}}(\mathcal{A}) = \check{v}_{\mathrm{s}}(\mathcal{C}) = -\check{v}_{\mathrm{s}}(\mathcal{B}) = -\check{v}_{\mathrm{s}}(\mathcal{D}) = l_{\mathrm{f}} D_{12}^\dagger. \end{aligned}\right\} \tag{3 e 9}$$

In view of the uniformity and the symmetries on opposite sides it is sensible to

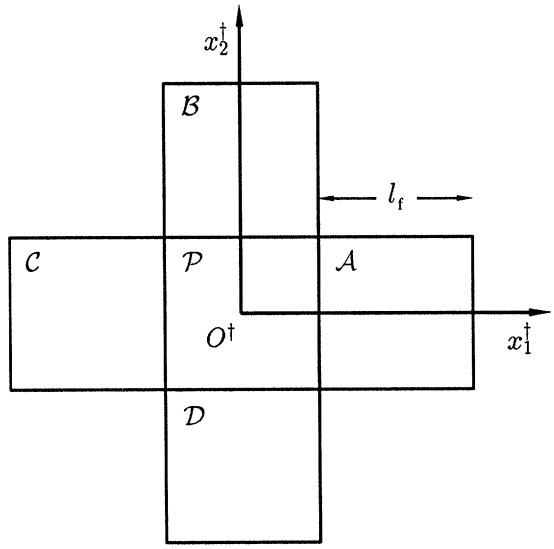

Figure 7. Geometry of adjacent square floes.

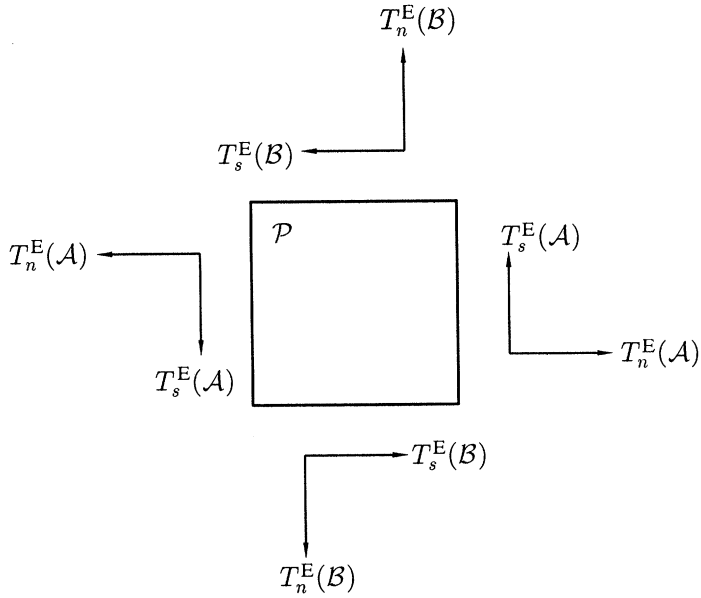

Figure 8. Tractions on the central square floe.

propose uniform tractions

$$\left.\begin{aligned} T_1^{\mathrm{E}\dagger}(\mathcal{A}) = -T_1^{\mathrm{E}\dagger}(\mathcal{C}) = T_n^{\mathrm{E}}(\mathcal{A}), \quad T_2^{\mathrm{E}\dagger}(\mathcal{B}) = -T_2^{\mathrm{E}\dagger}(\mathcal{D}) = T_n^{\mathrm{E}}(\mathcal{B}), \\ T_2^{\mathrm{E}\dagger}(\mathcal{A}) = -T_2^{\mathrm{E}\dagger}(\mathcal{C}) = T_s^{\mathrm{E}}(\mathcal{A}), \quad T_1^{\mathrm{E}\dagger}(\mathcal{B}) = -T_1^{\mathrm{E}\dagger}(\mathcal{D}) = -T_s^{\mathrm{E}}(\mathcal{B}), \end{aligned}\right\} \tag{3e10}$$

as illustrated by figure 8. It is clear that the zero moment requirement implies

$$T_s^{\mathrm{E}}(\mathcal{B}) = -T_s^{\mathrm{E}}(\mathcal{A}), \tag{3e11}$$

PHILOSOPHICAL TRANSACTIONS OF THE ROYAL SOCIETY A MATHEMATICAL, PHYSICAL & ENGINEERING SCIENCES

which is consistent with the tangential velocity result $\check{v}_{\rm s}(\mathcal{B}) = -\check{v}_{\rm s}(\mathcal{A})$ in (3 e 9). However, if we assumed a frictional law of the form $T_s^{\rm E} \propto T_n^{\rm E}$, then since $T_n^{\rm E}(\mathcal{A}) \neq T_n^{\rm E}(\mathcal{B})$ in general, the moment condition (3 e 11) would not be satisfied and this elementary view fails. The requirement (3 e 11) further implies that both of $T_s^{\rm E}(\mathcal{B})$, $T_s^{\rm E}(\mathcal{A})$ are zero or non-zero, so interfaces must both diverge or converge, which implies $D_{11}^{\dagger}$ and $D_{22}^{\dagger}$ have the same sign. This is consistent with the tight packing and rigid rotation assertion, but it is not guaranteed everywhere by the differential equations. The model assumption must therefore be to define divergence and convergence for all interfaces by $\eta \gtrless 0$, as in the ridging model, and set

$$\boldsymbol{T}^{\rm E} \equiv \boldsymbol{0}, \quad \bar{\boldsymbol{N}}^{\rm E} \equiv \boldsymbol{0} \quad \text{for} \quad \eta \geqslant 0. \tag{3 e 12}$$

We can evaluate the integral (3 e 3) for the square floe and uniform tractions on each side, with $\boldsymbol{r}^{\rm p} = \boldsymbol{0}$ in the floe coordinates $x_\alpha^{\dagger}$. Thus, for $\eta < 0$:

$$\bar{N}_{11}^{\rm E\dagger} = T_n^{\rm E}(\mathcal{A}), \quad \bar{N}_{22}^{\rm E\dagger} = T_n^{\rm E}(\mathcal{B}), \quad \bar{N}_{12}^{\rm E\dagger} = T_s^{\rm E}(\mathcal{A}). \tag{3 e 13}$$

The interaction mechanism is described by (postulated) relations between $T_n^{\rm E}(\mathcal{A})$, $T_s^{\rm E}(\mathcal{A})$ and $\check{v}_{\rm n}(\mathcal{A})$, $\check{v}_{\rm n}(\mathcal{B})$, $\check{v}_{\rm s}(\mathcal{A})$, which in turn relate the $\bar{N}_{\alpha\beta}^{\rm E\dagger}$ to the $D_{\alpha\beta}^{\dagger}$ to determine a viscous relation. This must be a tensor relation (coordinate invariant) and frame indifferent (independent of observer), and the general form in two-dimensions can be expressed as

$$\bar{\boldsymbol{N}}^{\rm E} = \{\phi_0 \boldsymbol{1} + \phi_1 \boldsymbol{D}\}\, H(-\eta), \tag{3 e 14}$$

where ϕ_0 and ϕ_1 are functions of the two independent invariants of $\boldsymbol{D}$, say η and positive γ given by

$$\eta = \frac{\partial v_\alpha}{\partial x_\alpha} = \operatorname{tr} \boldsymbol{D}, \quad \gamma^2 = \tfrac{1}{2}\operatorname{tr} \hat{\boldsymbol{D}}^2, \tag{3 e 15}$$

where

$$\hat{\boldsymbol{D}} = \boldsymbol{D} - \tfrac{1}{2}\eta \boldsymbol{1} \tag{3 e 16}$$

is the deviatoric strain rate. In components,

$$\eta = D_{11} + D_{22}, \quad \gamma^2 = D_{12}^2 + \tfrac{1}{4}(D_{11} - D_{22})^2. \tag{3 e 17}$$

η measures the rate of increase of element area per unit area, and γ measures a rate of change of shape (shearing). Corresponding integrated stress invariants $\bar{P}$, $\bar{J}$ are given by

$$\bar{P} = -\tfrac{1}{2}\operatorname{tr} \bar{\boldsymbol{N}}^{\rm E}, \quad \bar{J} = \tfrac{1}{2}\operatorname{tr} (\hat{\bar{\boldsymbol{N}}}^{\rm E})^2, \quad \hat{\bar{\boldsymbol{N}}}^{\rm E} = \bar{\boldsymbol{N}}^{\rm E} + \bar{P}\boldsymbol{1}, \tag{3 e 18}$$

defining a mean pressure and a shear stress magnitude. The equivalent inverse form of (3 e 14) is

$$\boldsymbol{D} = \psi_0 \boldsymbol{1} + \psi_1 \bar{\boldsymbol{N}}^{\rm E}, \quad \eta < 0, \tag{3 e 19}$$

where ψ_0, ψ_1 are functions of $\bar{P}$ and $\bar{J}$, and from (3 e 18), (3 e 14) and (3 e 16),

$$\bar{P} = -(\phi_0 + \tfrac{1}{2}\phi_1 \eta) H(-\eta), \quad \bar{J} = \phi_1^2 \gamma^2 H(-\eta), \quad \psi_0 = -\phi_0/\phi_1, \quad \psi_1 = 1/\phi_1. \tag{3 e 20}$$

We assert that the corresponding shear stresses and strain rates have the same sign; that is, they are not in opposite directions, so that $\phi_1 \geqslant 0$, and that $\bar{P}$ is positive in converging flow $\eta < 0$, so that $\phi_0 - \tfrac{1}{2}\phi_1(-\eta) > 0$ for all $\eta < 0$. Further,

we require continuity with the diverging flow result $\bar{\boldsymbol{N}}^{\mathrm{E}} = \boldsymbol{0}$ as $\boldsymbol{D} \to \boldsymbol{0}$, $\eta \to 0$. Thus

$$\phi_1 \geqslant 0, \quad \phi_0 < 0, \quad \phi_0 \to 0 \quad \text{as} \quad \eta \to 0 \quad \text{through negative values} \qquad (3\,e\,21)$$

for all γ; ϕ_0, ϕ_1 are not relevant in $\eta > 0$. In diverging flow, $\eta \geqslant 0$, $\boldsymbol{D}$ is not determined by $\bar{\boldsymbol{N}}^{\mathrm{E}}$.

Comparing (3 *e* 13) with (3 *e* 14) and (3 *e* 9) shows the underlying traction–relative-velocity relations,

$$\left.\begin{aligned} T_n^{\mathrm{E}}(\mathcal{A}) &= \left\{\phi_0 + \frac{\phi_1}{l_{\mathrm{f}}}\check{v}_{\mathrm{n}}(\mathcal{A})\right\} H(-\eta), \\ T_n^{\mathrm{E}}(\mathcal{B}) &= \left\{\phi_0 + \frac{\phi_1}{l_{\mathrm{f}}}\check{v}_{\mathrm{n}}(\mathcal{B})\right\} H(-\eta), \\ T_s^{\mathrm{E}}(\mathcal{A}) &= \frac{\phi_1}{l_{\mathrm{f}}}\check{v}_{\mathrm{s}}(\mathcal{A}) H(-\eta), \end{aligned}\right\} \qquad (3\,e\,22)$$

where ϕ_0, ϕ_1 are functions of the invariants

$$\left.\begin{aligned} \eta &= \{\check{v}_{\mathrm{n}}(\mathcal{A}) + \check{v}_{\mathrm{n}}(\mathcal{B})\}/l_{\mathrm{f}}, && < 0, \\ \gamma &= \left\{\check{v}_{\mathrm{s}}^2(\mathcal{A}) + \tfrac{1}{4}[\check{v}_{\mathrm{n}}(\mathcal{A}) - \check{v}_{\mathrm{n}}(\mathcal{B})]^2\right\}^{1/2}/l_{\mathrm{f}}, && > 0. \end{aligned}\right\} \qquad (3\,e\,23)$$

If we require $T_n^{\mathrm{E}}(\mathcal{A})$ to depend only on $\check{v}_{\mathrm{n}}(\mathcal{A})$ and $T_n^{\mathrm{E}}(\mathcal{B})$ to depend only on $\check{v}_{\mathrm{n}}(\mathcal{B})$; that is, normal traction on an edge to depend only on the relative velocity normal to that edge, and not on the relative tangential velocity, then immediately both ϕ_0 and ϕ_1 must be independent of γ. Then, setting the derivative of $T_n^{\mathrm{E}}(\mathcal{A})$ with respect to $\check{v}_{\mathrm{n}}(\mathcal{B})$ and the derivative of $T_n^{\mathrm{E}}(\mathcal{B})$ with respect to $\check{v}_{\mathrm{n}}(\mathcal{A})$ to zero, shows that

$$l_{\mathrm{f}}\frac{\mathrm{d}\phi_0}{\mathrm{d}\eta} + \check{v}_{\mathrm{n}}(\mathcal{A})\frac{\mathrm{d}\phi_1}{\mathrm{d}\eta} = l_{\mathrm{f}}\frac{\mathrm{d}\phi_0}{\mathrm{d}\eta} + \check{v}_{\mathrm{n}}(\mathcal{B})\frac{\mathrm{d}\phi_1}{\mathrm{d}\eta} = 0, \qquad (3\,e\,24)$$

which must hold for independent $\check{v}_{\mathrm{n}}(\mathcal{A})$ and $\check{v}_{\mathrm{n}}(\mathcal{B})$, so that ϕ_0 and ϕ_1 must be independent of η, and hence constant. Further, with the limit condition (3 *e* 21), $\phi_0 \equiv 0$, and so (3 *e* 14) reduces to a linearly viscous law

$$\bar{\boldsymbol{N}}^{\mathrm{E}} = \phi_1 \boldsymbol{D} H(-\eta) \qquad (3\,e\,25)$$

with a single constant viscosity measure ϕ_1, corresponding to a shear viscosity $\frac{1}{2}\phi_1$ and a bulk viscosity $\frac{1}{3}\phi_1$. This is not a realistic ice pack model, but may have value for numerical testing. We must therefore allow T_n^{E} to depend on both $\check{v}_{\mathrm{n}}$ and $\check{v}_{\mathrm{s}}$, and T_s^{E} to depend on both $\check{v}_{\mathrm{s}}$ and $\check{v}_{\mathrm{n}}$, with a common form for $T_n^{\mathrm{E}}(\mathcal{A})$ and $T_n^{\mathrm{E}}(\mathcal{B})$ to be consistent with the frame indifferent relation (3 *e* 14). Given $T_n^{\mathrm{E}}(\check{v}_{\mathrm{n}}, \check{v}_{\mathrm{s}})$ and $T_s^{\mathrm{E}}(\check{v}_{\mathrm{n}}, \check{v}_{\mathrm{s}})$, (3 *e* 22) are two relations for $\phi_0(\eta, \gamma)$, $\phi_1(\eta, \gamma)$, but we can alternatively explore forms of ϕ_0 and ϕ_1 and examine the implied traction relations. The law (3 *e* 14) has isotropic compression and deviatoric responses

$$\bar{P} = -(\phi_0 + \tfrac{1}{2}\phi_1\eta)H(-\eta) = \phi_3 H(-\eta) \geqslant 0, \quad \hat{\bar{\boldsymbol{N}}}^{\mathrm{E}} = \phi_1 \hat{\boldsymbol{D}}, \qquad (3\,e\,26)$$

so that shear response is governed solely by ϕ_1, but compression involves both ϕ_0 and ϕ_1 through ϕ_3. Recall the weighting factor $Af(A)$ entering the pack stress $\boldsymbol{N}^{\mathrm{e}}$ given by (3 *e* 3), implying increase of pack stresses as A increases.

Since the ridging process accelerates as $-\eta$ increases to accommodate the horizontal convergence, and ridging implies that the local ice is fracturing, it is customary to assert that the stress field is obeying some failure criterion, which in turn prohibits excessive stress rise. The conventional viscoplasticity model assumes that the stress satisfies a yield criterion throughout a converging zone. We now show by example how this much simpler nonlinearly viscous model can bound a yield or failure function of the stress invariants between close lower and upper bounds when the convergence $-\eta$ is much greater than a positive threshold value η_0. This reflects the major features of the conventional view of the above process. Consider the typical form of a yield function,

$$\bar{P}^2 + \frac{a_3^2}{a_1^2}\bar{J} = \left\{\phi_3^2 + \frac{a_3^2}{a_1^2}\phi_1^2\gamma^2\right\} H(-\eta), \tag{3 e 27}$$

where a_1, a_3 are constants. Now choose the material response functions ϕ_3, ϕ_1 in the form,

$$\phi_3 = a_3(1 - \mathrm{e}^{\eta/\eta_0}), \quad \phi_1 = \frac{a_1(1 - \mathrm{e}^{\eta/\eta_0})}{(\gamma^2 + \gamma_0^2)^{1/2}}, \tag{3 e 28}$$

where η_0, γ_0 are constants, then

$$\bar{P}^2 + \frac{a_3^2}{a_1^2}\bar{J} = a_3^2\left(1 - \mathrm{e}^{\eta/\eta_0}\right)^2\left\{1 + \frac{\gamma^2}{\gamma^2 + \gamma_0^2}\right\} H(-\eta). \tag{3 e 29}$$

For $0 \leqslant \gamma^2 \leqslant \gamma_0^2$ and $-\eta \gg \eta_0$, the yield function lies between a_3^2 and $\frac{3}{2}a_3^2$, which implies that during rapid ridging the stress combination defined by this function lies between a_3 and $1.23\,a_3$ so that a_3 is a measure of the failure stress. The constant a_1 can be chosen to provide the required weighting of $\bar{J}$ in the yield function.

A linearly viscous fluid model with constant shear viscosity μ and bulk viscosity ζ is given by

$$\phi_1 = 2\mu h, \quad \phi_3 = -\zeta\eta h, \quad \phi_0 = (\mu - \zeta)(-\eta)h, \tag{3 e 30}$$

showing the explicit dependence on h which was not shown in the general relations above for the depth integrated stresses for which the functions ϕ_0, ϕ_1, ϕ_3, should incorporate the factor h. To obtain a factor h^2, used by Overland & Pease (1988) and Loewe (1990), it is necessary to assume that the edge tractions vary linearly with depth instead of being independent of x_3.

4. Model summary

(a) *Proposed theory*

The model is a system of partial differential equations and algebraic relations for a horizontal velocity field $v_\alpha(x_\alpha, t)$, layer thickness $h(x_\alpha, t)$, auxiliary thicknesses of coherent and ridging ice $h_{\mathrm{c}}(x_\alpha, t)$, $h_{\mathrm{r}}(x_\alpha, t)$, ice area fraction $A(x_\alpha, t)$ and ridging area fraction $A_{\mathrm{r}}(x_\alpha, t)$, ice temperature $\Theta^{\mathrm{I}}(x_\alpha, x_3, t)$, integrated water pressure $P^{\mathrm{W}}(x_\alpha, t)$ and integrated extra stress $N^{\mathrm{e}}_{\alpha\beta}(x_\alpha, t)$, given the dynamic water surface $x_3 = z_{\mathrm{w}}(x_\alpha, t)$. From (2 *a* 3) and (3 *d* 9) the layer base and surface are given by

$$x_3 = z_{\mathrm{b}} = z_{\mathrm{w}} - (\rho/\rho_{\mathrm{w}})h, \quad x_3 = z_{\mathrm{s}} = z_{\mathrm{w}} + (1 - \rho/\rho_{\mathrm{w}})h, \tag{4 a 1}$$

in terms of h, where ρ and ρ_w are the constant ice and water densities. Apart from atmospheric and ocean coupling, the energy balance (3 *b* 17) is an equation for the ice temperature Θ^I which can be solved independently once the velocity field $\boldsymbol{v}$, area fraction A and thickness h have been determined by the dynamics. Thus

$$\frac{D\Theta^I}{Dt} = \frac{\partial \Theta^I}{\partial t} + v_\alpha \frac{\partial \Theta^I}{\partial x_\alpha} = \frac{K^I}{\rho C^I}\frac{\partial^2 \Theta^I}{\partial x_3^2} + \tfrac{1}{2}\frac{kL}{\rho A C^I} + \frac{r^I}{\rho C^I}, \tag{4 a 2}$$

subject to base and surface conditions of the form (2 *b* 30) and (2 *b* 31):

$$x_3 = z_b: \quad \Theta^I = \Theta_M, \quad x_3 = z_s: \quad \Theta^I = \Theta^s \quad \text{or} \quad \left[K\frac{\partial \Theta}{\partial n}\right] = -\rho q^I L, \tag{4 a 3}$$

where Θ_M is the saline water freezing temperature, L is latent heat of ice, K^I and C^I are the ice thermal conductivity and specific heat respectively, and q^I is the intrinsic ice accumulation flux at the surface.

The two momentum equations (3 *d* 17) are, for $\alpha = 1, 2$,

$$\frac{\partial N^e_{\alpha\beta}}{\partial x_\beta} + A(\tau^{sI}_\alpha + \tau^{bI}_\alpha) - \rho h g \frac{\partial z_w}{\partial x_\alpha} + \varepsilon_{\alpha\beta 3} f_c \rho h v_\beta = \rho h \frac{Dv_\alpha}{Dt}, \tag{4 a 4}$$

where f_c is the Coriolis parameter, and $\boldsymbol{\tau}^{sI}$, $\boldsymbol{\tau}^{bI}$ are the intrinsic tangential tractions due to wind stress and ocean drag respectively on the ice base. Two common models for the ocean drag are the linear and quadratic relations,

$$\boldsymbol{\tau}^{bI} = -\rho_w c_1 [\boldsymbol{v}], \quad \boldsymbol{\tau}^{bI} = -\rho_w c_2 |[\boldsymbol{v}]|[\boldsymbol{v}], \tag{4 a 5}$$

in the relative velocity $[\boldsymbol{v}]$ of the ice to the ocean, with coefficients c_1, c_2, such that $\rho_w c_1 v^*$, or $\rho_w c_2 v^{*2}$, respectively are less than τ^* (drag less than wind stress); that is

$$c_1 < 10^{-3} \text{ m s}^{-1}, \quad c_2 < 10^{-2}. \tag{4 a 6}$$

If the ocean velocity is taken at the 10 m depth, then the velocity rotation in the upper layer is accounted for by a turning angle in relation (4 *a* 5).

Evolution of area fraction A and thickness h are governed by (3 *c* 15) and (3 *c* 16) independent of the auxiliary equations for A_r, h_r, h_c and are

$$\frac{DA}{Dt} + A\eta\{1 - \alpha(A)H(-\eta)\} = \frac{k}{\rho}, \tag{4 a 7}$$

$$\frac{Dh}{Dt} = q^I - b^I - h\eta\,\alpha(A)\,H(-\eta). \tag{4 a 8}$$

These involve the horizontal velocity divergence $\eta = \partial v_\alpha / \partial x_\alpha$, and the mass transfer k to ice from layer water per unit volume per unit time given by (3 *b* 18):

$$k = -2(1 - A)\frac{\rho_w (Q^W + R^W)}{\rho h L}. \tag{4 a 9}$$

Here b^I is the intrinsic volume flux from the ice base due to phase change, Q^W is the intrinsic energy flux into the water per unit surface area per unit time, and R^W is the intrinsic radiation energy deposit per unit time into the water layer per unit cross-sectional area. Recall that $\alpha(A)$ is a prescribed model function defining the ratio of the vertical ridging flux to the horizontal flux, which increases

with A. The area evolution (4 a 7) involves the velocity through the divergence η and with the material derivative $\mathrm{D}A/\mathrm{D}t$, and the velocity is governed by the momentum equations (4 a 4) which involve both A and h, and hence coupling with the evolution system (4 a 7), (4 a 8).

Finally, there is a constitutive law for the two-dimensional integrated extra stress $\boldsymbol{N}^{\mathrm{e}}$, defined in terms of the mean floe stress $\bar{\boldsymbol{N}}^{\mathrm{E}}$ by (3 e 3). As an example, a general nonlinearly viscous law (3 e 14) has the form,

$$\boldsymbol{N}^{\mathrm{e}} = Af(A)G(h)\left\{\phi_3(\eta,\gamma)\mathbf{1} + \phi_1(\eta,\gamma)\hat{\boldsymbol{D}}\right\}H(-\eta), \tag{4 a 10}$$

where the strain rate $\boldsymbol{D}$ and deviatoric strain rate $\hat{\boldsymbol{D}}$ are given by

$$D_{\alpha\beta} = \frac{1}{2}\left(\frac{\partial v_\alpha}{\partial x_\beta} + \frac{\partial v_\beta}{\partial x_\alpha}\right), \quad \hat{\boldsymbol{D}} = \boldsymbol{D} - \tfrac{1}{2}\eta\mathbf{1}, \tag{4 a 11}$$

with invariants

$$\eta = \operatorname{tr}\boldsymbol{D}, \quad \gamma = \left\{\tfrac{1}{2}\operatorname{tr}\hat{\boldsymbol{D}}^2\right\}^{1/2}. \tag{4 a 12}$$

A general factor $G(h)$ allows arbitrary variation of the edge tractions with depth. For example,

$$G(h) = h \quad \text{and} \quad G(h) = h^2, \tag{4 a 13}$$

describe edge tractions uniform with depth as adopted in (3 e 30), and edge tractions linear in depth considered by Overland & Pease (1988) and Loewe (1990), respectively. The former is more consistent with the depth-independent horizontal velocity $v_\alpha(x_\alpha, t)$ assumption. The contact length proportion $f(A)$ is a further prescribed model function to reflect increasing ice–ice contact as A increases.

At the ice pack boundary there may be sections in contact with a shore described by zero normal velocity and either zero tangential velocity or a slip condition, but also sections in contact with open water where the extra integrated stress is zero. If outer edge melting or freezing is negligible compared to horizontal velocities, such sections are material, moving with the ice velocity. There may, of course, be calving, which would require additional physical theory. There is also a possibility of internal boundaries with open water developing and evolving in diverging zones with sustained melting when A becomes zero.

Tentative proposals for the two model functions $\alpha(A)$ and $f(A)$ are

$$\alpha(A) = A^m \quad (0 \leqslant A \leqslant 1), \quad m > 0, \tag{4 a 14}$$

or

$$\alpha(A) = \begin{cases} \dfrac{A - A_{\mathrm{f}}}{1 - A_{\mathrm{f}}} & (0 < A_{\mathrm{f}} < A < 1), \\ 0 & (0 \leqslant A \leqslant A_{\mathrm{f}}), \end{cases} \tag{4 a 15}$$

and

$$f(A) = \frac{\mathrm{e}^{-\lambda(1-A)} - \mathrm{e}^{-\lambda}}{1 - \mathrm{e}^{-\lambda}} \quad (0 \leqslant A \leqslant 1), \quad \lambda \gg 1, \tag{4 a 16}$$

but the effects of different forms must be assessed in dynamic calculations. The contact length function $f(A)$ in (4 a 16) is analogous to the factor used by Hibler (1979) to couple the ice strength to the concentration, with a modification necessary to ensure $f(0) = 0$. Hibler suggests a value $\lambda = 20$. There can be

no direct measurement of $\alpha(A)$ and $f(A)$, but they provide a flexibility to adjust the effects of varying concentration A at least in a qualitatively plausible manner. In particular, $\alpha(A)$ and the more fundamental ridging process which determines a physically plausible evolution of A in the limit $A \to 1$, is a new theoretical feature. The constitutive model now has an interpretation in terms of ice–ice contact forces, but still lacks a constructive formulation. The balances have been formulated systematically with precise definition of all the variables, and the arguments for a valid approximate two-dimensional model have been laid out. An important feature is the different structure of the equations in converging and diverging zones, defined by $\eta \gtrless 0$ respectively, and the presence of moving interfaces separating such zones.

(*b*) *Comparison*

Before illustrating the ridging process we will draw distinctions between the proposed theory and the Hibler (1979) model, which is used in current numerical applications, highlighting both the new approach to ice area fraction evolution and the differences in the basic balances. A superscript H will be attached to Hibler variables for some of which a precise definition is lacking, and comparisons are drawn with appropriate interpretations which reveal inconsistencies. We set aside the constitutive model for the ice pack stress and focus on the momentum balance and evolution of A and h.

The ice area fraction A^{H} has the same definition as A, but the ice mass m^{H} per unit mixture area and the ice thickness h^{H} are equal to the partial mass m^{i} and partial thickness h^{i}, defined by (3 *a* 4) and (3 *b* 6), respectively,

$$A^{\mathrm{H}} = A, \quad m^{\mathrm{H}} = m^{\mathrm{i}} = Am, \quad h^{\mathrm{H}} = h^{\mathrm{i}} = Ah. \tag{4 b 1}$$

The Hibler (1979) ice concentration and thickness equations are

$$\frac{\mathrm{D}A}{\mathrm{D}t} + A\frac{\partial v_\alpha}{\partial x_\alpha} = S_A^{\mathrm{H}} + \text{diffusion}, \quad A \leqslant 1, \tag{4 b 2}$$

$$\frac{\mathrm{D}h^{\mathrm{i}}}{\mathrm{D}t} + h^{\mathrm{i}}\frac{\partial v_\alpha}{\partial x_\alpha} = S_h^{\mathrm{H}} + \text{diffusion}, \tag{4 b 3}$$

where S_A^{H}, S_h^{H} are source terms and where the diffusion terms are artificially introduced to obtain a convergent numerical algorithm. They mask a serious instability inherent to the complete system of equations, caused by applying the plasticity model in divergence (Gray 1992). The mass balance equations (4 *a* 7), (4 *a* 8) in diverging flow ($\eta > 0$) can be combined to obtain the relations,

$$\frac{\mathrm{D}A}{\mathrm{D}t} + A\frac{\partial v_\alpha}{\partial x_\alpha} = \frac{k}{\rho}, \tag{4 b 4}$$

$$\frac{\mathrm{D}h^{\mathrm{i}}}{\mathrm{D}t} + h^{\mathrm{i}}\frac{\partial v_\alpha}{\partial x_\alpha} = A(q^{\mathrm{I}} - b^{\mathrm{I}}) + \frac{h^{\mathrm{i}}k}{A\rho}. \tag{4 b 5}$$

To correlate (4 *b* 2), (4 *b* 3) with (4 *b* 4), (4 *b* 5) we need the source term interpretations

$$S_A^{\mathrm{H}} = k/\rho, \quad S_h^{\mathrm{H}} = A(q^{\mathrm{I}} - b^{\mathrm{I}}) + h^{\mathrm{i}}k/A\rho, \tag{4 b 6}$$

where the mass transfer k is determined by (4 *a* 9). The source terms in Hibler (1979) are quite different, postulated in terms of prescribed seasonal growth rates.

No direct comparison of the equations is possible in convergent flow as the ridging process is a new model feature that remains valid in sustained convergence as illustrated in § 3 *b*, *c*.

The Hibler (1979) momentum balance is not comparable to the extra integrated total stress momentum balance (4 *a* 4), which was formulated for the entire ice water layer. Instead we must derive the momentum balance for the ice constituent only and assume a form for the unknown interaction drag. The partial depth integrated ice stress $N^{\mathrm{i}}_{\alpha\beta}$ and water stress $N^{\mathrm{w}}_{\alpha\beta}$, are defined as

$$N^{\mathrm{i}}_{\alpha\beta} = \int_{z_{\mathrm{b}}}^{z_{\mathrm{s}}} \sigma^{\mathrm{i}}_{\alpha\beta}\, \mathrm{d}x_3, \quad N^{\mathrm{w}}_{\alpha\beta} = \int_{z_{\mathrm{b}}}^{z_{\mathrm{s}}} \sigma^{\mathrm{w}}_{\alpha\beta}\, \mathrm{d}x_3, \tag{4 b 7}$$

and the definition of the total integrated stress (3 *d* 5) ensures that

$$N_{\alpha\beta} = N^{\mathrm{i}}_{\alpha\beta} + N^{\mathrm{w}}_{\alpha\beta}. \tag{4 b 8}$$

The partial water stress $\sigma^{\mathrm{w}}_{\alpha\beta}$ is given explicitly by (3 *d* 10), assuming that in the water the in-plane viscous shear stresses are negligible compared to the partial water pressure p^{w}. Thus the partial integrated water stress is

$$N^{\mathrm{w}}_{\alpha\beta} = -P^{\mathrm{w}}\delta_{\alpha\beta} = -(1-A)P^{\mathrm{W}}\delta_{\alpha\beta}, \tag{4 b 9}$$

and the depth integrated ice stress $N^{\mathrm{i}}_{\alpha\beta}$ is related to the total extra stress $N^{\mathrm{e}}_{\alpha\beta}$ by applying (3 *d* 16), (4 *b* 8) and (4 *b* 9):

$$N^{\mathrm{e}}_{\alpha\beta} = N^{\mathrm{i}}_{\alpha\beta} + AP^{\mathrm{W}}\delta_{\alpha\beta}. \tag{4 b 10}$$

Integrating the ice momentum balance (3 *d* 1) through the thickness, using (4 *b* 7) and the small gradient approximation, gives

$$\frac{\partial N^{\mathrm{i}}_{\alpha\beta}}{\partial x_\beta} + t^{\mathrm{i}}_\alpha|_{z_{\mathrm{s}}} + t^{\mathrm{i}}_\alpha|_{z_{\mathrm{b}}} + \varepsilon_{\alpha\beta 3} A m f_{\mathrm{c}} v_\beta + \rho\mathcal{B}^{\mathrm{i}}_\alpha = Am\frac{\mathrm{D}v_\alpha}{\mathrm{D}t}, \tag{4 b 11}$$

where $\rho\mathcal{B}^{\mathrm{i}}_\alpha$ is the depth integrated interaction drag. We again suppose that there is a normal water pressure and intrinsic drag $\tau^{\mathrm{bI}}_\alpha$ acting on the ice base, and that the ice surface is subjected to a tangential intrinsic wind stress $\tau^{\mathrm{sI}}_\alpha$. Thus

$$t^{\mathrm{i}}_\alpha|_{z_{\mathrm{s}}} = A\tau^{\mathrm{sI}}_\alpha, \quad t^{\mathrm{i}}_\alpha|_{z_{\mathrm{b}}} = A\left\{\tau^{\mathrm{bI}}_\alpha - P^{\mathrm{W}}n_\alpha\right\}_{z_{\mathrm{b}}}. \tag{4 b 12}$$

The ice momentum balance, using (4 *b* 12) with (3 *d* 14), becomes

$$\frac{\partial N^{\mathrm{e}}_{\alpha\beta}}{\partial x_\beta} + A(\tau^{\mathrm{sI}}_\alpha + \tau^{\mathrm{bI}}_\alpha) - Amg\frac{\partial z_{\mathrm{w}}}{\partial x_\alpha} + \varepsilon_{\alpha\beta 3} A m f_{\mathrm{c}} v_\beta + \rho\mathcal{B}^{\mathrm{i}}_\alpha - P^{\mathrm{W}}\frac{\partial A}{\partial x_\alpha} = Am\frac{\mathrm{D}v_\alpha}{\mathrm{D}t}, \tag{4 b 13}$$

while the Hibler (1979) momentum balance is

$$\frac{\partial \sigma^{\mathrm{H}}_{\alpha\beta}}{\partial x_\beta} + \tau^{\mathrm{sH}}_\alpha + \tau^{\mathrm{bH}}_\alpha - Amg\frac{\partial z_{\mathrm{w}}}{\partial x_\alpha} + \varepsilon_{\alpha\beta 3} A m f_{\mathrm{c}} v_\beta = Am\frac{\mathrm{D}v_\alpha}{\mathrm{D}t}. \tag{4 b 14}$$

Correlation of (4 *b* 13) with (4 *b* 14) requires

$$\sigma^{\mathrm{H}}_{\alpha\beta} = N^{\mathrm{e}}_{\alpha\beta}, \tag{4 b 15}$$

PHILOSOPHICAL TRANSACTIONS OF THE ROYAL SOCIETY A MATHEMATICAL, PHYSICAL & ENGINEERING SCIENCES

which is the first precise definition of what is meant by $\sigma^{\mathrm{H}}_{\alpha\beta}$, and

$$\tau^{\mathrm{sH}}_{\alpha} = A\tau^{\mathrm{sI}}_{\alpha} = \tau^{si}_{\alpha}, \quad \tau^{\mathrm{bH}}_{\alpha} = A\tau^{\mathrm{bI}}_{\alpha} = \tau^{bi}_{\alpha}, \tag{4 b 16}$$

which are partial tangential surface tractions, and

$$\rho\mathcal{B}^{\mathrm{i}}_{\alpha} = P^{\mathrm{W}}\frac{\partial A}{\partial x_{\alpha}}. \tag{4 b 17}$$

With the common horizontal ice and water velocity condition, (3 *a* 9), the total momentum and ice momentum equations (4 *a* 4) and (4 *a* 11) determine the interaction drag $\rho\mathcal{B}^{\mathrm{i}}_{\alpha}$. Eliminating the stress gradients and Coriolis force in turn gives the alternative forms

$$\begin{aligned}\rho\mathcal{B}^{\mathrm{i}}_{\alpha} &= (1-A)\left\{\varepsilon_{\alpha\beta 3}mf_{\mathrm{c}}v_{\beta} - mg\frac{\partial z_{\mathrm{w}}}{\partial x_{\alpha}} - m\frac{\mathrm{D}v_{\alpha}}{\mathrm{D}t}\right\} + P^{\mathrm{W}}\frac{\partial A}{\partial x_{\alpha}},\\ &= -(1-A)\left\{\frac{\partial N^{\mathrm{e}}_{\alpha\beta}}{\partial x_{\beta}} + A(\tau^{\mathrm{sI}}+\tau^{\mathrm{bI}})\right\} + P^{\mathrm{W}}\frac{\partial A}{\partial x_{\alpha}}.\end{aligned} \tag{4 b 18}$$

Suppose that the layer water has a depth independent horizontal velocity field v^{w}_{α}, then on integrating (3 *d* 2) through the layer thickness h_{w} the interaction drag (4 *b* 17) determines the motion of the water

$$m\frac{\mathrm{D}v^{\mathrm{W}}_{\alpha}}{\mathrm{D}t} = (\tau^{\mathrm{sW}}+\tau^{\mathrm{bW}}) + \varepsilon_{\alpha\beta 3}mf_{\mathrm{c}}v^{\mathrm{w}}_{\beta} - mg\frac{\partial z_{\mathrm{w}}}{\partial x_{\alpha}}, \tag{4 b 19}$$

where τ^{sW}, τ^{bW} are the tangential intrinsic wind stress and basal drag on the layer water. Essentially (4 *b* 17) is a minimum interaction force which allows the layer water to move freely in the leads unimpeded by the surrounding ice, while (4 *b* 18) is in some sense a maximum interaction force, which carries the layer water with the ice. Any alternative would require an analysis of the three-dimensional layer water motion.

Furthermore, the explicit forms used by Hibler (1979) for the surface and base tractions are

$$\left.\begin{aligned}\boldsymbol{\tau}^{\mathrm{sH}} &= \rho_{\mathrm{a}}C^{\mathrm{H}}_{\mathrm{a}}|\boldsymbol{V}^{\mathrm{H}}_{\mathrm{g}}|(\boldsymbol{V}^{\mathrm{H}}_{\mathrm{g}}\cos\phi^{\mathrm{H}} + \boldsymbol{k}\wedge\boldsymbol{V}^{\mathrm{H}}_{\mathrm{g}}\sin\phi^{\mathrm{H}}),\\ \boldsymbol{\tau}^{\mathrm{bH}} &= \rho_{\mathrm{w}}C^{\mathrm{H}}_{\mathrm{w}}|\boldsymbol{V}^{\mathrm{H}}_{\mathrm{w}}-\boldsymbol{v}|[(\boldsymbol{V}^{\mathrm{H}}_{\mathrm{w}}-\boldsymbol{v})\cos\theta^{\mathrm{H}} + \boldsymbol{k}\wedge(\boldsymbol{V}^{\mathrm{H}}_{\mathrm{w}}-\boldsymbol{v})\sin\theta^{\mathrm{H}}],\end{aligned}\right\} \tag{4 b 20}$$

which are quadratic drag relations analogous to (4 *a* 5), where $V^{\mathrm{H}}_{\mathrm{g}}$ is the geostrophic wind, $V^{\mathrm{H}}_{\mathrm{w}}$ is the geostrophic ocean current, $C^{\mathrm{H}}_{\mathrm{a}}$ and $C^{\mathrm{H}}_{\mathrm{w}}$ are air and water drag coefficients, ρ_{a} is the air density, and ϕ^{H} and θ^{H} are additional air and water turning angles associated with the planetary boundary layer. These do not include the area fraction scaling A, since $C^{\mathrm{H}}_{\mathrm{a}}$, $C^{\mathrm{H}}_{\mathrm{w}}$ are supposed to be constants, and so are inconsistent with (4 *b* 16).

5. One-dimensional analytic solution

(*a*) *One-dimensional equations*

The prime purpose of the model is to predict the dynamics and thermal processes of the ice pack coupled with atmosphere and ocean dynamics, necessarily a large-scale numerical computation. An important step will be to solve uncoupled problems, in which the driving and responding conditions at the surface and

base are prescribed, still a complex numerical problem. Section 4 has summarized the two-dimensional equations, and drawn distinctions with the model at present in use, in particular highlighting the ridging model which prevents the ice area fraction exceeding unity, and noting the different structure of the equations in converging and diverging zones, and the presence of moving interfaces separating such zones. It is essential to establish numerical algorithms which can solve accurately some idealized problems which include the main physical features of the equations and which include such moving interfaces, and so one-dimensional motions are worthy of serious investigation. Two basic problems are onshore and alongshore drift (Pritchard & Schwaegler 1975), and there have been various numerical treatments – see, for example, Leppäranta & Hibler (1985), Häikinien (1987) and Overland & Pease (1988) – making different assumptions. These have not treated the auxiliary ridging process nor dealt with a moving interface, and, most importantly, had no comparison analytic solution to verify numerical accuracy (or even the general validity of the algorithm).

A class of one-dimensional onshore drift solutions will now be constructed analytically, ignoring the Coriolis force to maintain the uni-axial motion, and ignoring the phase change and thermal fluxes at the surface and base. The ocean is assumed to remain at rest with dynamic surface $z_{\rm w} = 0$. These assumptions do not change the structure of the differential equations, so solutions will serve to test general numerical algorithms. The physical variables depend only on time t and one space coordinate $x_1 = x$, and the pack velocity and surface and base tractions have only axial components v, $\tau^{\rm sI}$, $\tau^{\rm bI}$, and only the integrated extra stress component $N^{\rm e}_{11} = N^{\rm e}$ enters the axial momentum balance. Let the pack be initially at rest with uniform thickness h_0 and ice area fraction A_0, and occupy $0 \leqslant x \leqslant l_0$, with $x = 0$ a rigid coast and $x = l_0$ the free edge bounded by water. For $t > 0$ the pack is driven onshore by a wind stress $\tau^{\rm sI}$ (< 0) such that the coast edge $x = 0$ is stationary, $v = 0$, and the ocean edge $x = l(t)$ is free of extra stress, $N^{\rm e} = 0$. In the first phase $0 \leqslant t \leqslant t_1$ the entire pack is in converging flow, and in the second phase $t_1 \leqslant t \leqslant t_2$ an expanding zone of diverging flow spreads from the floe edge $x = l(t)$, reaching the coast at time t_2.

This two phase motion is illustrated in figure 9, where $x = l_z(t)$ is the moving interface between converging and diverging flow zones labelled $R_{\rm C}$ and $R_{\rm D}$ respectively. Note that in the second phase $t > t_1$ the free edge is shown to continue to move towards the coast during the initial period of divergence, and only to reverse direction in the final stage. This was always the situation for calculated examples of the class of motions introduced later. By definition, the interface is at neutral flow, $\eta = 0$, and the velocity field is continuous. Furthermore, independent of the adopted constitutive law, we suppose the extra stress $N^{\rm e}$ is strictly negative during convergence $\eta < 0$, but approaches zero continuously as $\eta \to 0$ for continuity across the interface with the diverging zone $\eta > 0$ where $N^{\rm e} \equiv 0$. In addition, we must exclude discontinuity of wind stress across the interface, since the changing interface location has no influence on the weather system. The momentum balance $(4\,a\,4)$ therefore implies that the stress gradient $\partial N^{\rm e}/\partial x$ must be continuous across the interface, and hence zero since $N^{\rm e} \equiv 0$ in the diverging zone. Strengthening the above continuity of $N^{\rm e}$ to differentiability as $\eta \to 0$, it follows that $\partial \eta/\partial x$ must vanish at the interface. This is true for a viscous behaviour in which $N^{\rm e}$ is a differentiable function of η. The motion therefore satisfies the following conditions:

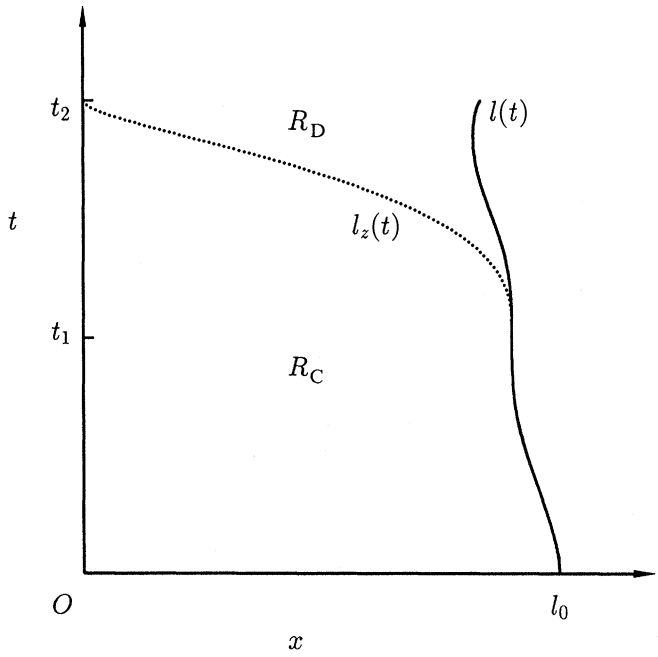

Figure 9. Free edge $l(t)$ (solid curve) and interface path $l_z(t)$ (dotted curve) separating zones of convergence R_C and divergence R_D.

$$t = 0: \quad h = h_0, \quad A = A_0, \quad v = 0; \tag{5 a 1}$$

$$x = 0: \quad v = 0; \tag{5 a 2}$$

$$x = l(t): \quad \eta = \frac{\partial v}{\partial x} = 0; \tag{5 a 3}$$

$$x = l_z(t): \quad \eta = 0, \quad \frac{\partial \eta}{\partial x} = 0, \quad v \quad \text{continuous}; \tag{5 a 4}$$

$$R_C \ (0 < x < l_z): \quad v \leqslant 0, \quad \eta \leqslant 0; \tag{5 a 5}$$

$$R_D \ (l_z < x < l): \quad \eta > 0; \tag{5 a 6}$$

$$t_1 < t < t_2: \quad 0 \leqslant l_z(t) \leqslant l(t), \quad l_z(t_1) = l(t_1), \quad l_z(t_2) = 0, \quad l_z'(t) \leqslant 0. \tag{5 a 7}$$

The ice area fraction A and thickness h evolution are governed by

$$\frac{\mathrm{D}A}{\mathrm{D}t} + A\{1 - \alpha(A)H(-\eta)\}\eta = 0, \tag{5 a 8}$$

$$\frac{\mathrm{D}h}{\mathrm{D}t} + h\eta\alpha(A)\,H(-\eta) = 0, \tag{5 a 9}$$

where

$$\eta = \frac{\partial v}{\partial x}, \quad \frac{\mathrm{D}}{\mathrm{D}t} = \frac{\partial}{\partial t} + v\frac{\partial}{\partial x}. \tag{5 a 10}$$

The momentum balance is

$$\frac{\partial N^{\mathrm{e}}}{\partial x} + A(\tau^{\mathrm{sI}} + \tau^{\mathrm{bI}}) = \rho h \frac{\mathrm{D}v}{\mathrm{D}t}, \tag{5 a 11}$$

and the two ocean drag models considered are

$$\tau^{\mathrm{bI}} = -\rho_{\mathrm{w}} c_1 v \quad \text{or} \quad \tau^{\mathrm{bI}} = -\rho_{\mathrm{w}} c_2 |v| v. \tag{5 a 12}$$

The inverse solution construction proceeds from an assumed smooth deformation field and interface motion satisfying the properties (5 *a* 2)–(5 *a* 7) and solving (5 *a* 8), (5 *a* 9) subject to (5 *a* 1) for A and h. The balance (5 *a* 11) together with a constitutive law for N^{e} and drag law (5 *a* 12) then determines the required wind stress τ^{sI}. Continuity of v and $\mathrm{D}v/\mathrm{D}t$ through $t = t_1$ will also be imposed to obtain a continuously varying wind stress through $t = t_1$. For illustrations of required wind stresses we use a linearly viscous model

$$N^{\mathrm{e}} = hAf(A)\zeta \frac{\partial v}{\partial x} H(-\eta), \tag{5 a 13}$$

where ζ is the axial viscosity and $f(A)$ is given by (4 *a* 16):

$$f(A) = \frac{\mathrm{e}^{-\lambda(1-A)} - \mathrm{e}^{-\lambda}}{1 - \mathrm{e}^{-\lambda}} \quad (0 \leqslant A \leqslant 1), \quad \lambda \gg 1. \tag{5 a 14}$$

The ridging flux ratio $\alpha(A)$ given by (4 *a* 15), which allows an analytic solution, is adopted, namely

$$\alpha(A) = \begin{cases} \alpha_{\mathrm{f}}(A - A_{\mathrm{f}}) & (0 \leqslant A_{\mathrm{f}} < A \leqslant 1), \\ 0 & (0 \leqslant A \leqslant A_{\mathrm{f}}), \end{cases} \tag{5 a 15}$$

where

$$\alpha_{\mathrm{f}} = \frac{1}{1 - A_{\mathrm{f}}} \geqslant 1. \tag{5 a 16}$$

(*b*) *Normalized variables and deformation gradient*

We adopt the normalized variables introduced in § 2 *d* with $l^* = l_0$, so that the pack length in X is initially unity, and for convenience introduce a timescale $t^{\#}$ and dimensionless time $\tilde{t}$ by

$$v^* t^{\#} = l^* = l_0, \quad t = t^{\#} \tilde{t} \tag{5 b 1}$$

with h^* and v^* prescribed as before, and $\epsilon = h^*/l_0 \ll 1$ still holds for pack lengths l_0 envisaged. Note that the timescales $t^{\#}$ and t^* defined by (2 *d* 19) are different, and $t^{\#} = 10t^*$ for $v^* = 10^{-1}$ m s^{-1}, $l_0 = 10^6$ m. Now

$$\frac{\mathrm{D}}{\mathrm{D}t} = \frac{1}{t^{\#}} \left(\frac{\partial}{\partial \tilde{t}} + \tilde{v} \frac{\partial}{\partial X} \right) = \frac{1}{t^{\#}} \frac{\tilde{\mathrm{D}}}{D\tilde{t}}, \quad \eta = \frac{\partial v}{\partial x} = \frac{1}{t^{\#}} \frac{\partial \tilde{v}}{\partial X} = \frac{1}{t^{\#}} \tilde{\eta}. \tag{5 b 2}$$

The solution is most easily constructed in material coordinates $(\xi, \tilde{t})$, where ξ is the particle position X at $\tilde{t} = 0$, and the ice pack occupies $0 \leqslant \xi \leqslant 1$ for all $\tilde{t}$. Denote a particle path by

$$X = \chi(\xi, \tilde{t}), \tag{5 b 3}$$

then the deformation gradient $F(\xi,\tilde{t})$ and velocity $\breve{v}(\xi,\tilde{t})$ are given by

$$F=\frac{\partial\chi}{\partial\xi}>0,\quad \breve{v}=\frac{\partial\chi}{\partial\tilde{t}}, \tag{5 b 4}$$

which satisfy the connexion

$$\frac{\partial F}{\partial\tilde{t}}=\frac{\partial\breve{v}}{\partial\xi}=\breve{\eta}. \tag{5 b 5}$$

Given $F(\xi,\tilde{t})$, the particle ξ position at any fixed time $\tilde{t}$ is recovered by

$$X=\int_0^{\xi}F(\xi',\tilde{t})\,\mathrm{d}\xi'. \tag{5 b 6}$$

For any function $\tilde{w}(X,\tilde{t})=\breve{w}(\xi,\tilde{t})$,

$$\frac{\partial\breve{w}}{\partial\xi}=F\frac{\partial\tilde{w}}{\partial X},\quad \frac{\partial\breve{w}}{\partial\tilde{t}}=\frac{\partial\tilde{w}}{\partial\tilde{t}}+\tilde{v}\frac{\partial\tilde{w}}{\partial X}=\frac{\tilde{D}\tilde{w}}{D\tilde{t}} \tag{5 b 7}$$

since $\tilde{v}=(\partial X/\partial\tilde{t})_{\xi}$ with the definition (5 *b* 4). In particular

$$\tilde{\eta}=\frac{\partial\tilde{v}}{\partial X}=\frac{1}{F}\frac{\partial\breve{v}}{\partial\xi}=\frac{1}{F}\frac{\partial F}{\partial\tilde{t}}=\frac{\breve{\eta}}{F}. \tag{5 b 8}$$

The evolution equations (5 *a* 8), (5 *a* 9) become

$$\frac{\partial\breve{A}}{\partial\tilde{t}}+\frac{\breve{A}}{F}\left\{1-\alpha(\breve{A})H(-\breve{\eta})\right\}\frac{\partial F}{\partial\tilde{t}}=0, \tag{5 b 9}$$

$$\frac{\partial\breve{h}}{\partial\tilde{t}}+\frac{\breve{h}}{F}\frac{\breve{A}-A_{\mathrm{f}}}{1-A_{\mathrm{f}}}H(-\breve{\eta})\frac{\partial F}{\partial\tilde{t}}=0, \tag{5 b 10}$$

with the additional condition

$$F(\xi,0)\equiv 1. \tag{5 b 11}$$

The momentum balance (5 *a* 11) becomes

$$\breve{A}\hat{\kappa}(\breve{\tau}^{\mathrm{sI}}+\breve{\tau}^{\mathrm{bI}})=\frac{v^*}{gt^{\#}\epsilon}\breve{h}\frac{\partial\breve{v}}{\partial\tilde{t}}-\frac{1}{F}\frac{\partial\breve{N}^{\mathrm{e}}}{\partial\xi}, \tag{5 b 12}$$

where

$$\hat{\kappa}=\kappa\epsilon^{-1}=O(1),\quad \breve{\tau}^{\mathrm{bI}}=-\hat{c}_1\breve{v}\ \text{ or }\ -\hat{c}_2|\breve{v}|\breve{v}, \tag{5 b 13}$$

and

$$\hat{c}_1=\frac{\rho_{\mathrm{w}}c_1v^*}{\tau^*}\lesssim O(1),\quad \hat{c}_2=\frac{\rho_{\mathrm{w}}c_2v^{*2}}{\tau^*}\lesssim O(1). \tag{5 b 14}$$

The linearly viscous law (5 *a* 13) gives a stress gradient contribution in a converging zone

$$\frac{1}{F}\frac{\partial\breve{N}^{\mathrm{e}}}{\partial\xi}=\hat{\zeta}\frac{H(-\breve{\eta})}{F^2}\left\{\breve{h}\breve{A}f(\breve{A})\left[\frac{\partial^2\breve{v}}{\partial\xi^2}-\frac{1}{F}\frac{\partial F}{\partial\xi}\frac{\partial\breve{v}}{\partial\xi}\right]+\frac{\partial\breve{v}}{\partial\xi}\frac{\partial}{\partial\xi}\left[\breve{h}\breve{A}f(\breve{A})\right]\right\}, \tag{5 b 15}$$

where

$$\hat{\zeta}=\zeta/\rho gh^*t^{\#}. \tag{5 b 16}$$

Since $\breve{v}(\xi,\tilde{t})$ is continuous through $\tilde{t}=\tilde{t}_1$, and $\breve{v}$, $\partial\breve{v}/\partial\xi$, $\partial^2\breve{v}/\partial\xi^2$ are continuous across the interface by continuity of $\tilde{v}$, $\partial\tilde{v}/\partial X$, $\partial^2\tilde{v}/\partial X^2$, the stress gradient $\partial\breve{N}^{\mathrm{e}}/\partial\xi$ is continuous throughout the motion. Continuity of the wind stress $\breve{\tau}^{\mathrm{sI}}$ through $\tilde{t}=\tilde{t}_1$, determined by (5 *b* 12), therefore requires the further restriction on the assumed motion that $\partial v/\partial t$ is continuous through $\tilde{t}=\tilde{t}_1$. For a given net force $\tau^{\mathrm{sI}}+\tau^{\mathrm{bI}}<0$ in the momentum balance (5 *b* 12), since $\partial\breve{v}/\partial\tilde{t}<0$ and $\partial\breve{N}/\partial\xi>0$ in the converging zone, the coastward acceleration decreases as $\partial\breve{N}/\partial\xi$ increases with increasing interaction resistance. Furthermore, the balance cannot be between negative $\partial\breve{v}/\partial\tilde{t}$ and positive $\partial^2\breve{v}/\partial\xi^2$ which follows from positive $\partial N^{\mathrm{e}}/\partial\xi$ in the viscous model (5 *b* 15), so the equation does not have a diffusion structure.

The solution domains are now

$$R_{\mathrm{C}}:\ \left\{\begin{array}{ll} 0\leqslant\xi\leqslant 1 & (0\leqslant\tilde{t}\leqslant\tilde{t}_1),\\ 0\leqslant\xi\leqslant\breve{L}_z(\tilde{t}) & (\tilde{t}_1\leqslant\tilde{t}\leqslant\tilde{t}_2),\end{array}\right\} \tag{5 b 17}$$

$$R_{\mathrm{D}}:\ \breve{L}_z(\tilde{t})\leqslant\xi\leqslant 1\quad(\tilde{t}_1\leqslant\tilde{t}\leqslant\tilde{t}_2), \tag{5 b 18}$$

where

$$\breve{L}_z(\tilde{t}_1)=1,\quad \breve{L}_z(\tilde{t}_2)=0,\quad \breve{L}_z'(\tilde{t})\leqslant 0. \tag{5 b 19}$$

(*c*) *Area fraction and thickness*

We will suppose that $A_0\geqslant A_{\mathrm{f}}$ so that the $\alpha(A)$ variation (5 *a* 15) applies throughout the converging flow. A solution while A first increases from $A_0<A_{\mathrm{f}}$ to A_{f} could be constructed similarly. At a given ξ, the converging flow continues to a time $\tilde{t}_z(\xi)\geqslant\tilde{t}_1$ when $\xi=\breve{L}_z(\tilde{t}_z)$, unique since $\breve{L}_z$ is monotonic. With (5 *a* 15), (5 *b* 9) becomes

$$0\leqslant\tilde{t}\leqslant\tilde{t}_z(\xi):\quad \frac{\partial\breve{A}}{\partial\tilde{t}}+\frac{\alpha_{\mathrm{f}}\breve{A}(1-\breve{A})}{F}\frac{\partial F}{\partial\tilde{t}}=0, \tag{5 c 1}$$

subject to $\breve{A}=A_0$, $F=1$, at $\tilde{t}=0$, which has the explicit integral,

$$0\leqslant\tilde{t}\leqslant\tilde{t}_z(\xi):\quad \breve{A}=\frac{A_0}{A_0+(1-A_0)F^{\alpha_{\mathrm{f}}}}. \tag{5 c 2}$$

At time $\tilde{t}_z$,

$$\tilde{t}=\tilde{t}_z(\xi):\quad \breve{A}=\breve{A}_z(\xi)=\frac{A_0}{A_0+(1-A_0)F_z^{\alpha_{\mathrm{f}}}(\xi)},\quad F_z(\xi)=F[\xi,\tilde{t}_z(\xi)], \tag{5 c 3}$$

which are the initial function values for the subsequent diverging flow described by

$$\tilde{t}_z(\xi)\leqslant\tilde{t}\leqslant\tilde{t}_2:\quad \frac{\partial\breve{A}}{\partial\tilde{t}}+\frac{\breve{A}}{F}\frac{\partial F}{\partial\tilde{t}}=0, \tag{5 c 4}$$

which has explicit integral,

$$\tilde{t}_z(\xi)\leqslant\tilde{t}\leqslant\tilde{t}_2:\quad \breve{A}=\breve{A}_z(\xi)F_z(\xi)/F. \tag{5 c 5}$$

During the converging flow (5 *b* 10) with (5 *a* 15), becomes

$$0\leqslant\tilde{t}\leqslant\tilde{t}_z(\xi):\quad \frac{\partial\breve{h}}{\partial\tilde{t}}+\frac{\alpha_{\mathrm{f}}\breve{h}(\breve{A}-A_{\mathrm{f}})}{F}\frac{\partial F}{\partial\tilde{t}}=0, \tag{5 c 6}$$

subject to $\breve{h} = h_0$, $F = 1$, at $\tilde{t} = 0$, which has the explicit integral,

$$0 \leqslant \tilde{t} \leqslant \tilde{t}_z(\xi): \quad \breve{h} = h_0 A_0/F + h_0(1 - A_0)F^{\alpha_f - 1} = h_0 A_0/FA. \tag{5 c 7}$$

At time $\tilde{t}_z$,

$$\tilde{t} = \tilde{t}_z(\xi): \quad \breve{h} = \breve{h}_z(\xi) = h_0 A_0/F_z(\xi)\breve{A}_z(\xi), \tag{5 c 8}$$

and since in the subsequent diverging flow $\partial\breve{h}/\partial\tilde{t} = 0$,

$$\tilde{t}_z(\xi) \leqslant \tilde{t} \leqslant \tilde{t}_2, \quad \breve{h} = \breve{h}_z(\xi). \tag{5 c 9}$$

If the thermal terms k, q^{I}, b^{I} are prescribed functions of t at each particle ξ, then particular integrals can be added to the solutions (5 c 2), (5 c 5), (5 c 7), leading to modified $\breve{A}$ and $\breve{h}$. The above explicit solutions for $\breve{A}(\xi, \tilde{t})$ and $\breve{h}(\xi, \tilde{t})$ depend only on the deformation gradient $F(\xi, \tilde{t})$, so solutions can be constructed for any $F(\xi, \tilde{t})$ defining a motion and interface path with the properties listed in § 5 *a*.

(*d*) *Deformation field*

The analytic expressions for $\breve{A}(\xi, \tilde{t})$, $\breve{h}(\xi, \tilde{t})$ are explicitly in terms of $F(\xi, \tilde{t})$, the deformation gradient, from which the velocity field $\breve{v}(\xi, \tilde{t})$ is determined through the connexion (5 b 5). We assume forms of $F(\xi, \tilde{t})$ in $0 \leqslant \tilde{t} \leqslant \tilde{t}_1$ and $\tilde{t}_1 \leqslant \tilde{t} \leqslant \tilde{t}_2$ which immediately satisfy some of the required conditions listed in § 5 *a*, and with flexibility to meet the others. Consider for the first phase

$$0 \leqslant \tilde{t} \leqslant \tilde{t}_1: \quad F = 1 - \Gamma(\tilde{t})(1 - \xi)^n, \quad n > 0, \tag{5 d 1}$$

where $F = 1$ initially implies $\Gamma(0) = 0$. Then by (5 b 5) and (5 b 6)

$$\frac{\partial\breve{v}}{\partial\xi} = \frac{\partial F}{\partial\tilde{t}} = -\Gamma'(\tilde{t})(1 - \xi)^n, \tag{5 d 2}$$

$$\frac{\partial^2\breve{v}}{\partial\xi^2} = n\Gamma'(\tilde{t})(1 - \xi)^{n-1}, \tag{5 d 3}$$

$$\breve{v} = -\frac{\Gamma'(\tilde{t})}{n+1}\left\{1 - (1 - \xi)^{n+1}\right\}, \tag{5 d 4}$$

$$X = \xi - \frac{\Gamma(\tilde{t})}{n+1}\left\{1 - (1 - \xi)^{n+1}\right\}, \tag{5 d 5}$$

satisfying $\breve{v} = 0$ on $\xi = 0$ and $\partial\breve{v}/\partial\xi = 0$ on $\xi = 1$, and $\breve{v} = 0$, $F = 1$ at $\tilde{t} = 0$. Then the converging flow condition $\breve{v} < 0$, $F < 1$, for $0 < \tilde{t} < \tilde{t}_1$ is satisfied provided that

$$\Gamma(0) = 0, \quad \Gamma'(0) = 0, \quad \Gamma'(\tilde{t}) > 0, \quad 0 < \Gamma(\tilde{t}) < 1 \quad (0 < \tilde{t} < \tilde{t}_1). \tag{5 d 6}$$

At the transition time $\tilde{t}_1$ the acceleration is

$$\tilde{t} = \tilde{t}_1: \quad \frac{\partial\breve{v}}{\partial\tilde{t}} = -\frac{\Gamma''(\tilde{t}_1)}{n+1}\left\{1 - (1 - \xi)^{n+1}\right\}. \tag{5 d 7}$$

The second phase $\tilde{t}_1 \leqslant \tilde{t} \leqslant \tilde{t}_2$ incorporates the interface $\xi = \breve{L}_z(\tilde{t})$ with properties (5 b 19) and interface conditions (5 a 4) which imply $\breve{v}$ and F continuous,

and $\partial\breve{v}/\partial\xi$, $\partial^2\breve{v}/\partial\xi^2$ vanishing. Consider

$$\tilde{t}_1 \leqslant \tilde{t} \leqslant \tilde{t}_2: \quad F = 1 - \Gamma_1(1-\xi)^n - c(1-\xi)\left\{(1-\xi)^n - [\breve{L}_z(\tilde{t}) - \xi]^n\right\}, \tag{5 d 8}$$

where c is a free positive parameter such that

$$\Gamma_1 = \Gamma(\tilde{t}_1) > 0, \quad c > 0, \quad \Gamma_1 + c < 1. \tag{5 d 9}$$

The latter inequality guarantees $F > 0$ at $\xi = 0$, $\tilde{t} = \tilde{t}_2$, and hence throughout the phase since $\partial F/\partial\xi > 0$ at $\tilde{t} = \tilde{t}_1$ and we will see that $\partial^2 F/\partial\xi\partial\tilde{t} = \partial^2\breve{v}/\partial\xi^2 > 0$. F is continuous at $\tilde{t} = \tilde{t}_1$ since $\breve{L}_z(\tilde{t}_1) = 1$. Now

$$\frac{\partial\breve{v}}{\partial\xi} = \frac{\partial F}{\partial\tilde{t}} = nc\breve{L}_z'(\tilde{t})(1-\xi)\left[\breve{L}_z(\tilde{t}) - \xi\right]^{n-1}, \tag{5 d 10}$$

$$\frac{\partial^2\breve{v}}{\partial\xi^2} = -nc\breve{L}_z'(\tilde{t})\left[\breve{L}_z(\tilde{t}) - \xi\right]^{n-2}\left\{\breve{L}_z(\tilde{t}) - \xi + (n-1)(1-\xi)\right\}, \tag{5 d 11}$$

$$\begin{aligned}\breve{v} = c\breve{L}_z'(\tilde{t})\{&\breve{L}_z^n(\tilde{t}) - (1-\xi)[\breve{L}_z(\tilde{t}) - \xi]^n \\ &- (n+1)^{-1}(\breve{L}_z^{n+1}(\tilde{t}) - [\breve{L}_z(\tilde{t}) - \xi]^{n+1})\},\end{aligned} \tag{5 d 12}$$

$$\begin{aligned}X = \xi &- \frac{\Gamma_1}{n+1}\{1-(1-\xi)^{n+1}\} - \frac{c}{n+2}\{1-(1-\xi)^{n+2}\} \\ &+ \frac{c}{n+1}\left\{\breve{L}_z^{n+1}(\tilde{t}) - (1-\xi)\left[\breve{L}_z(\tilde{t}) - \xi\right]^{n+1}\right\} \\ &- \frac{c}{(n+1)(n+2)}\left\{\breve{L}_z^{n+2}(\tilde{t}) - \left[\breve{L}_z(\tilde{t}) - \xi\right]^{n+2}\right\},\end{aligned} \tag{5 d 13}$$

so that $\partial\breve{v}/\partial\xi = \partial^2\breve{v}/\partial\xi^2 = 0$ at $\xi = \breve{L}_z(\tilde{t})$ and, with $\breve{L}_z' < 0$, $\partial\breve{v}/\partial\xi$ changing from negative to positive as ξ increases through $\breve{L}_z(\tilde{t})$ requires

$$n \text{ even integer } > 2 \Rightarrow \quad n = 4, 6, \ldots \tag{5 d 14}$$

Continuity of $\breve{v}$ through $\tilde{t} = \tilde{t}_1$, when $\breve{L}_z(\tilde{t}) = 1$, requires

$$nc\breve{L}_z'(\tilde{t}_1) = -\Gamma'(\tilde{t}_1) \leqslant 0. \tag{5 d 15}$$

At the transition time $\tilde{t}_1$ the acceleration is

$$\begin{aligned}\tilde{t} = \tilde{t}_1: \quad \frac{\partial\breve{v}}{\partial\tilde{t}} &= c\breve{L}_z''(\tilde{t}_1)\left\{\frac{n}{n+1}\left[1-(1-\xi)^{n+1}\right]\right\} \\ &+ (n-1)c\left[\breve{L}_z'(\tilde{t})\right]^2\{1-(1-\xi)^n\},\end{aligned} \tag{5 d 16}$$

so continuity requires

$$\breve{L}_z'(\tilde{t}_1) = \Gamma'(\tilde{t}_1) = 0, \quad nc\breve{L}_z''(\tilde{t}_1) = -\Gamma''(\tilde{t}_1). \tag{5 d 17}$$

Since $\Gamma'(\tilde{t}) > 0$ for $\tilde{t} < \tilde{t}_1$, and $\Gamma'(\tilde{t}_1) = 0$, then $\Gamma''(\tilde{t}_1) \leqslant 0$. Similarly, $\breve{L}_z'(\tilde{t}) < 0$ for $\tilde{t} > \tilde{t}_1$ and $\breve{L}_z'(\tilde{t}_1) = 0$, so $\breve{L}_z''(\tilde{t}_1) \leqslant 0$. Compatibility with (5 d 17) requires that

$$\breve{L}_z''(\tilde{t}_1) = \Gamma''(\tilde{t}_1) = 0, \tag{5 d 18}$$

and so this class of motions have the property

$$\tilde{t} = \tilde{t}_1 : \quad \breve{v} = \frac{\partial \breve{v}}{\partial \tilde{t}} \equiv 0. \tag{5 d 19}$$

Thus $\Gamma(\tilde{t})$ and $\breve{L}_z(\tilde{t})$ have the properties

$$\left.\begin{aligned} &\Gamma(0) = 0, \quad \Gamma'(0) = 0, \quad \Gamma(\tilde{t}_1) = \Gamma_1, \\ &\Gamma'(\tilde{t}_1) = \Gamma''(\tilde{t}_1) = 0, \quad \Gamma(\tilde{t}) > 0 \quad (0 \leqslant \tilde{t} \leqslant \tilde{t}_1), \end{aligned}\right\} \tag{5 d 20}$$

$$\left.\begin{aligned} &\breve{L}_z(\tilde{t}_1) = 1, \quad \breve{L}'_z(\tilde{t}_1) = \breve{L}''_z(\tilde{t}_1) = 0, \\ &\breve{L}_z(\tilde{t}_2) = 0, \quad \breve{L}'_z(\tilde{t}) < 0 \quad (\tilde{t}_1 < \tilde{t} < \tilde{t}_2). \end{aligned}\right\} \tag{5 d 21}$$

The most simple polynomials meeting these requirements are

$$\left.\begin{aligned} \Gamma(\tilde{t}) &= \Gamma_1 \left(\frac{\tilde{t}}{\tilde{t}_1}\right)^2 \left\{6 - 8\left(\frac{\tilde{t}}{\tilde{t}_1}\right) + 3\left(\frac{\tilde{t}}{\tilde{t}_1}\right)^2\right\}, \\ \Gamma'(\tilde{t}) &= 12\frac{\Gamma_1}{\tilde{t}_1}\left(\frac{\tilde{t}}{\tilde{t}_1}\right)\left\{1 - \left(\frac{\tilde{t}}{\tilde{t}_1}\right)\right\}^2, \\ \Gamma''(\tilde{t}) &= 12\frac{\Gamma_1}{\tilde{t}_1^2}\left\{1 - 4\left(\frac{\tilde{t}}{\tilde{t}_1}\right) + 3\left(\frac{\tilde{t}}{\tilde{t}_1}\right)^2\right\}, \end{aligned}\right\} \tag{5 d 22}$$

$$1\breve{L}_z(\tilde{t}) = 1 - \frac{(\tilde{t} - \tilde{t}_1)^3}{(\tilde{t}_2 - \tilde{t}_1)^3}, \quad \breve{L}'_z(\tilde{t}) = -3\frac{(\tilde{t} - \tilde{t}_1)^2}{(\tilde{t}_2 - \tilde{t}_1)^3}, \quad \breve{L}''_z(\tilde{t}) = -6\frac{(\tilde{t} - \tilde{t}_1)}{(\tilde{t}_2 - \tilde{t}_1)^3}, \tag{5 d 23}$$

which give a deformation gradient field

$$0 \leqslant \tilde{t} \leqslant \tilde{t}_1 : \; F = 1 - \Gamma_1 \left(\frac{\tilde{t}}{\tilde{t}_1}\right)^2 \left\{6 - 8\left(\frac{\tilde{t}}{\tilde{t}_1}\right) + 3\left(\frac{\tilde{t}}{\tilde{t}_1}\right)^2\right\}(1 - \xi)^n, \tag{5 d 24}$$

$$\tilde{t}_1 \leqslant \tilde{t} \leqslant \tilde{t}_2 : \; F = 1 - \Gamma_1(1 - \xi)^n - c(1 - \xi)\left\{(1 - \xi)^n - \left[1 - \xi - \frac{(\tilde{t} - \tilde{t}_1)^3}{(\tilde{t}_2 - \tilde{t}_1)^3}\right]^n\right\}. \tag{5 d 25}$$

A choice

$$\Gamma_1 = c = \tfrac{1}{8} \tag{5 d 26}$$

determines a maximum compression at the coast at time $\tilde{t} = \tilde{t}_2$ corresponding to $F = 0.75$.

(*e*) *Illustrations*

The above construction is now used to illustrate a motion with converging and diverging zones. We determine the ice thickness and area evolution, and the required wind stress when the ice response is described by a linearly viscous fluid model, for both linear and quadratic drags. We adopt the parameters,

$$h^* = 5 \text{ m}, \quad l^* = l_0 = 10^6 \text{ m}, \quad v^* = 10^{-1} \text{ m s}^{-1}, \quad \tau^* = 10^{-1} \text{ N m}^{-2}, \tag{5 e 1}$$

Figure 10 Figure 11

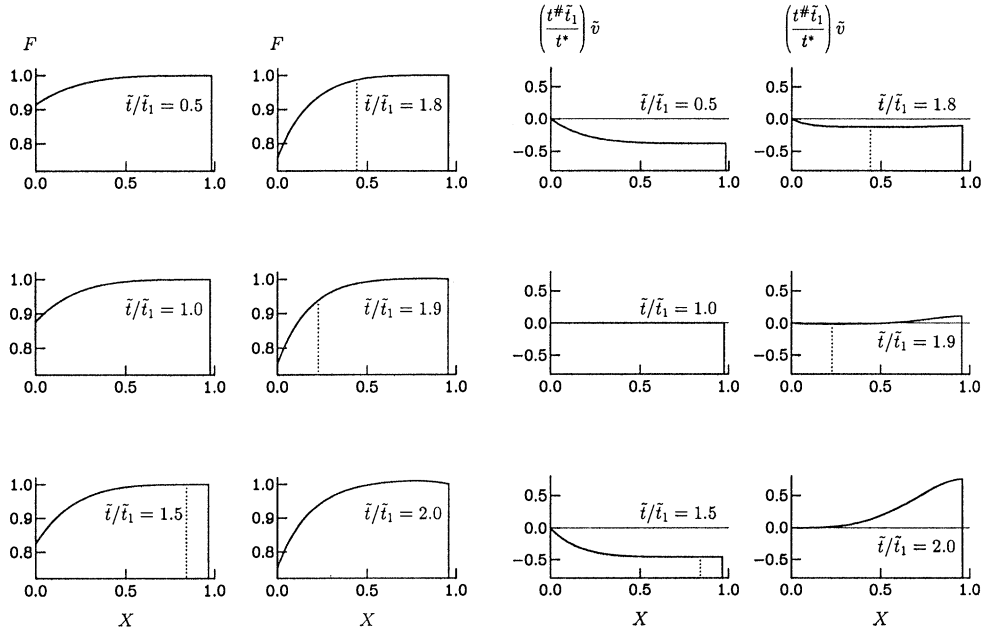

Figure 10. The deformation gradient variations F with X are shown at a sequence of time ratios. These hold for cases (i)–(iii) and (a), (b), because F is independent of the concentrations A_f, A_0 and the times $\tilde{t}_1$, $\tilde{t}_2$. The dotted line shows location of the interface $L_z(\tilde{t})$ and the vertical solid line shows location of the free edge $L(\tilde{t})$.

Figure 11. The velocity distribution $\tilde{v}$ as a function of X is shown at a sequence of time ratios, common to cases (i)–(iii). The factor $\tilde{t}_1$ is included to eliminate explicit dependence on $\tilde{t}_1$ and a further factor $t^{\#}/t^*$ is used to renormalize. In case (a) $t^{\#}\tilde{t}_1/t^* = 1$ and in case (b) $t^{\#}\tilde{t}_1/t^* = 0.5$, so in case (b) $\tilde{v}$ is double the shown velocity scale. The dotted line shows location of the interface $L_z(\tilde{t})$ and the vertical solid line shows location of the free edge $L(\tilde{t})$.

so that

$$\epsilon = 5 \times 10^{-6}, \quad \kappa = 2.22 \times 10^{-6}, \quad \hat{\kappa} = 0.444, \tag{5 e 2}$$

and

$$t^{\#} = 10^7 \text{ s} = 10t^*, \quad v^*/g\epsilon t^{\#} = 2.04 \times 10^{-4}, \quad \rho g h^* t^{\#} = 4.5 \times 10^{11} \text{ N m}^{-2} \text{ s}. \tag{5 e 3}$$

For the wind stress calculations we need further drag properties. The linear and quadratic drag relations (5 *b* 13) with coefficients

$$\hat{c}_1 = 10^3 c_1 = 0.55, \quad \hat{c}_2 = 10^2 c_2 = 0.55, \tag{5 e 4}$$

where c_1 has unit m s^{-1} and c_2 is dimensionless, are chosen on the basis of Hibler's (1979) quadratic drag value. We adopt a contact length fraction function $f(A)$ defined by (5 *a* 14) with

$$\lambda = 20, \tag{5 e 5}$$

which corresponds to the Hibler (1979) approximation. Two linearly viscous models are considered, with distinct viscosities. The first provides a competitive balance between the stress gradient (5 *b* 15) in (5 *b* 12) with the wind stress and basal

PHILOSOPHICAL TRANSACTIONS OF THE ROYAL SOCIETY A MATHEMATICAL, PHYSICAL & ENGINEERING SCIENCES

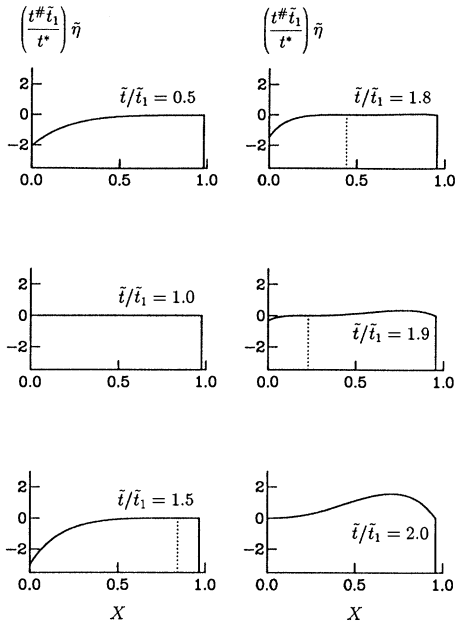

Figure 12. The divergence $\tilde{\eta} = \partial\tilde{v}/\partial X$ as a function of X is shown at a sequence of time ratios, common to cases (i)–(iii). The factor $\tilde{t}_1$ is included to eliminate explicit dependence on $\tilde{t}_1$ and a further factor $t^{\#}/t^*$ is used to renormalise. In case (*a*) $t^{\#}\tilde{t}_1/t^* = 1$ and in case (*b*) $t^{\#}\tilde{t}_1/t^* = 0.5$, so in case (*b*) $\tilde{\eta}$ is double the shown divergence scale. The dotted line shows location of the interface $L_z(\tilde{t})$ and the vertical solid line shows location of the free edge $L(\tilde{t})$.

drag, and the second corresponds to Hibler's (1979) integrated viscous law:

$$\left.\begin{aligned} \zeta = \zeta_1 = 5 \times 10^{10}\ \text{kg m}^{-1}\ \text{s}^{-1}, \qquad \hat{\zeta}_1 = 0.111, \\ \zeta = \zeta_2 = 1.25 \times 10^{12}\ \text{kg m}^{-1}\ \text{s}^{-1}, \qquad \hat{\zeta}_2 = 2.777. \end{aligned}\right\} \tag{5 e 6}$$

The examples all use

$$n = 4, \quad \breve{h}_0 = 0.5, \quad h_0 = 2.5\ \text{m}, \tag{5 e 7}$$

and three sets of critical and initial area fractions are explored:

$$\left.\begin{aligned} &\text{(i)} \quad A_{\text{f}} = 0.5, \quad \alpha_{\text{f}} = 2, \quad A_0 = 0.5; \\ &\text{(ii)} \quad A_{\text{f}} = 0.5, \quad \alpha_{\text{f}} = 2, \quad A_0 = 0.75; \\ &\text{(iii)} \quad A_{\text{f}} = 0.75, \quad \alpha_{\text{f}} = 4, \quad A_0 = 0.75. \end{aligned}\right\} \tag{5 e 8}$$

In view of the distinct magnitudes $t^{\#}$, t^* related by (5 *e* 3), the dimensionless phase times $\tilde{t}_1$, $\tilde{t}_2$ are chosen to reflect weather system scales, and two pairs have been investigated:

$$\left.\begin{aligned} &(a) \quad \tilde{t}_1 = t^*/t^{\#}, \qquad \tilde{t}_2 = 2t^*/t^{\#}; \\ &(b) \quad \tilde{t}_1 = t^*/(2t^{\#}), \qquad \tilde{t}_2 = t^*/t^{\#}. \end{aligned}\right\} \tag{5 e 9}$$

In both, the ratio $\tilde{t}_2/\tilde{t}_1$ has the same value 2. The second pair represents the deformation evolution at double the rate of the first in view of the dependence of F, (5 *d* 24), (5 *d* 25), on $\tilde{t}/\tilde{t}_1$ and $\tilde{t}_1/\tilde{t}_2$ only, but not so the velocity, divergence, stress gradient and wind stress which have explicit dependence on $\tilde{t}_1$ as well as on

Figure 13 Figure 14

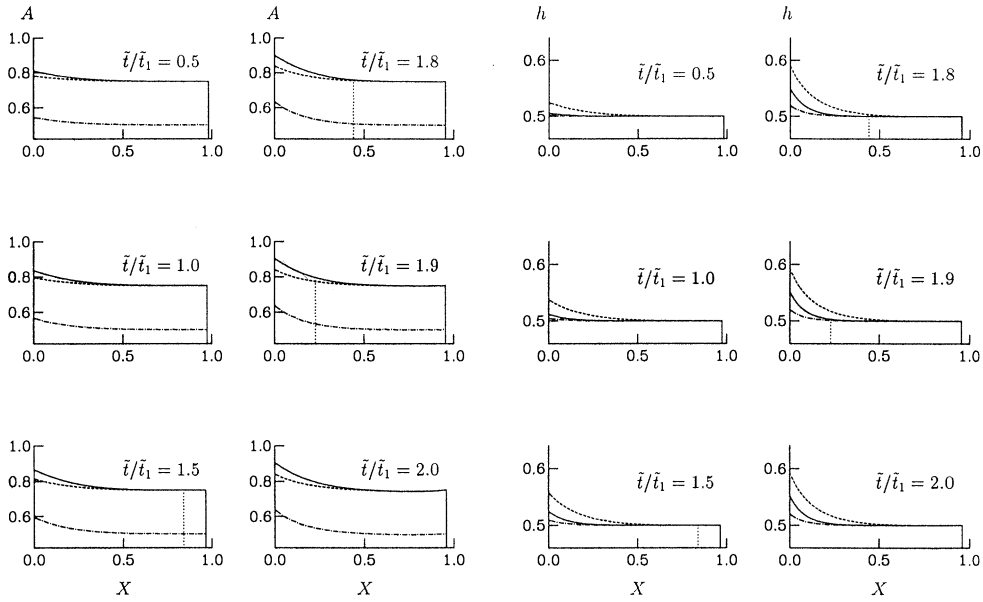

Figure 13. Ice area fraction distribution A at a sequence of time ratios, for sets (i) (dot–dash curve), (ii) (dashed curve) and (iii) (solid curve). These hold for cases (a) and (b), because A is independent of the times $\tilde{t}_1$ and $\tilde{t}_2$. The dotted line shows location of the interface $L_z(\tilde{t})$ and the vertical solid line shows location of the free edge $L(\tilde{t})$.

Figure 14. Ice thickness distribution $\tilde{h}$ at a sequence of time ratios, for sets (i) (dot–dash curve), (ii) (dashed curve) and (iii) (solid curve). These hold for cases (a) and (b), because $\tilde{h}$ is independent of the times $\tilde{t}_1$ and $\tilde{t}_2$. The dotted line shows location of the interface $L_z(\tilde{t})$ and the vertical solid line shows location of the free edge $L(\tilde{t})$.

$\tilde{t}/\tilde{t}_1$. It is therefore convenient to display calculated physical variables as functions of X at a sequence of fixed times ratios $\tilde{t}/\tilde{t}_1$, with the major distinctions occurring in the wind stress displays.

The free edge path $X = L(\tilde{t})$, interface path $X = L_z(\tilde{t})$, and the kinematic variables F, $\tilde{v}$, $\tilde{\eta}$ are independent of A_f and A_0. Further, $\tilde{t}_1\tilde{v}$ and $\tilde{t}_1\tilde{\eta}$ are functions only of $\tilde{t}/\tilde{t}_1$ in view of $(5\,d\,4)$, $(5\,d\,12)$, $(5\,d\,2)$, $(5\,d\,10)$ and $(5\,d\,22)$, $(5\,d\,23)$. Figure 10 shows a sequence of deformation gradient variations F with X at different time ratios $\tilde{t}/\tilde{t}_1$. These are independent of A_f, A_0 and the times $\tilde{t}_1$, $\tilde{t}_2$ and hence are common to cases (i)–(iii) and (a), (b). Also shown are the free edge path $X = L(\tilde{t})$ and the interface path $X = L_z(\tilde{t})$. In figure 11 the velocity $\tilde{v}$ is shown with the factor $\tilde{t}_1$ to eliminate explicit dependence on $\tilde{t}_1$ and a further factor $t^{\#}/t^*$ to renormalize. In case (a) $t^{\#}\tilde{t}_1/t^* = 1$ and in case (b) $t^{\#}\tilde{t}_1/t^* = 0.5$, so in case (b) $\tilde{v}$ is double the shown scaled velocity. The figure shows velocity as a function of X at a sequence of different time ratios $\tilde{t}/\tilde{t}_1$, common to cases (i)–(iii). Figure 12 shows the divergence η in a similarly scaled form, common to cases (i)–(iii). The more rapid changes arise near the end of the second phase, particularly the velocity and divergence in the diverging zone to the right of the interface, indicated by the dotted line.

Figures 13 and 14 show the area fraction A and thickness $\tilde{h}$ at the same times for each of the sets (i)–(iii) in $(5\,e\,8)$. The distinctions between cases (i) and (ii)

PHILOSOPHICAL TRANSACTIONS OF THE ROYAL SOCIETY A MATHEMATICAL, PHYSICAL & ENGINEERING SCIENCES

Figure 15

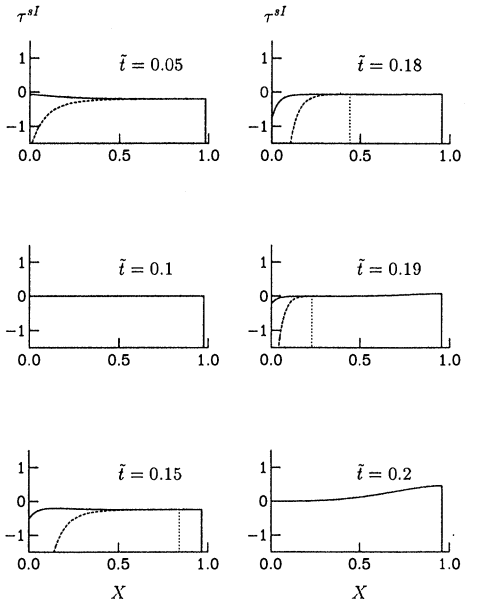

Figure 16

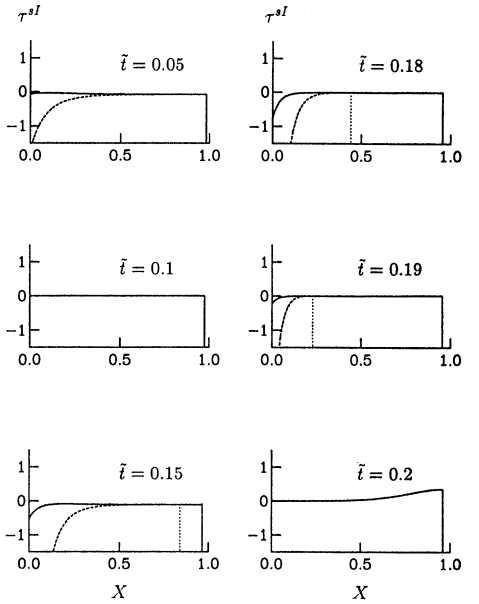

Figure 15. Wind stress distribution $\tilde{\tau}^{\mathrm{sI}}$ at a sequence of time in case (a) for viscosity ζ_1 (solid curve) and viscosity ζ_2 (dashed curve) with linear drag relation. The dotted line shows location of the interface $L_z(\tilde{t})$ and the vertical solid line shows location of the free edge $L(\tilde{t})$.

Figure 16. Wind stress distribution $\tilde{\tau}^{\mathrm{sI}}$ at a sequence of time in case (a) for viscosity ζ_1 (solid curve) and viscosity ζ_2 (dashed curve) with quadratic drag relation. The dotted line shows location of the interface $L_z(\tilde{t})$ and the vertical solid line shows location of the free edge $L(\tilde{t})$.

and case (iii) reflect the influence of α_{f}, and the distinction between case (i) and cases (ii) and (iii) reflect the influence of A_0. Specifically, the influence of A_0 for given α_{f} is shown by a comparison of the results for the sets (i) and (ii). For the larger A_0 there is less room for A to increase during convergence, and so the ridging process enhances the increase in thickness $\tilde{h}$. Increase of A_{f} is reflected by increase of α_{f}, and the influence of α_{f} at given A_0 is shown by a comparison of the results for sets (ii) and (iii). Larger A_{f} implies that the ridging starts at larger A so that thickness increase is less pronounced, compensated by greater increase in area fraction A. The influence of ridging is naturally confined to the region of greatest convergence.

Figures 15 and 16 show the required wind stress for set (iii), $(5\,e\,8)$, and case (a), $(5\,e\,9)$, at a sequence of times for the linear and quadratic drag relations respectively, comparing the smaller and larger viscosity, ζ_1, ζ_2, results. The change between linear and quadratic drag relations is not great, except near the free edge at later times when the velocity becomes large enough for the quadratic dependence to be more significant. The viscosity change is significant, showing the large coastward wind stress necessary near the coast during the convergence with higher viscosity. This implies that a moderate prescribed wind stress in the direct problem must result in a lower convergence than constructed in the present situation if the viscosity is so high. Note that the acceleration term is not significant because the coefficient $v^*/(g\epsilon t^{\#})$ is negligible $(5\,e\,3)$.

Figures 17 and 18 show the corresponding results for case (b), $(5\,e\,9)$, when

PHILOSOPHICAL TRANSACTIONS OF THE ROYAL SOCIETY A MATHEMATICAL, PHYSICAL & ENGINEERING SCIENCES

Figure 17 Figure 18

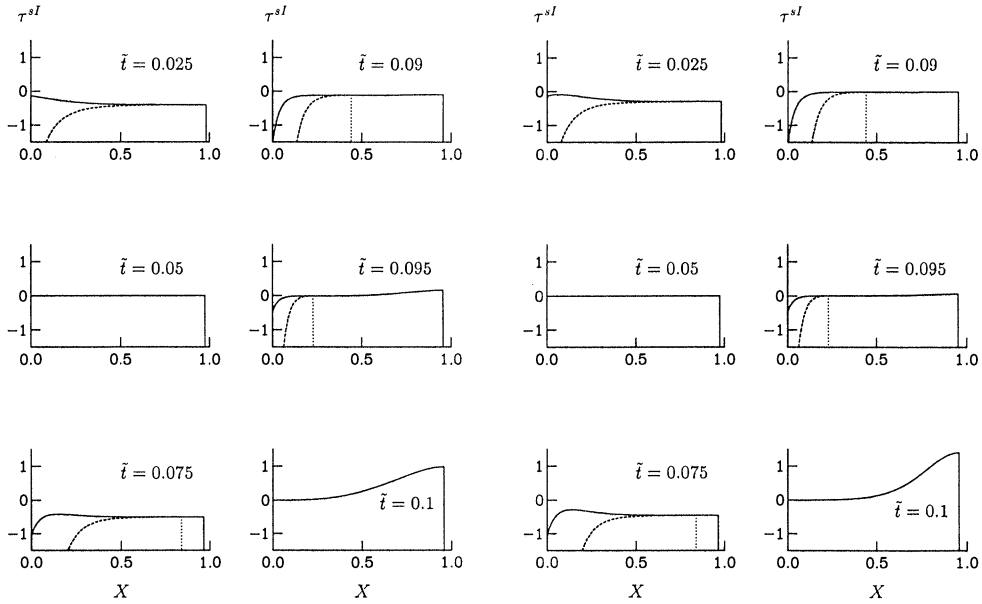

Figure 17. Wind stress distribution $\tilde{\tau}^{sI}$ at a sequence of time in case (b) for viscosity ζ_1 (solid curve) and viscosity ζ_2 (dashed curve) with linear drag relation. The dotted line shows location of the interface $L_z(\tilde{t})$ and the vertical solid line shows location of the free edge $L(\tilde{t})$.

Figure 18. Wind stress distribution $\tilde{\tau}^{sI}$ at a sequence of time in case (b) for viscosity ζ_1 (solid curve) and viscosity ζ_2 (dashed curve) with quadratic drag relation. The dotted line shows location of the interface $L_z(\tilde{t})$ and the vertical solid line shows location of the free edge $L(\tilde{t})$.

$\tilde{t}_1$ is halved so that the deformation evolves at double the rate. The viscosity comparison remains the same as above. It can be seen, however, that increasing the deformation rate both increases the wind stress magnitudes and increases their gradient in the regions of high convergence and high divergence. Moreover, this effect is more pronounced with the quadratic drag relation than with the linear drag relation, because of the velocity influence.

In addition to showing some qualitative effects of different parameters, this exact solution provides an important test problem for any numerical algorithm constructed to solve the coupled system of partial differential equations over a domain with a moving edge and with distinct regions of convergence and divergence separated by an unknown moving interface. The applied wind stress at all points and times for the direct problem is calculated from the algebraic relations (5 b 14) and (5 b 17) once the differentials are calculated and the known deformation, velocity and velocity gradients are substituted.

6. Concluding remarks

The mathematical analysis we have presented makes precise the many assumptions and approximations necessary to model the dynamics of a large-scale sea ice pack by two-dimensional theory. It rests on the use of dimensionless variables normalized through observed magnitudes and recognition of the essential momentum balances, and on the use of stretched coordinates to reflect the assumed

PHILOSOPHICAL TRANSACTIONS OF THE ROYAL SOCIETY A MATHEMATICAL, PHYSICAL & ENGINEERING SCIENCES

slow and smooth variation of quantities over the length scales of an individual floe and of the pack. The physical notions underpinning the formulation are implicit in other treatments, but our theoretical mechanics approach determines a structure in which quantities are fully defined and in which both the validity and weakness of many of the approximations are exposed. It therefore complements the more direct physical approaches, but, more significantly, provides a mathematical framework in which physical assumptions can be interpreted and assessed. Moreover, the mathematical approximation scheme based on a small dimensionless parameter determines a leading-order reduced model in which the neglected terms are consistently of higher order in the small parameter.

We can highlight some of the main features which we see as significant theoretical developments. An explicit formulation of the ice floe and lead water motions and conservation laws within an interacting continua framework (mixture theory) exposes the accompanying smoothness assumptions and required relations between partial and intrinsic variables. Integration of the full three-dimensional equations through the ice pack thickness introduces the assumptions of smoothly varying layer thickness h and ice area fraction A, and defines a thickness integrated stress field. A detailed analysis of a single coherent floe demonstrates that the mean depth integrated stress is, to leading order, determined by the extra edge tractions induced by interactions between adjacent converging floes. This allows an interpretation of pack stress as a mean stress in the local floe, in turn related to the relative motions of local floes described in terms of the pack velocity field. From this we have the first formal interpretation of a constitutive law for the ice pack stress, and its dependence on the converging or diverging nature of the local flow. A major weakness of this theory, which applies to all the implicit treatments, is that the individual floes should be much smaller then the pack, so that mean values over floes can be sensibly interpreted as local values of the pack scale variables. This fails for the larger floes which occur in practice, so solution of pack equations will not represent real variations over the larger floes.

A serious deficiency in earlier models is that the ice area fraction can, and would without artificial numerical cut-off, exceed unity in maintained convergence. This has been recognized as a consequence of neglecting the redistribution of converging ice into thicker ridges (in the evolution equation). Here we formulate a simple ridging mechanism, which could be generalized, that accounts for this redistribution and leads to consistent area fraction evolution, allowing only an asymptotic approach to unity in maintained convergence. We also illustrate that even an elementary viscous model for the ice pack stress can predict that the stress field in a highly converging zone must satisfy approximately some failure criterion based on a combination of the stress invariants.

The theory also emphasizes the distinction between the equations in converging and diverging flow regions, both in relation to the ice pack stress and to the ridging process. This highlights the occurrence of moving interfaces between such regions, across which appropriate matching conditions must be satisfied. These unknown moving boundaries must be determined as part of the solution evolution. This is the first time this significant, and complex, feature of the ice pack evolution has been identified. A final one-dimensional analytic solution is constructed for a particular class of problems which involve the formation of such an interface and its subsequent motion through the pack. While not necessarily of direct physical

PHILOSOPHICAL TRANSACTIONS OF THE ROYAL SOCIETY A MATHEMATICAL, PHYSICAL & ENGINEERING SCIENCES

interest, it can serve as a first test solution for numerical algorithms which must be constructed to treat realistic two-dimensional motions.

7. Nomenclature

$\boldsymbol{a}$	Particle acceleration with respect to the Earth
$\boldsymbol{a}^{\mathrm{c}}$	Coriolis acceleration
$\boldsymbol{a}^{\mathrm{N}}$	Acceleration in fixed stars Newtonian frame
$\bar{\boldsymbol{a}}^{\mathrm{N}}$	Mean horizontal Newtonian acceleration
b	Volume flux of ice ablating from the floe base per unit area
b^{i}	Partial ice volume flux per unit cross-section
b^{I}	Intrinsic ice volume flux per unit cross-section
b^{W}	Intrinsic downward water volume flux per unit cross-section, needed to maintain the layer base
c_1	Linear water drag coefficient
c_2	Quadratic water drag coefficient
$\hat{c}_1$	Scaled linear drag coefficient
$\hat{c}_2$	Scaled quadratic drag coefficient
$\boldsymbol{e}_1, \boldsymbol{e}_2$	Tangent vectors
f	Mean proportion of ice–ice contact length on floe boundaries
f_{c}	Coriolis parameter
g	Gravitational acceleration
$\boldsymbol{g}^*$	Gravity due to Earth's mass
h	Ice thickness
h_{c}	Coherent ice thickness
h_d	Thickness difference between ridged and coherent ice
h^{H}	Ice thickness, used in Hibler (1979)
h^{i}	Partial ice thickness
h_{r}	Ridged ice thickness
h_{w}	Layer water depth
h_0	Initial ice thickness
h^*	Ice thickness magnitude
$\tilde{h}, \breve{h}$	Non-dimensional ice thickness, as functions of spatial and material coordinates
$\boldsymbol{i}, \boldsymbol{j}, \boldsymbol{k}$	Unit coordinate base vectors
k	Mass transfer per unit pack volume per unit time, due to phase change
k^{r}	Mass transfer per unit pack volume per unit time, from coherent to ridging ice
l	One-dimensional ice pack length
l_{f}	Horizontal ice floe length scale
l_z	Position of the moving interface between converging and diverging zones, in the one-dimensional motion example
l_0	Initial one-dimensional pack length
l^*	Ice pack and weather system length scale
$m, \tilde{m}$	Physical and non-dimensional intrinsic ice column mass
m^{H}	Ice column mass, used in Hibler (1979)
m^{i}	Partial ice column mass

m^{w}	Partial water column mass
$\boldsymbol{n}$	Unit normal vector to a material surface
p^{w}	Partial water pressure
p^{W}	Intrinsic water pressure
q	Volume flux of ice accreting to the surface of the floe per unit area
q^{i}	Partial ice flux to the ice surface
q^{I}	Intrinsic ice flux to the ice surface
q^{W}	Accumulation rate of water per unit water surface area
r^{I}	Radiation energy deposit to the ice per unit volume per unit time
$\boldsymbol{r}^{\mathrm{p}}$	Position vector of particle P
r^{W}	Radiation energy deposit to the water per unit volume per unit time
$\boldsymbol{s}$	Tangential vector to a material surface
$t, \tilde{t}$	Time and non-dimensional time
$t_1, t_2, \tilde{t}_1, \tilde{t}_2$	Times and non-dimensional times at which the first and second phases end, in the one-dimensional motion example
t^*	Evolution timescale
$t^{\#}$	Time scale for one-dimensional illustration
$\boldsymbol{t}$	Total traction
$t_{\mathrm{n}}^{\mathrm{b}}, t_{\mathrm{n}}^{\mathrm{s}}$	Normal traction on the base and surface of the ice
$\boldsymbol{t}_{\mathrm{s}}^{\mathrm{b}}, \boldsymbol{t}_{\mathrm{s}}^{\mathrm{s}}$	Tangential traction on the base and surface of the ice
$\boldsymbol{t}^{\mathrm{i}}$	Partial ice traction
$\boldsymbol{t}^{\mathrm{I}}$	Intrinsic ice traction
$t_{\mathrm{n}}^{\mathrm{I}}, \boldsymbol{t}_{\mathrm{s}}^{\mathrm{I}}$	Intrinsic normal and tangential ice tractions
$\boldsymbol{t}^{\mathrm{w}}$	Partial water traction
$\boldsymbol{t}^{\mathrm{W}}$	Intrinsic water traction
v^*	Horizontal ice velocity magnitude
$\boldsymbol{v}$	Pack velocity
$\tilde{\boldsymbol{v}}, \breve{\boldsymbol{v}}$	Non-dimensional pack velocity, as functions of spatial and material coordinates
$\breve{\boldsymbol{v}}$	Relative velocity to floe $\mathcal{P}$
$\boldsymbol{v}^{\mathrm{D}}$	Distortional velocity
$\boldsymbol{v}^{\mathrm{i}}$	Ice velocity
$\boldsymbol{v}^{\mathrm{p}}$	Rigid body velocity
v_3^{r}	Vertical velocity component which transports ice into sails and keels
$\boldsymbol{v}^{\mathrm{w}}$	Layer water velocity
x	Axial position
$\boldsymbol{x}$	Position vector
$\boldsymbol{x}^{\dagger}$	Position vector in local floe coordinates
$\boldsymbol{y}$	Position vector relative to the centre of floe $\mathcal{P}$
$z_{\mathrm{b}}, \tilde{z}_{\mathrm{b}}$	Physical and non-dimensional ice base
$z_{\mathrm{s}}, \tilde{z}_{\mathrm{s}}$	Physical and non-dimensional ice surface
$z_{\mathrm{w}}, \tilde{z}_{\mathrm{w}}$	Physical and non-dimensional water surface
$\mathcal{A}, \mathcal{B}, \mathcal{C}, \mathcal{D}$	Floe labels
$A, \breve{A}$	Ice concentration, as functions of spatial and material coordinates
A_0	Initial ice concentration
A_{c}	Concentration of coherent ice per unit mixture area
A^{H}	Ice concentration, used in Hibler (1979)
A_{r}	Concentration of ridging ice per unit mixture area

$\boldsymbol{B}, \tilde{\boldsymbol{B}}$	Physical and non-dimensional body force
$C, \tilde{C}$	Physical and non-dimensional floe edge contour
$C_{\mathrm{a}}^{\mathrm{H}}, C_{\mathrm{w}}^{\mathrm{H}}$	Quadratic drag coefficients for air and water used in Hibler (1979)
C^{I}	Specific heat of ice
$\boldsymbol{D}$	Strain rate tensor
$\hat{\boldsymbol{D}}$	Deviatoric strain rate tensor
E^{W}	Evaporation rate per unit water surface area
F	Deformation gradient
$\boldsymbol{F}^{\mathrm{E}}, \tilde{\boldsymbol{F}}^{\mathrm{E}}$	Physical and non-dimensional net force due to extra tractions
G	Thickness dependence for the integrated stress
H	Heaviside unit function
H_{w}	Non-dimensional layer water depth
$I, \tilde{I}$	Physical and non-dimensional moment of inertia of an ice floe about a vertical axis through P
$\bar{J}$	Integrated stress invariant
K	Thermal conductivity
K^{I}	Thermal conductivity of ice
L	Latent heat
$\breve{L}_z$	Non-dimensional position of the moving interface between converging and diverging zones, as a function of material coordinates
$\boldsymbol{L}$	Velocity gradient
$M, \tilde{M}$	Physical and non-dimensional ice floe mass
O	Origin
N^{e}	Axial integrated extra stress
$\boldsymbol{N}$	Integrated total stress
$\boldsymbol{N}^{\mathrm{e}}$	Integrated extra stress
$\bar{\boldsymbol{N}}^{\mathrm{E}}$	Mean integrated extra stress
$\tilde{\boldsymbol{N}}^{\mathrm{E}}$	Non-dimensional integrated extra stress
$\bar{\tilde{\boldsymbol{N}}}^{\mathrm{E}}$	Mean non-dimensional integrated extra stress
$\hat{\bar{\boldsymbol{N}}}^{\mathrm{E}}$	Deviatoric mean integrated extra stress
$\boldsymbol{N}^{\mathrm{i}}$	Integrated partial ice stress
$\boldsymbol{N}^{\mathrm{I}}$	Integrated intrinsic ice stress
$\boldsymbol{N}^{\mathrm{w}}$	Integrated partial water stress
$\mathcal{P}$	Label for the central floe
P^{w}	Partial integrated water pressure
P^{W}	Intrinsic integrated water pressure
$\bar{P}$	Integrated stress invariant
Q^{W}	Surface energy flux into the water per unit water area
$\boldsymbol{Q}$	Horizontal ice flux per unit width of vertical section
R_{C}	Converging flow zone
R_{D}	Diverging flow zone
$\boldsymbol{R}^{\mathrm{p}}$	Position vector of the centre of mass in non-dimensional coordinates
$S, \tilde{S}$	Physical and non-dimensional horizontal cross-section floe domain
$S_A^{\mathrm{H}}, S_h^{\mathrm{H}}$	Ice concentration and thickness source terms, used in Hibler (1979)
$\boldsymbol{T}$	Integrated traction

$\boldsymbol{T}^{\mathrm{E}}$	Integrated extra traction
$\boldsymbol{V}_{\mathrm{g}}^{\mathrm{H}}$, $\boldsymbol{V}_{\mathrm{w}}^{\mathrm{H}}$	Geostrophic wind and ocean current, used in Hibler (1979)
$\boldsymbol{W}$	Spin tensor
$\boldsymbol{X}$	Non-dimensional position vector
$\rho\beta^{\mathrm{i}}$	Interaction drag per unit mixture volume on the ice due to the water (the body drag)
$\rho\hat{\beta}^{\mathrm{i}}$	Interaction thrust on the ice due to momentum production during phase change
$\rho\hat{\beta}^{\mathrm{w}}$	Interaction thrust on the water due to momentum production during phase change
α	Ratio of vertical ridging ice flux to available horizontal flux
γ	Strain rate invariant
γ_0	Invariant threshold
$\delta_{\alpha\beta}$	Kronecker delta
ϵ	Coordinate scaling parameter
ϵ_{f}	Floe aspect ratio
ϵ^*	Pack aspect ratio
$\varepsilon_{\alpha\beta 3}$	Permutation tensor
ζ	Bulk viscosity
η	Horizontal velocity divergence of pack
$\tilde{\eta}, \breve{\eta}$	Non-dimensional divergence as functions of spatial and material coordinates
η_0	A divergence threshold
θ^{H}	Air turning angle, used in Hibler (1979)
κ	Ratio of wind stress to basal pressure
$\hat{\kappa}$	Scaled ratio of wind stress to basal pressure
μ	Shear viscosity
ξ	One-dimensional position vector in material coordinates
ρ	Ice density
ρ_{a}	Air density
ρ^{c}	Partial density of coherent ice
ρ^{r}	Partial density of ridging ice
ρ_{w}	Water density
ρ^{w}	Partial density of water
$\boldsymbol{\sigma}$	Total stress
$\boldsymbol{\sigma}^{\mathrm{e}}$	Total extra stress
$\boldsymbol{\sigma}^{\mathrm{H}}$	Two-dimensional stress tensor, used in Hibler (1979)
$\boldsymbol{\sigma}^{\mathrm{i}}$	Partial ice stress
$\boldsymbol{\sigma}^{\mathrm{I}}$	Intrinsic ice stress
$\tilde{\boldsymbol{\sigma}}^{\mathrm{I}}$	Non-dimensional intrinsic ice stress
$\boldsymbol{\sigma}^{\mathrm{w}}$	Partial water stress
$\boldsymbol{\sigma}^{\mathrm{W}}$	Intrinsic water stress
$\tau^{\mathrm{bI}}, \tau^{\mathrm{sI}}$	Axial intrinsic basal and surface stress on the ice
$\breve{\tau}^{\mathrm{bI}}, \breve{\tau}^{\mathrm{sI}}$	Axial non-dimensional intrinsic basal and surface stress on the ice, as functions of material coordinates
τ^*	Wind stress magnitude
$\boldsymbol{\tau}^{\mathrm{b}}, \boldsymbol{\tau}^{\mathrm{s}}, \tilde{\boldsymbol{\tau}}^{\mathrm{b}}, \tilde{\boldsymbol{\tau}}^{\mathrm{s}}$	Physical and non-dimensional basal and surface stress on an ice floe
$\boldsymbol{\tau}^{\mathrm{bH}}, \boldsymbol{\tau}^{\mathrm{sH}}$	Water drag and winds stress, used in Hibler (1979)

$\boldsymbol{\tau}^{\mathrm{bI}}, \boldsymbol{\tau}^{\mathrm{bI}}$	Intrinsic basal and surface stress on the ice
$\boldsymbol{\tau}^{\mathrm{bW}}, \boldsymbol{\tau}^{\mathrm{sW}}$	Intrinsic basal and surface stress on the layer water
ϕ	Latitude
ϕ^{H}	Water turning angle, used in Hibler (1979)
ϕ_0, ϕ_1, ϕ_3	Functions of strain rate invariants
χ	Mapping from material to spatial coordinates
ψ	Energy absorption by the ice per unit layer volume due to phase change at the layer water interfaces
ψ_0, ψ_1	Functions of the stress invariants
ω	Physical and non-dimensional angular velocity of an ice floe
ω^*	Floe angular velocity magnitude
$\rho\mathcal{B}^{\mathrm{i}}$	Integrated interaction drag between the ice and layer water
Θ	Temperature
Θ^{I}	Ice temperature
Θ_M	Uniform layer water temperature, assumed to be saline water freezing temperature
Θ^{s}	Prescribed surface temperature
Ω	Angular velocity of the Earth about its North–South axis
$\boldsymbol{\Omega}$	Angular velocity of the Earth
Δ_{b}	Magnitude of the gradient of z_{b}
Δ_{s}	Magnitude of the gradient of z_{s}
$\mathbf{1}$	Unit tensor
tr	Trace

The early development of this work took place as part of the FRAM Special Topic, under which Dr J. M. N. T. Gray was supported by a NERC Ph.D. studentship at the Scott Polar Research Institute, Cambridge. We are very grateful to Professor K. Hutter, who reviewed the original manuscript very thoroughly, and provided us with a detailed commentary. He drew attention to several places where the arguments presented lacked the steps and clarity necessary to justify the results. We have therefore been able to rewrite those parts and, we trust, present a more convincing account of the model construction.

References

Bourke, R. H. & Garrett, R. P. 1987 Sea ice thickness distribution in the Arctic Ocean. *Cold Reg. Sci. Tech.* **13**, 259–280.

Campbell, W. & Rasmussen, A. 1970 *a* *AIDJEX Bull.* **1**, 4.

Campbell, W. & Rasmussen, A. 1970 *b* Latest experiments with ice rheology. *AIDJEX Bull.* **2**, 11–12.

Colony, R. 1975 The simulation of Arctic sea ice dynamics. *AIDJEX Bull.* **31**, 151–168.

Colony, R. & Pritchard, R. S. 1975 Integration of elastic-plastic constitutive laws. *AIDJEX Bull.* **30**, 55–80.

Coon, M. D. 1972 Mechanical behaviour of compacted Arctic ice floes. Offshore Technology Conference, Houston, Texas, Paper no. OTC 1684. American Institute of Metallurgical, Mining and Petroleum Engineers.

Coon, M. D., Maykut, G. A., Pritchard, R. S., Rothrock, D. A. & Thorndike, A. S. 1974 Modeling the pack ice as an elastic-plastic material. *AIDJEX Bull.* **24**, 1–105.

Flato, G. M. & Hibler, W. D. 1989 On a simple sea-ice dynamics model for climate studies. *Annls Glaciol.* **14**, 72–77.

Flato, G. M. & Hibler, W. D. 1990 A cavitating fluid sea ice model. *Cold Reg. Res. Engng Lab. Monograph* **90-1**.

PHILOSOPHICAL TRANSACTIONS OF THE ROYAL SOCIETY A MATHEMATICAL, PHYSICAL & ENGINEERING SCIENCES

Flato, G. M. & Hibler, W. D. 1992 Modeling pack ice as a cavitating fluid. *J. Phys. Ocean* **22**(6), 626–651.

Fowler, A. C. 1979 The use of a rational model in the mathematical analysis of a polythermal glacier. *J. Glaciol.* **24**, 443–456.

Glen, J. W. 1970 Thoughts on a viscous model for sea ice. *AIDJEX Bull.* **2**, 18–27.

Gordon, A. L. & Comiso, J. C. 1988 Polynyas in the Southern ocean. *Scientific Am.* **256**(6), 90–97.

Gray, J. M. N. T. 1992 Sea ice dynamics. Ph.D. thesis, University of Cambridge, U.K.

Häkkinen, S. 1987 Feedback between ice flow, Barotropic flow, and baroclinic flow in the presence of bottom topography. *J. geophys. Res.* **92**(C4), 3807–3820.

Hibler, W. D. 1979 A dynamic Thermodynamic sea ice model. *J. Phys. Ocean* **9**, 815–845.

Hibler, W. D. 1980 *a* Modeling pack ice as a viscous-plastic continuum: preliminary results. In *Sea ice processes and models* (ed. R. S. Pritchard), pp. 163–176. Seattle and London: University of Washington Press.

Hibler, W. D. 1980 *b* Documentation for a two-level dynamic thermodynamic sea ice model. *Cold Reg. Res. Engng Lab. Special Rep.* **80–8**.

Hibler, W. D. 1980 *c* Sea ice growth, drift and decay. In *Dynamics of snow and ice masses* (ed. S. C. Colbeck), pp. 141–209. Academic Press.

Hibler, W. D. 1980 *d* Modeling a variable thickness sea ice cover. *Mon. Weather Rev.* **108**, 1944–1973.

Hibler, W. D. 1984 The role of sea ice dynamics in modeling CO_2 increases. Climate processes and climate sensitivity. *Geophys. Monograph* **5**, 238–253.

Hibler, W. D. 1985 *a* Numerical modeling of sea ice dynamics and ice thickness characteristics – a final report. *Cold Reg. Res. Engng Lab. Rep.* **85–5**.

Hibler, W. D. 1985 *b* Modeling sea-ice dynamics. In *Advances in geophysics* (ed. B. Saltzman), vol. 28. Part A. Climate dynamics, pp. 549–579. Academic Press.

Hibler, W. D. 1986 Ice Dynamics. In *The geophysics of sea ice* (ed. N. Untersteiner), pp. 577–640. NATO ASI series B: Physics 146. Plenum Press.

Hibler, W. D. & Ackley, S. F. 1983 Numerical simulation of the Weddell sea pack ice. *J. geophys. Res.* **88**(C5), 2873–2887.

Hibler, W. D. & Bryan, K. 1987 A diagnostic ice-ocean model. *J. Phys. Ocean* **17**, 987–1015.

Hibler, W. D. & Tucker, T. 1979 Some results of a linear-viscous model of the Arctic ice cover. *J. Glaciol.* **22**, 293–304.

Hibler, W. D., Udin, I. & Ullerstig, A. 1983 On forecasting mesoscale ice dynamics and build-up. *Annls Glaciol.* **4**, 110–115.

Hopkins, M. A. & Hibler, W. D. 1991 On the ridging of a thin sheet of lead ice. *Annls Glaciol.* **15**, 81–86.

Hutter, K. 1982 A mathematical model of polythermal glaciers and ice sheets. *Geophys. Astrophys. Fluid Dynamics* **21**, 201–224.

Hutter, K. 1983 *Theoretical glaciology.* Dordrecht and Boston: Reidel.

Kelly, R. J., Morland, L. W. & Boulton, G. S. 1990 Deep penetration of permafrost through saturated ground. *Cold Reg. Sci. Tech.* **18**, 9–27.

Kelly, R. J., Morland, L. W. & Morris, E. M. 1990 A mixture theory for a phase-changing snowpack. *Cold Reg. Sci. Tech.* **17**, 271–285.

Lemke, P., Owens, W. B. & Hibler, W. D. 1990 A coupled sea ice-mixed layer-pycnocline model for the Weddell-sea. *J. geophys. Res.* **95**(C6), 9513–9525.

Leppäranta, M. & Hibler, W. D. 1985 The role of plastic ice interaction in marginal ice zone dynamics. *J. geophys. Res.* **90**(C11), 11,899–11,909.

Loewe, P. 1990 Full sea ice model forced with GCM atmosphere. In *Sea ice properties and processes: Proc. of the W. F. Weeks Sea Ice Symp.* (ed. S. F. Ackley & W. F. Weeks), pp. 251–255. *Cold Reg. Res. Engng Lab. Monograph* **90–1**.

PHILOSOPHICAL TRANSACTIONS OF THE ROYAL SOCIETY A MATHEMATICAL, PHYSICAL & ENGINEERING SCIENCES

Maykut, G. A. & Untersteiner, N. 1971 Some results from a time-dependent thermodynamic model of sea ice. *J. geophys. Res.* **76**(6), 1550–1575.

Maykut, G. A. 1976 Energy exchange over young sea ice in the central Arctic. *AIDJEX Bull.* **31**, 45–74.

Mellor, M. 1980 Mechanical properties of polycrystalline ice. In *Proc. IUTAM Symp. Physics and Mechanics of Ice* (ed. P. Tryde), pp. 217–245. Berlin: Springer.

Millero, F. J. 1978 Freezing point of seawater. In *Eighth Rep. Joint Panel on Oceanographic Tables and Standards. UNESCO Tech. Pap. Mar. Sci. no. 28, Annex 6.* Paris: UNESCO.

Morland, L. W. 1972 A simple constitutive theory for a fluid-saturated porous solid. *J. geophys. Res.* **76**, 890–900.

Morland, L. W. 1978 A theory of slow fluid flow through a porous thermoelastic matrix. *Geophys. J. R. astr. Soc.* **55**, 393–410.

Morland, L. W. 1982 A fixed domain method for diffusion with a moving boundary. *J. Engng Math.* **16**, 259–269.

Morland, L. W. 1984 Thermomechanical balances in ice sheet floes. *Geophys. Astrophys. Fluid Dynamics* **29**, 237–266.

Morland, L. W. 1987 Unconfined ice-shelf flow. In *Dynamics of the west Antarctic ice sheet* (ed. C. J. Van der Veen & J. Oerlemans), pp. 99–116. Reidel.

Morland, L. W. 1992 Flow of viscous fluids through a porous deformable matrix. *Surv. Geophys.* **13**, 209–268.

Morland, L. W. & Johnson, I. R. 1980 The steady motion of ice sheets. *J. Glaciol.* **25**, 229–246.

Morland, L. W. & Johnson, I. R. 1982 Effects of bed inclination and topography on steady isothermal ice sheets. *J. Glaciol.* **28**, 71–90.

Morland, L. W. & Kelly, R. J. 1990 Comparisons of Laplace transform and finite difference solutions for evolving permafrost regions. *Int. J. numer. analyt. Meth. Geomech.* **14**, 631–648.

Morland, L. W. & Shoemaker, E. M. 1982 Ice shelf balances. *Cold Reg. Sci. Tech.* **5**, 235–251.

Nansen, F. 1902 The oceanography of the north polar basin. The Norwegian polar expedition 1893–1896. Scientific Results **3**, 357–386.

Nikiforov, Ye. G. 1957 Changes in the compactness of the ice cover in relation to the dynamics of the ice cover. *Problems of the Arctic*, vol. 2. Leningrad.

Nikiforov, Ye. G., Gudkovich, Z. M., Yefimov, Yu. n. & Romanov, M. A. 1967 Principles of a method for calculating the ice redistribution under the influence of the wind during the navigation period in the Arctic seas. *Tr. Arkt. Antartkt. Inst.* **257**, 5–25. (English transl. *AIDJEX Bull.* **3**, 40–64.)

Nye, J. F. 1973 The physical meaning of the two-dimensional stresses in a floating ice cover. *AIDJEX Bull.* **21**, 1–8.

Nye, J. F. & Thomas, D. R. 1974 The use of satellite photographs to give the movement and deformation of sea ice. *AIDJEX Bull.* **27**, 1–21.

Olmsted, C. 1991 Measuring sea ice deformation with imaging radar satellites. In *Proc. Int. Conf on the Role of the Polar Regions in Global Change, University of Alaska Fairbanks, 11–15 June 1990* (ed. G. Weller, C. L. Wilson & B. A. B. Severin), vol. 1, pp. 141–146. University of Alaska Fairbanks.

Overland, J. E. & Pease, C. H. 1988 Modeling ice dynamics in coastal seas. *J. geophys. Res.* **93**(C12), 619–637.

Owens, W. B. & Lemke, P. 1990 Sensitivity studies with a sea ice-mixed layer-pycnocline model in the Weddell sea. *J. geophys. Res.* **95**(C6), 9527–9538.

Pai, S. I. & Li, H. 1971 Mathematical model for two-phase flow for the dynamics of pack ice in the Arctic ocean. *AIDJEX Bull.* **9**, 35–40.

Pai, S. I. & Li, H. 1975 A note on the dynamics model of pack ice in the Arctic ocean and its surrounding seas. *AIDJEX Bull.* **28**, 167–172.

Parkinson, C. L. & Washington, W. M. 1979 A large-scale numerical model of sea ice. *J. geophys. Res.* **84**(C1), 311–337.

PHILOSOPHICAL TRANSACTIONS OF THE ROYAL SOCIETY A MATHEMATICAL, PHYSICAL & ENGINEERING SCIENCES

Parmerter, R. R. & Coon, M. D. 1972 Model of pressure ridge formation in sea ice. *J. geophys. Res.* **77**, 6565–6575.

Parmerter, R. R. & Coon, M. D. 1973 Mechanical model of ridging in the Arctic sea ice cover. *AIDJEX Bull.* **19**, 59–112.

Preller, R. H. 1985 The NORDA/FNOC Polar Ice Prediction System (PIPS) – Arctic: A technical description. Naval ocean research and development activity, Rep. 108.

Preller, R. H. & Posey, P. G. 1989*a* The Regional Polar Ice Prediction System – Barents sea (RPIPS–B): A technical description. Naval ocean research and development activity, Rep. 182.

Preller, R. H. & Posey, P. G. 1989*b* The Polar Ice Prediction System – a sea ice forecasting system. Naval ocean research and development activity, Rep. 212.

Preller, R. H., Cheng A. & Posey, P. G. 1990 Preliminary testing of a sea ice model for the Greenland sea. In *Sea Ice Properties and Processes. Proc. of the W. F. Weeks Sea Ice Symp.* (ed. S. F. Ackley & W. F. Weeks), pp. 259–277. *Cold Reg. Res. Engng Lab. Monograph* **90**–**1**.

Pritchard, R. S. & Schwaegler, R. T. 1975 Applications of the AIDJEX ice model. *AIDJEX Bull.* **31**, 137–150.

Pritchard, R. S. & Colony, R. 1975 A difference scheme for the AIDJEX sea ice model. *AIDJEX Bull.* **31**, 188–203.

Pritchard, R. S., Coon, M. D., & McPhee, M. G. 1976 Simulation of sea ice dynamics during AIDJEX. *AIDJEX Bull.* **34**, 73–93.

Pritchard, R. S. (ed.) 1980*a* *Sea ice processes and models*. Seatle and London: University of Washington Press.

Pritchard, R. S. 1980*b* A simulation of nearshore winter ice dynamics in the Beaufort sea. In *Sea ice processes and models* (ed. R. S. Pritchard), pp. 49–61. Seattle and London: University of Washington Press.

Reed, R. J. & Campbell, W. J. 1960 Theory and Observations of the drift of ice station Alpha. ONR final report, task number NR 307–250. University of Washington, Seattle, 255.

Rossby, C. G. & Montgomery, R. B. 1935 The layer of frictional influence in wind and water currents. *Papers Phys. Oceanog. Meteorol. MIT Woods Hole Oceanog. Inst.* **3**, 1–100.

Rothrock, D. A. 1970 The kinematics and mechanical behaviour of pack ice: the state of the subject. *AIDJEX Bull.* **2**, 1–10.

Ruzin, M. I. 1959 The wind drift of ice in a heterogeneous pressure field. *Tr. Arkt. Antartkt. Inst.* **226**, 123–135.

Schulekin, V. V. 1938 The drift of ice fields. *C.r. Acad. Sci. USSR* **54**, 589–594.

Semtner, A. J. 1976 A model for the thermodynamic growth of sea ice in numerical investigations of climate. *J. Phys. Ocean* **6**, 379–389.

Shen, H. H. & Ackermann, N. L. 1982 Constitutive relationships for fluid–solid mixtures. *J. Mech. Div ASCE* **108**(EM5), 748–763.

Shen, H. H. & Ackermann, N. L. 1984 Constitutive equations for a simple shear flow of a disk shaped granular mixture. *Int. J. Engng Sci.* **22**, 829–843.

Shen, H. H., Hibler, W. D. & Leppäranta, M. 1986 On applying granular flow theory to a deforming broken ice field. *Acta Mech.* **63**, 143–160.

Shen, H. H., Hibler, W. D. & Leppäranta, M. 1987 The role of floe collisions in sea ice rheology. *J. geophys. Res.* **92**(C7), 7085–7096.

Solomon, H. 1970 A study of ice dynamics relevant to AIDJEX. *AIDJEX Bull.* **2**, 33–50.

Stössel, A., Lemke, P. & Owens, W. B. 1990 Coupled sea ice-mixed layer simulations for the Southern ocean. *J. geophys. Res.* **95**(C6), 9527–9538.

Sverdrup, H. U. 1928 The wind-drift of the ice in the north Siberian shelf. The Norwegian North Polar expedition with the Maud 1918–1925. *Scientific results*, vol. 4.

Thorndike, A. S. & Maykut, G. A. 1973 On the thickness distribution of sea ice. *AIDJEX Bull.* **21**, 31–47.

Thorndike, A. S., Rothrock, D. A., Maykut, G. A. & Colony, R. 1975 The thickness distribution of sea ice. *J. geophys. Res.* **80**, 4501–4513.

PHILOSOPHICAL TRANSACTIONS OF THE ROYAL SOCIETY A MATHEMATICAL, PHYSICAL & ENGINEERING SCIENCES

Timokhov, L. A. 1971 On the relation between turbulent and averaged ice-floe motion. *AIDJEX Bull.* **6**, 27–36.

Wadhams, P. 1981 Sea ice topography of the Arctic ocean in the region 70° W to 25° E. *Phil. Trans. R. Soc. Lond.* A **302**, 45–85.

Wadhams, P. 1987 The ice thickness distribution across the Atlantic sector of the Antarctic ocean in midwinter. *J. geophys. Res.* **92**(C13), 535–552.

Walsh, J. E. W., Hibler, W. D. & Ross, B. 1985 Numerical simulation of Northern Hemisphere sea ice variability, 1951–1980. *J. geophys. Res.* **90**(C3), 4847–4865.

Weeks, W. F. 1976 Sea ice conditions in the Arctic. *AIDJEX Bull.* **34**, 173–206.

Yegorov, K. L. 1971 Theory of the drift in ice fields in a horizontally inhomogeneous wind field. *AIDJEX Bull.* **6**, 37–45.

Received 27 November 1992; accepted 26 February 1993

PHILOSOPHICAL TRANSACTIONS OF THE ROYAL SOCIETY A MATHEMATICAL, PHYSICAL & ENGINEERING SCIENCES